APPLICATIONS OF SUBSTRATE ANALOGUES FOR STUDIES OF PRENYLTRANSFERASE ENZYMES

A DISSERTATION
SUBMITTED TO THE FACULTY OF THE GRADUATE SCHOOL
OF THE UNIVERSITY OF MINNESOTA
BY

Amanda Jane DeGraw

IN PARTIAL FULFILLMENT OF THE REQUIREMENTS
FOR THE DEGREE OF DOCTOR OF PHILOSOPHY

ADVISOR:
Dr. Mark D. Distefano

APRIL 2010

Acknowledgements

It never ceases to amaze me that I made it this far. I did not do it alone though. There are so many friends, family members, and colleagues that have helped me along the way. I am truly grateful for all that they have done and would like to take the time to acknowledge them.

To my advisor, Mark Distefano: Thank you for allowing me to be a member your group and helping me see I made the right decision when everything up to that point had felt wrong. You always knew what to say to motivate me, and I appreciate your belief that I could do it. You've helped me to realize the kind of scientist I want to be and that I can accomplish anything I set me mind to.

To the past and present MDD group members: While quite dysfunctional at times, we have been a family over the years. Each and everyone one of you has helped me at some point along the way, whether it be an idea for an experiment, or just someone to laugh and chat with, and I thank you for that. In particular, Dr. Ben Duckworth, Dr. James Wollack, Dr. Dan Mullen, Josh Ochocki, Jon Dozier, and Dr. Rita Majerle. Ben: you're my hero. Thank you for your friendship over the years. I couldn't have made it without you. Josh and Jon: I am really going to miss you guys. You have been so good to me.

To the Taton group: You guys are the best! Thanks for always making me smile. In particular Alexi Young.

I have had the distinct pleasure of working with a number of other groups, not just within the University of Minnesota, and each deserves a special thank you. The Wattenberg Lab (U of MN): Thanks to Aaron Charlson for always providing cells for me. Nicholette Zeliadt, thank you for teaching me westerns, letting me steal your sonicator,

and always being a smiling face when I came in to the lab. And thank you to Dr. Elizabeth Wattenberg for providing excellent feedback and suggestions with my projects. The Beese Lab (Duke University), Dr. Lorena Beese and Michael Hast: It was truly a pleasure working on the cage compounds project with you. A special thanks to Mike for providing the MDD group with a mammalian PFTase clone that has worked wonders! So many of our projects have benefited from it. The Shoichet Lab (UCSF), Dr. Brian Shoichet and Dr. Michael Keiser: I could not have asked for better collaborators. It was great working with you. Thank you to EVERYONE involved in the Rubber Project. This includes the past and present scientists at the USDA; Dr. Wenshuang Xie, Dr. Fred Hahn, Dr. Colleen McMahan, and Dr. Maureen Whalen, the scientists at the University of Nevada Reno; Dr. David Shintani and Dr. Huma Nural, and Dr. Katrina Cornish from Yulex Corp. Thank you to everyone working at the various U of MN research facilities, especially Dr. Lorraine Anderson and Dr. Todd Markowski from the mass spectrometry and proteomics center.

To Dr. Rita Majerle: You have always been and will always be a great mentor and friend to me. I would not be where I am today if not for you. It never occurred to me to go to graduate school, let along obtain a Ph.D. You saw something in me no one else had, including myself. You were there for me when I was confused and upset about the choices I had made, and you showed me there was still hope. And when I was at my lowest and ready to quit, you helped me to come to my senses. I cannot begin to tell you what it has meant to have you working right along side me in my final year. It was such a joy to have you there. You lent an ear when I needed one most and strengthened my resolve to get through it. Thank you from the bottom of my heart.

To all of my family: The amount of love you have to give is amazing and has kept me going all these years. Mom, you are one of my best friends and an endless source of encouragement. Dad, your tenacity and "spunk" are things that I adore. I have the best of both you in me. My big brother Chris, thank you for protecting me and always being there for me. A special thank you goes to my Grandpa Larson for believing in me so much that he paid me a dollar for every "A" I received from 1st grade through 5th grade. Grandpa, your faith and pride in me gave me more strength than you know.

To Amy Klein: Thank you for believing in me and keeping Shawn company while I did my homework. You're the best.

And last, but certainly not least, to my amazing husband, Shawn: We have been through so much together. You have always been my rock. Thank you for always loving me, no matter how much time I spent doing homework in college, or in the lab in graduate school. You may not always understand what it is that I am doing, but you always listen when I want to share my good news with you, or gripe about something else. You are my best friend. You always understood that even though I was busy all the time and not around a lot, I still loved you and needed you. I would not have made this far without you. All of my successes are your successes too.

To my wonderful and amazing family and friends

To my parents, Jane and Gary

And especially to my husband, Shawn

By lending an ear, a shoulder to cry on, laughter,
and endless amounts of support and love,
you helped me see the light when I thought it would always be dark.

Abstract

Prenyltransferase enzymes serve a variety of important biological functions from the creation of natural rubber to the modification of signal transduction proteins. The focus of this thesis is twofold; to understand better the isoprenoid chain elongation enzyme prenyltransferase, which catalyzes the extension of isoprene units, and the protein prenyltransferases, which catalyze the transfer of an isoprenyl diphosphate to a protein or peptide. Substrate analogues have proven to be versatile tools for probing the identity, structure, mechanism, and function of various prenyltransferase enzymes. Described here are a variety of analogues of prenyltransferase substrates towards the study of prenyltransferase enzymes.

A photoactive phosphonophosphate-containing analogue of farnesyl diphosphate (FPP) that can covalently modify proteins it is bound to upon irradiation with light was characterized and applied towards the identification of *cis*-prenyltransferase protein(s) involved in rubber biosynthesis. Kinetic and structural studies with this analogue and protein farnesyltransferase (PFTase) or protein geranylgeranyltransferase type-I (PGGTase-I) demonstrate that this probe is a good mimic of isoprenoid diphosphates. The phosphonophosphate linkage resulted in enhanced stability of the analogues, allowing it to be used as a label and identify a specific protein in rubber biosynthesis, rubber elongation factor (REF). The cross-linking of REF with a photoactivatible analogue of FPP suggests that REF can interact with isoprenoid diphosphates during rubber biosynthesis and this interaction may be key for the process. However, results indicated it is unlikely that REF is the sole protein responsible for rubber synthesis, thus prompting further work in the area.

A caged compound is a biologically relevant molecule rendered inactive by a link to a chemical group (the "cage") through a photolabile bond. A series of photoactivatable protein prenyltransferase substrate analogues were created to achieve temporal control of prenyltransferase activity. Detailed characterization of these probes was performed to explore their applicability in protein prenylation studies. The first generation of caged PFTase analogues contain a nitrobenzyl-based photolabile group incorporated at the distal phosphate of the isoprenoid diphosphate substrate or the sulfhydryl side-chain of

the cysteine residue in a CAAX peptide substrate. Kinetic studies of caged isoprenoid diphosphates demonstrated that they are poor substrates for PFTase but, upon irradiation, can efficiently release FPP upon irradiation which can be utilized for catalysis. The caged CAAX peptide photo releases the parent peptide with similar kinetics to the caged isoprenoid diphosphates. When caged the CAAX peptide does not function as a substrate, but is able to bind with efficient capacity and nearly identical conformation as compared to the photo-released peptide and does not interfere with the binding of the isoprenoid diphosphate substrate. These results lead to a wide variety of experiments where temporal control over protein prenylation is necessary.

A second set of isoprenoid diphosphate analogues was created, bearing an azide or alkyne moiety. These analogues were applied as chemical proteomic probes for studying the mammalian protein prenylome. Cells were treated with either the alcohol, which is converted into the diphosphate by cellular kinases or the diphosphate isoprenoid analogue. These analogues were then appended onto prenylated proteins and through Cu(I)-catalyzed cycloaddition with a corresponding azide- or alkyne-modified fluorophore, and direct visualization of prenylated proteins accomplished. Application of this same reaction with a biotinylated capture reagent allowed for enrichment of the modified proteins and subsequent identification by liquid chromatography-tandem mass spectrometry (LC-MS). This work is still in progress.

Table of Contents

List of Tables

List of Figures

List of Schemes

List of Abbreviations

PPTase: protein prenyltransferase, IPP: isopentenyl diphosphate, DMAPP: dimethylallyl diphosphate, MVA: mevalonate, MEP: 2C-methyl-D-erythritol, AACT: acetyl-CoA C-acetyltransferase, HMGS: 3-hydroxy-3-methylglutaryl-CoA synthase, MK: mevalonate kinase, PMK: phosphomevalonate kinase, MDC: mevalonate 5-diphosphate decarboxylase, DXPS: 1-deoxy-D-xylulose-5-phosphate synthase, DXR: 1-deoxy-D-xylulose-5-phosphate reductase, CMT: MEP cytidyltransferase, CMK: 4-(cytidine 5'-diphospho)-2C-methylerythritol kinase, MECPS: 2C-methylerythritol 2,4-cyclodiphosphate synthase, MER: 2C-methyl-D-erythritol 2,4-cyclodiphosphate reductase, HMR: 1-hydroxy-2-methyl-2-(E)-butenyl-4-diphosphate reductase, UPP: undecaprenyl diphosphate, FPP: farnesyl diphosphate, GGPP: geranylgeranyl diphosphate, PFTase: protein farnesyltransferase, PGGTase-I: protein geranylgeranyltransferase type I, PGGTase-II: protein geranylgeranyltransferase type II, APP: allylic diphosphate, WRP: washed rubber particle, GPP: geranyl diphophosphate, Bz: benzophenone, DATFP: diazotrifluoropropionate, REF: rubber elongation factor, NBz: nitrobenzyl, DMNPE: dimethoxynitrophenethyl, CNBz: α-carboxy-nitrobenzyl, DMNBz: dimethoxy-nitrobenzyl, FTI: protein farnesyltransferase inhibitor, GGTI: protein geranylgeranyltransferase inhibitor, PTM: post-translational modification, DIFO: difluorinated cylcooctyne, TAMRA: tetramethylcarboxy rhodamine, AD: Alzheimer's disease, LC-MS/MS: liquid chromatography-tandem mass spectrometry, SCX: strong cation exchange, RP: reverse phase, RFP: red fluorescent protein, SEA: similarity ensemble approach, GPCR: G-protein coupled receptor, TIPT: tetraiodophenolphthalein, GFP: green fluorescent protein

Preface

Please note the following:

Chapter 2: Reproduced in part with permission from a) DeGraw, A.J.; Zhao, Z.; Strickland, C.L.; Taban, A.H.; Hsieh, J.; Jefferies, M.; Xie, W.; Shintani, D.K.; McMahan, C.M.; Cornish, K.; and Distefano, M.D. A photoactive isoprenoid diphosphate analogue containing a stable phosphonate linkage: synthesis and biochemical studies with prenyltransferases. *J. Org. Chem.* **2007,** *72*, 4587-4595. © American Chemical Society and b) Xie, W.; McMahan, C.M.; DeGraw, A.J.; Distefano, M.D.; Cornish, K.; Whalen, M.C.; and Shintani, D.K. Initiation of rubber biosynthesis: In vitro comparisons of benzophenone-modified diphosphate analogues in three rubber-producing species. *Phytochemistry* **2008,** *69*, 2539-2545. © Elsevier

Chapter 3: Reproduced in part with permission from DeGraw, A.J.; Hast, M.A.; Xu, J.; Mullen, D.; Beese, L.S.; Barany, G.; and Distefano, M.D. Caged protein prenyltransferase substrates: tools for understanding protein prenylation. *Chem. Biol. Drug Des.* **2008,** *72*, 171-181. © Wiley-VCH

Appendix B: Reproduced in part with permission from DeGraw, A.J.; Keiser, M.J.; Ochocki, J.D.; Shoichet, B.K.; and Distefano, M.D. Prediction and Evaluation of protein farnesyltransferase inhibition by commercial drugs. *J. Med. Chem.* **2010**, *53*, 2464-2471 © American Chemical Society

Chapter 1. Background – Prenyltransferase Enzymes

1.1 Introduction

There are three known classes of prenyltransferase enzymes: isoprenoid chain elongation prenyltransferases, small molecule prenyltransferases, and protein prenyltransferases.[1] The products of these enzymes are widely distributed in nature and serve a variety of important biological functions.[2] This thesis focuses on two of the three classes. Isoprenoid chain elongation prenyltransferases catalyze the extension of isoprene units, thus generating linear isoprenoid polymers of defined chain length. These polymers can serve as lipid carriers[3] or be utilized in cell wall biosynthesis.[4] Some have a yet unidentified biological function, as in the case of *cis*-1,4-polyisoprene rubber.[5] The protein prenyltransferases (PPTases) catalyze the transfer of an isoprenyl diphosphate to a protein or peptide.[6] These prenylated products are involved in specific signal transduction pathways, some of which have been implicated in oncogenesis.[7-9] Despite serving two very different functions, both of these classes of enzymes rely on the biosynthesis of isopentenyl diphosphate (IPP) and dimethylallyl diphosphate (DMAPP) to function.

1.2 Biosynthesis of IPP and DMAPP

Until the early 1990's, the isoprenoid building blocks utilized by prenyltransferase enzymes were believed to be made by only one biosynthetic route known as the mevalonate (MVA) pathway (Scheme 1.1, Panel A).[10] It was at that time that an alternative route was discovered, now known as the 2C-methyl-D-erythritol (MEP) pathway (Scheme 1.1, Panel B). These two distinct pathways appear to be clearly distributed among organisms.[11] The MVA pathway is used mostly by eukaryotes (including all mammals) a small number of eubacteria, fungi, the cytosol and mitochondria of plants, and some parasites such as *Trypanosoma* and *Leishmania*. The MEP pathway is employed in algae, cyanobacteria, most eubacteria, chloroplasts of plants, and apicomplexan parasites.

The MVA pathway[11] (Scheme 1.1, Panel A) begins with coupling of two molecules of Acetyl-CoA (**1**) catalyzed by acetyl-CoA C-acetyltransferase (AACT) to form acetoacetyl-CoA (**2**). 3-Hydroxy-3-methylglutaryl-CoA synthase (HMGS) then catalyzes the condensation of **2** with **1** to yield HMG-CoA (**3**). HMG-CoA reductase (HMGR) catalyzes the reduction of **3** to mevalonate (**4**). A mevalonate kinase (MK) phosphorylates at the C_5 position and phosphomevalonate kinase (PMK) adds a second phospho group. Mevalonate 5-diphosphate decarboxylase (MDC) leads to the conversion of phosphomevalonate phosphate (**6**) to IPP (**7**). An IPP isomerase converts IPP to DMAPP (**8**).

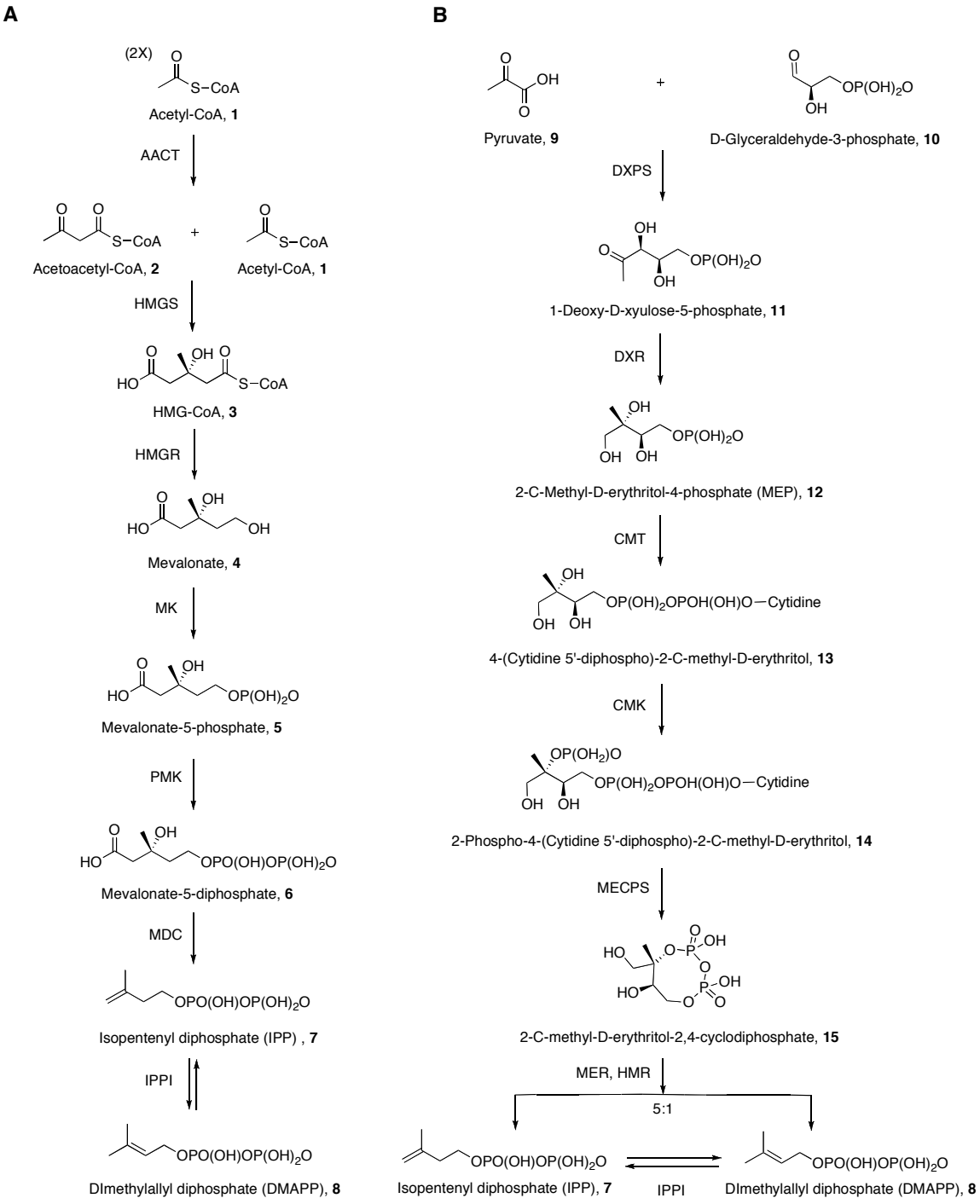

Scheme 1.1 Biosynthetic pathways for IPP and DMAPP

The head-to-tail condensation of pyruvate (**9**) with glyceraldehye 3-phosphate (**10**), catalyzed by 1-deoxy-D-xylulose-5-phosphate synthase (DXPS) is the first step in the MEP pathway[10] (Scheme 1.1b). A reductoisomerase (DXR) catalyzes both the rearrangement and reduction of 1-deoxy-D-xylulose-5-phosphate to MEP (**12**). MEP is conjugated with cytidine diphophsate by MEP cytidyltransferase (CMT) to form 4-(cytidine 5'-diphospho)-2C-methylerythritol (**13**). A kinase enzyme (CMK) catalyzes the phosphorylation of 2-position. **13** is then cyclized by 2C-methylerythritol 2,4-cyclodiphosphate synthase (MECPS). Two reduction reactions catalyzed by 2C-methyl-D-erythritol 2,4-cyclodiphosphate reductase (MER) and 1-hydroxy-2-methyl-2-(E)-butenyl-4-diphosphate reductase (HMR) lead to the formation of IPP (**7**) and DMAPP (**8**) in approximately a 5:1 ratio.

1.3 Prenyltransferase class I: isoprenoid chain-elongation enzymes

Elongation of allylic diphosphate substrates like DMAPP occurs through consecutive condensation reactions with IPP. The first class of prenyltransferase enzymes catalyze these reactions, which can proceed in either a *cis*-chain elongation or *trans*-chain elongation, as shown in Scheme 1.2.[12] In *trans*-elongation, the reaction has been shown to begin with the elimination of the pyrophoshate ion from the allylic diphosphate, thus generating an allylic cation[1]. Addition of IPP occurs through stereospecific removal of a proton to generate a new C-C bond. The resulting product contains a new double bond and is one C_5-isoprene unit longer. Repetition of this condensation reaction results in

prenyl chains of varying length. The mechanism of *cis*-elongation is not as well understood as hydrolysis of the allylic substrate has not been observed.[1]

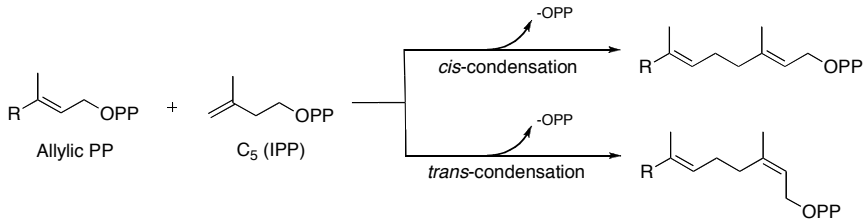

Scheme 1.2. Configuration of isoprenoid chain enlongation

Within this class of prenyltransferase enzymes there are considered to be four different sub-classes based on the length and stereochemistry of the isoprenoid formed and the catalytic requirements or structures of the enzymes.[13, 14] Group 1 contains enzymes that catalyze the synthesis of short chain compounds like farnesyl diphosphate (C_{15}) and geranylgeranyl diphosphate (C_{20}), shown in Figure 1.1. The only requirement of these enzymes for catalytic function is a divalent metal ion such as Mg^{2+} or Mn^{2+}. Of all the prenyltransferase enzymes, these have been the most extensively studied and characterized. Their structure is a tightly bound homodimer.[12]

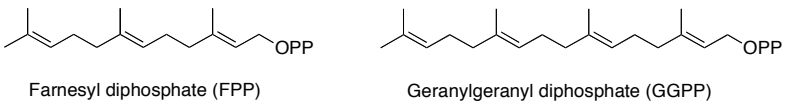

Figure 1.1. Small chain isoprenoid diphosphates

The second and third groups synthesize the medium (C_{30} and C_{35}) and longer chain (C_{40}, C_{45}, and C_{50}) prenyl diphosphates, all in the *trans*-configuration. Besides the length of their isoprenoid products, what sets these groups apart are differences in their catalytic requirements. Group 2 prenyltransferases are compromised of two non-identical protein

components that are not covalently bound. Catalytic activity is dependent on the association of these two parts.[15] Group 3 prenyltransferases are homodimers like Group 1, but require a carrier protein, whose role may be to facilitate the removal of the hydrophobic polyprenyl products from their active sites.[16] The length of prenyl products produced by these three groups are dictated by amino-acid residues located within the allylic diphosphate substrate binding site.[1, 12]

The fourth group catalyzes *cis*-chain elongation and requires phospholipids or detergents for their catalytic activity, as well as divalent cations like Mg^{2+}. These enzymes are homodimers[12]. Products of these enzymes include undecaprenyl diphosphate (UPP, C_{55}), dehydrodolichyl diphosphate (C_{80}) and natural rubber ($C_{>100}$). All *cis*-prenyltransferases thus far identified have products of C_{55} or longer chain length.[17, 18] To date, only one *cis*-prenyltransferase enzyme structure (UPP) has been studied by X-ray crystallography.[19]

1.4 Prenyltransferase class II: protein prenyltransferases

The second class of prenyltransferase enzymes are quite different from those previously described. These catalyze the post-translational attachment of a C_{15} (farnesyl diphosphate, FPP) or a C_{20} (geranylgeranyl diphosphate, GGPP) isoprenoid to a C-terminal cysteine residue through a thioether linkage[6] (Scheme 1.3). The attachment of this isoprenoid allows for membrane localization of proteins involved in a number of signal transduction pathways. This isoprenoid can also help to stabilize protein-protein interactions.[6]

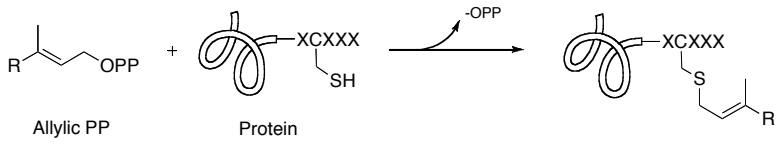

Scheme 1.3. Reaction catalyzed by protein prenyltransferases

There are two types of protein prenyltransferases; those that recognize a C-terminal cysteine residue located within a -CAAX consensus sequence or those that recognize a C-terminal -CXC, -CXXC, or -CC- sequence.[6] Protein farnesyltransferase (PFTase) and protein geranylgeranyltransferase type I (PGGTase-I) recognize the CAAX box, where C is the cysteine that is prenylated, A is typically aliphatic, and X is serine, methionine, or glutamine, which is prenylated by PFTase; or leucine, isoleucine, or valine; which is prenylated by PGGTase-I[20]. Protein geranylgeranyltransferase type II (PGGTase-II) recognizes the less stringent CXC or CXXC motif, where the first C is the cysteine that is prenylated, and X can be any amino acid.[6] PFTase and PGGTase-I are both heterodimers having identical α subunits and homologous β subunits. PGGTase-II is also a heterodimer, but shares only 27% identity with the PFTase/PGGTase-I α subunit and 29% identity with the PFTase β subunit.[6]

A search of the Swiss-Prot database revealed that there are approximately 300 proteins that end in the CXXX consensus sequence and are thus potentially prenylated.[8] The prenylation prediction (PRENbase) suite created by Maurer-Stroh and coworkers predicts that over a thousand different protein families are substrates for the three protein prenyltransferase enzymes.[21] As of yet, only the Rab family of proteins have been shown to be prenylated by PGGTase-II.[6] Proteins that have been confirmed to be farnesylated by PFTase include H-, K-, and N-Ras, the nuclear lamins, and the kinetechores CENP-E and

-F.[6, 22] Geranylgeranylated proteins include the Rho GTPases (RhoA, RhoB and RhoC), Rac1, CDC-42, and R-Ras.[6, 20] RhoB has been shown to be both farnesylated and geranylgeranylated *in vivo*.[23]

The reactions catalyzed by PFTase and PGGTase-I are currently under intense scrutiny given that their protein substrates have implications in oncogenesis and parasitic infection. A greater understanding of the catalytic mechanism and transition state would aid in the design of potent, specific inhibitors of these enzymes. Both enzymes are known to function through an ordered sequential mechanism, where the isoprenoid diphosphate binds first, creating a portion of the binding pocket for the CAAX peptide.[24, 25] The cysteine's thiol group ionizes upon coordination with the active site Zn^{2+}, and reaction with the C1 carbon of the isoprenoid occurs.[26] Whether this reaction occurs as an associative or dissociative type mechanism is currently being investigated.[27-30] Amino acid residues located within the enzyme active site dictate the length of isoprenoid substrate accepted.[1] While these residues appear to have tight control over chain length, there does not appear to be as much control over the chain shape. PFTase has been shown to be a highly promiscuous enzyme, accepting a number of non-natural FPP analogues as substrates.[31-35] The ability of PGGTase-I to utilize non-natural GGPP analogues as substrates has not been as extensively explored.[36]

1.5 Summary

Prenyltransferases are unique enzymes serving a variety of functions. Much still remains unknown about these enzymes. A *cis*-prenyl-chain elongation enzyme

contributes to the biosynthesis of natural rubber, but the identity of this enzyme or enzymes is yet to be determined. Among the protein prenyltransferase class, the targets of these enzymes have not been fully characterized leaving a good deal to be learned about the function and consequences of protein prenylation in *vivo*. Substrate analogues have proven to be versatile tools for probing the identity, structure, mechanism, and function of various prenyltransferase enzymes.[32,37-39]

1.6 References

1. Liang, P.-H.; Ko, T.-P.; Wang, A. H. J., Structure, mechanism and function of prenyltransferases. *Eur. J. Biochem.* **2002,** *269*, 3339-3354.

2. Poulter, C. D.; Rilling, H. C., Prenyl transferases and isomerase. *Biosynth. Isoprenoid Compd.* **1981,** *1*, 161-224.

3. Robyt, J. F., *Essentials of Carbohydrate Chemistry*. **1998**; p 400.

4. Sato, M.; Sato, K.; Nishikawa, S.-I.; Hirata, A.; Kato, J.-I.; Nakano, A., The yeast RER2 gene, identified by endoplasmic reticulum protein localization mutations, encodes cis-prenyltransferase, a key enzyme in dolichol synthesis. *Mol. Cell. Biol.* **1999,** *19*, 471-483.

5. Cornish, K., Biochemistry of natural rubber, a vital raw material, emphasizing biosynthetic rate, molecular weight and compartmentalization, in evolutionarily divergent plant species (1963 to 2000). *Nat. Prod. Rep.* **2001,** *18*, 182-189.

6. Zhang, F. L.; Casey, P. J., Protein prenylation: molecular mechanisms and functional consequences. *Annu. Rev. Biochem.* **1996,** *65*, 241-269.

7. Gelb, M. H.; Brunsveld, L.; Hrycyna, C. A.; Michaelis, S.; Tamanoi, F.; Van Voorhis, W. C.; Waldmann, H., Therapeutic intervention based on protein prenylation and associated modifications. *Nat. Chem. Biol.* **2006,** *2*, 518-528.

8. Sebti, S. M., Protein farnesylation: Implications for normal physiology, malignant transformation, and cancer therapy. *Cancer Cell* **2005,** *7*, 297-300.

9. Lowy, D. R.; Willumsen, B. M., Function and regulation of ras. *Annu. Rev. Biochem.* **1993,** *62*, 851-891.

10. Hirsch, A. K. H.; Diederich, F., The non-mevalonate pathway to isoprenoid biosynthesis: a potential source of new drug targets. *Chimia* **2008,** *62*, 226-230.

11. Lange, B. M.; Rujan, T.; Martin, W.; Croteau, R., Isoprenoid biosynthesis: the evolution of two ancient and distinct pathways across genomes. *Proc. Natl. Acad. Sci. U. S. A.* **2000,** *97*, 13172-13177.

12. Koyama, T., Molecular analysis of prenyl chain elongating enzymes. *Biosci., Biotechnol., Biochem.* **1999,** *63*, 1671-1676.

13. Koyama, T.; Ogura, K., Isopentenyl diphosphate isomerase and prenyltransferases. *Compr. Nat. Prod. Chem.* **1999,** *2*, 69-96.

14. Ogura, K.; Koyama, T., Enzymic aspects of isoprenoid chain elongation. *Chem. Rev.* **1998,** *98*, 1263-1276.

15. Zhang, Y. W.; Koyama, T.; Marecak, D. M.; Prestwich, G. D.; Maki, Y.; Ogura, K., Two subunits of heptaprenyl diphosphate synthase of *Bacillus subtilis* form a catalytically active complex. *Biochemistry* **1998,** *37*, 13411-13420.

16. Ohnuma, S.; Koyama, T.; Ogura, K., Purification of solanesyl-diphosphate synthase from *Micrococcus luteus*. A new class of prenyltransferase. *J. Biol. Chem.* **1991,** *266*, 23706-23713.

17. Takahashi, S.; Koyama, T., Structure and function of cis-prenyl chain elongating enzymes. *Chem. Rec.* **2006,** *6*, 194-205.

18. Kharel, Y.; Koyama, T., Molecular analysis of cis-prenyl chain elongating enzymes. *Nat. Prod. Rep.* **2003,** *20*, 111-118.

19. Fujihashi, M.; Zhang, Y.-W.; Higuchi, Y.; Li, X.-Y.; Koyama, T.; Miki, K., Crystal structure of cis-prenyl chain elongating enzyme, undecaprenyl diphosphate synthase. *Proc. Natl. Acad. Sci. U. S. A.* **2001,** *98*, 4337-4342.

20. Reid, T. S.; Terry, K. L.; Casey, P. J.; Beese, L. S., Crystallographic analysis of CaaX prenyltransferases complexed with substrates defines rules of protein substrate selectivity. *J. Mol. Biol.* **2004,** *343*, 417-433.

21. Maurer-Stroh, S.; Koranda, M.; Benetka, W.; Schneider, G.; Sirota, F. L.; Eisenhaber, F., Towards complete sets of farnesylated and geranylgeranylated proteins. *PLoS Comput. Biol.* **2007,** *3*, e66.

22. Tamanoi, F.; Kato-Stankiewicz, J.; Jiang, C.; Machado, I.; Thapar, N., Farnesylated proteins and cell cycle progression. *J. Cell. Biochem. Suppl.* **2001,** *37*, 64-70.

23. Armstrong, S. A.; Hannah, V. C.; Goldstein, J. L.; Brown, M. S., CAAX geranylgeranyl transferase transfers farnesyl as efficiently as geranylgeranyl to RhoB. *J. Biol. Chem.* **1995,** *270*, 7864-7868.

24. Dolence, J. M.; Cassidy, P. B.; Mathis, J. R.; Poulter, C. D., Yeast protein farnesyltransferase: steady-state kinetic studies of substrate binding. *Biochemistry* **1995,** *34*, 16687-16694.

25. Furfine, E. S.; Leban, J. J.; Landavazo, A.; Moomaw, J. F.; Casey, P. J., Protein farnesyltransferase: kinetics of farnesyl pyrophosphate binding and product release. *Biochemistry* **1995,** *34*, 6857-6862.

26. Rozema, D. B.; Poulter, C. D., Yeast protein farnesyltransferase. pKas of peptide substrates bound as zinc thiolates. *Biochemistry* **1999,** *38*, 13138-13146.

27. Sousa, S. F.; Fernandes, P. A.; Ramos, M. J., Unraveling the mechanism of the farnesyltransferase enzyme. *J. Biol. Inorg. Chem.* **2005,** *10*, 3-10.

28. Dolence, J. M.; Poulter, C. D., A mechanism for posttranslational modifications of proteins by yeast protein farnesyltransferase. *Proc. Natl. Acad. Sci. U. S. A.* **1995,** *92*, 5008-5011.

29. Lenevich, S.; Hosokawa, A.; Cramer, C. J.; Distefano, M. D., Transition state analysis of model and enzymatic prenylation reactions. *J. Am. Chem. Soc.* **2007,** *129*, 5796-5797.

30. Pais, J. E.; Bowers, K. E.; Fierke, C. A., Measurement of the α-secondary kinetic isotope effect for the reaction catalyzed by mammalian protein farnesyltransferase. *J. Am. Chem. Soc.* **2006,** *128*, 15086-15087.

31. Turek, T. C.; Gaon, I.; Distefano, M. D.; Strickland, C. L., Synthesis of farnesyl diphosphate analogues containing ether-linked photoactive benzophenones and their application in studies of protein prenyltransferases. *J. Org. Chem.* **2001,** *66*, 3253-3264.

32. Kale, T. A.; Hsieh, S. A.; Rose, M. W.; Distefano, M. D., Use of synthetic isoprenoid analogues for understanding protein prenyltransferase mechanism and structure. *Curr. Top. Med. Chem.* **2003,** *3*, 1043-1074.

33. Scholte, A. A.; Eubanks, L. M.; Poulter, C. D.; Vederas, J. C., Synthesis and biological activity of isopentenyl diphosphate analogues. *Bioorg. Med. Chem.* **2004,** *12*, 763-770.

34. Labadie, G. R.; Viswanathan, R.; Poulter, C. D., Farnesyl diphosphate analogues with omega-bioorthogonal azide and alkyne functional groups for protein farnesyl transferase-catalyzed ligation reactions. *J. Org. Chem.* **2007,** *72*, 9291-9297.

35. Duckworth, B. P.; Zhang, Z.; Hosokawa, A.; Distefano, M. D., Selective labeling of proteins by using protein farnesyltransferase. *Chembiochem* **2007,** *8*, 98-105.

36. Hosokawa, A.; Wollack, J.W.; Zhang, Z.; Chen, L.; Barany, G.; Distefano, M.D., Evaluation of an alkyne-containing analogue of farnesyldiphosphate as a dual substrate for protein-prenyltransferases. *Int. J. Pep. Res. Ther.* **2007,** *13*, 345-354.

37. Chen, A. P.; Chen, Y. H.; Liu, H. P.; Li, Y. C.; Chen, C. T.; Liang, P. H., Synthesis and application of a fluorescent substrate analogue to study ligand interactions for undecaprenyl pyrophosphate synthase. *J. Am. Chem. Soc.* **2002,** *124*, 15217-15224.

38. DeGraw, A. J.; Zhao, Z.; Strickland, C. L.; Taban, A. H.; Hsieh, J.; Jefferies, M.; Xie, W.; Shintani, D. K.; McMahan, C. M.; Cornish, K.; Distefano, M. D., A photoactive isoprenoid diphosphate analogue containing a stable phosphonate linkage: synthesis and biochemical studies with prenyltransferases. *J. Org. Chem.* **2007,** *72*, 4587-4595.

39. Henry, O.; Lopez-Gallego, F.; Agger, S. A.; Schmidt-Dannert, C.; Sen, S.; Shintani, D.; Cornish, K.; Distefano, M. D., A versatile photoactivatable probe designed

to label the diphosphate binding site of farnesyl diphosphate utilizing enzymes. *Bioorg. Med. Chem.* **2009,** *17*, 4797-4805.

Chapter 2. Photoactive isoprenoid diphosphate analogues for the identification of proteins involved in rubber biosynthesis

2.1 Introduction

Natural rubber, *cis*-1,4-polyisoprene, is a strategically important plant-derived material used in thousands of industrial, consumer, and medical applications. Due to its superior mechanical properties, synthetic polymers cannot be used in place of natural rubber in the manufacture of high performance products such as aircraft tires and critical medical devices. The military and transportation sectors of most industrialized economies are thus highly dependent on a reliable supply of natural rubber.

Currently, *Hevea brasiliensis* (Brazilian rubber tree) is the sole source of natural rubber for industrial applications and, due to its limited geographic range, most countries depend on imports of *H. brasiliensis* rubber to sustain industrial demand. Further, decades of inbreeding have rendered the commercial *H. brasiliensis* varieties highly susceptible to abiotic stress and pathogen attack.

Because of natural rubber's importance as a strategic material, many countries, including the United States, have ongoing programs to develop alternative sources of natural rubber capable of growing in temperate climates. Currently, the most promising candidate is guayule, *Parthenium argentatum*, a natural rubber-producing woody desert shrub native to the southwestern United States and northern Mexico.[1-4] Recently, guayule rubber has been commercialized as an alternative to *H. brasiliensis* rubber for the

manufacture of medical devices that can be used by persons with life-threatening Type I *H. brasiliensis* latex allergies. Supplies of this material are growing, but the need for natural rubber far outweighs the projected growth of the guayule rubber supply. While expanded plantings and selective breeding improvements are underway, genetic engineering of guayule holds significant potential for increased rubber yields, thereby enhancing the competitiveness of the U.S. domestic rubber crop. Overexpression of key metabolic pathway genes in genetically transformed guayule has been successful[5] but to date no studies have confirmed an increase in rubber production. Unfortunately, such efforts in crop improvement have been hampered by a lack of genetic and gene sequence knowledge, especially for gene(s) encoding the rubber transferase.

Rubber transferase is localized to the surface of cytosolic vesicles known as rubber particles, and biosynthesis is initiated through the binding of an allylic pyrophosphate (APP) primer. The progressive additions of isopentenyl pyrophosphate (IPP) molecules ultimately result in the formation of a high molecular weight cis-1,4 polyisoprene product.[6-8] Enzymatically active, partially-purified rubber particles (also known as washed rubber particles, WRPs) can be isolated such that, when provided with an appropriate allylic pyrophosphate primer, magnesium cofactor, and isopentenyl pyrophosphate monomer, rubber is produced *in vitro*.[3, 9, 10] Kinetic studies determined that rubber transferase is highly tolerant of allylic pyrophosphate primers of differing lengths and stereochemistry, including dimethly allyl pyrophosphate (DMAPP), geranyl pyrophosphate (GPP), farnesyl pyrophosphate (FPP), geranyl geranyl pyrophosphate (GGPP), and others.[6, 11] However, based on the results from structural analyses of natural

rubber[7, 12, 13] and kinetic analyses of the rubber transferase[6] it is likely that FPP functions as the actual APP primer *in vivo*.

Although rubber transferase is the key enzyme in rubber biosynthesis, it has not yet been purified and its corresponding gene sequences remain unknown. The primary reason is that rubber transferase is a membrane associated enzyme that is present in relatively low abundance.[14-16] In addition, classic biochemical approaches have failed to purify the rubber transferase because they are highly dependent on their ability to follow enzymatic activity throughout protein purification schemes. While relatively high levels of rubber transferase activity can be obtained from intact rubber particles, enzymatic activity is rapidly lost upon disruption of rubber particle structural integrity. As an alternative, we have chosen an approach involving the covalent photoaffinity tagging of rubber transferase using a specific benzophenone (Bz)-containing analog of the rubber biosynthetic initiator, FPP. This approach allows rubber transferase to be followed throughout purification even after enzymatic activity is lost.

Substrate analogues that covalently modify their cognate targets upon photolysis have proven useful for identifying previously uncharacterized enzymes. By creating a photoaffinity labeling reagent structurally based on suberoylanilide hydroxamic acid, Webb and coworkers were able to identify a potential target for hybrid polar cytodifferentiation agents through isolation of labeled proteins and mass spectral analysis.[17] Zhang and coworkers identified proteins that interact with platinum modified DNA using a photoreactive analogue of cisplatin.[18] The critical component in studies of this type is the ability to detect cross-linked proteins in order to isolate and identify them. Photoaffinity analogues of isoprenoid diphosphates have often employed a ^{32}P radiolabel

for detection given the ease of synthesis of these compounds.[19-21] However, because of the facile loss of the radiolabel due to the acid labile nature of the allylic diphosphate linkage, the use of such compounds has been less than ideal. The development of more stable photoreactive analogues may successfully accomplish such studies.

Because farnesyl diphosphate (FPP) is an isoprenoid building block utilized in a variety of cellular processes, we and others have developed a number of analogues that can be used for the study of isoprenoid binding enzymes like those involved in rubber biosynthesis.[22-25] Initial photoactive isoprenoid analogues incorporated a diazotrifluoropropionate (DATFP) photophore into the isoprenoid chain.[23, 25] Despite being accurate mimetics of FPP, they suffer from low cross-linking efficiency and require prolonged short wavelength UV irradiation for photoactivation. Molecules that utilize benzophenone moieties proved to be an attractive alternative for a number of reasons. Besides being more chemically stable than diazo esters, they can be easily manipulated in ambient light and require longer UV wavelengths for activation, avoiding protein degradation.[26] Given the significant overlap in the benzophenone and isoprenoid structures, analogues incorporating the benzophenone moiety as part of the isoprenoid chain were developed.[19, 20, 22, 24, 27, 28] X-ray crystallographic analysis of these molecules revealed that they are nearly superimposable with FPP in the active site of rat protein farnesyltransferase, confirming they are structurally analogous to FPP.[21, 24]

2.2 Research Objectives

We have created a benzophenone-based farnesyl diphosphate analogue (Figure 2.1) containing a stable phosphonophosphate group that replaces the labile allylic diphosphate. A number of polyprenyl phosphonophosphates have been reported as isoprenoid diphosphate mimics in the design of inhibitors[29, 30], immunoregulators[30, 31], as well as affinity purification reagents.[32, 33] Because the prenylation of proteins containing the C-terminal CAAX sequence by protein farnesyltransferase (PFTase) or protein geranylgeranyltransferase type I (PGGTase-I) is a well studied process, and a number of photoactivatable analogues of FPP have been used to study PFTase and/or PGGTase-I, we have chosen to use this a model system for probe validation. If the designed analogue can function as an FPP mimic in this CAAX-protein prenylation system, it should also function as an FPP mimic in the rubber biosynthesis initiation system. Described here is the characterization of probe **3** as well as its use in photoaffinity labeling studies aimed at identifying the protein(s) involved in rubber biosynthesis.

2.3 Results and Discussion

2.3.1 Probe stability

Towards the design of a more stable photoactive analogue, we envisioned compound **3**, based on **2**, that would incorporate a C-P bond at C-1 in lieu of the C-O bond present in **2** and FPP (**1**, Figure 2.1).

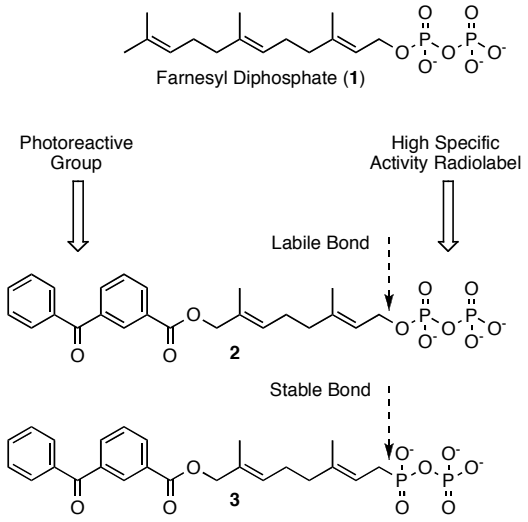

Figure 2.1. Photoactivatable isoprenoid analogue design.

In earlier work, it was noted that the ester linkage between the benzophenone and isoprenoid moieties present in compounds similar to **3** are stable to the acidic conditions typically used in reversed-phase chromatography to separate and identify cross-linked peptides obtained from photoaffinity labeling experiments with proteins. Unfortunately, this is not the case for the C-O bond at C-1 between the isoprenoid and phosphate moieties in allylic diphosphates such as **1** and **2**. In such molecules, while the phosphate anhydride linkage between the α and β phosphates is relatively stable to acid, the bond between C-1 and O-1 is labile. As illustrated in Figure 2.2, treatment of GPP, which contains a C-O bond at C-1 like **2**, with a mixture of H_2O and CH_3CN containing 0.2% TFA (common conditions for peptide analysis) results in hydrolysis of the allylic diphosphate with a half-life of approximately 2 hours.

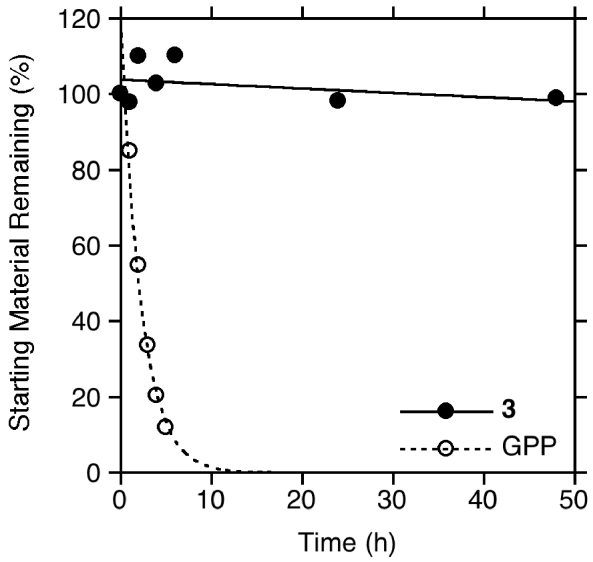

Figure 2.2. Stability of phosphonophosphate **3** compared to GPP.

This significant rate of degradation via phosphate loss makes it impractical to use ^{32}P-labeled allylic diphosphates for photoaffinity labeling applications when tryptic digestion and subsequent peptide sequencing are desired. In contrast, treatment of phosphonophosphate **3** under the same conditions results in less than 5% hydrolysis even after 50 hours of reaction. This enhanced stability significantly increases the utility of this benzophenone-containing analogue.

2.3.2 Probe validation with protein farnesyltransferase and protein geranylgeranyltransferase

2.3.2.1 Inhibition Kinetics

Given the inherent stability of the C-P bond at position C-1, phosphonophosphate **3** was tested as a competitive inhibitor of PFTase. The rate of PFTase-catalyzed farnesylation of the fluorescently tagged pentapeptide, *N*-Dansyl-GCVIA, was measured in the presence of a fixed concentration of FPP and varying concentrations of **3**. An IC_{50} value of 960 nM was calculated for **3**, which is comparable to previously synthesized benzophenone-based FPP analogues (see Table 2.1). The similarity in values between the ether-linked analogue **2** and **3** was unexpected, given the previously observed reduction in binding when a carbonyl group is involved in linkage between the benzophenone moiety and the isoprenoid.

Table 2.1. IC_{50} Values for Inhibition of PFTase by Benzophenone-Based Isoprenoid Diphosphate Photoaffinity Labeling Analogues.

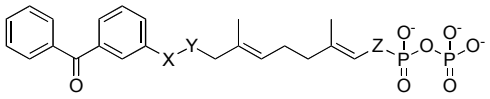

2 (X = CO, Y = O, Z = CH_2O)
3 (X = CO, Y = O, Z = CH_2)
4 (X = CO, Y = NH, Z = CH_2O)
5 (X = CH2, Y = O, Z = CH_2)

Compound	IC_{50} (μM)
2[a]	0.85
4[b]	2.3
5[c]	3.7
3	0.96

a From ref 25. *b* From ref 24. *c* From ref 19.

2.3.2.2 X-ray Crystallography

In contrast to our earlier work that always employed analogues containing an allylic diphosphate, compound **3** possesses a phosphonate linkage that is one carbon out of register relative to FPP. Crystals of **3** bound to PFTase were obtained and the structure of the resulting complex was determined via x-ray diffraction experiments to investigate the effect of this modification. The structure of **3** bound to PFTase is shown in Figure 2.3; for comparison the structure of FPP bound to rPFTase is shown in a superposition (panel A). Figure 2.4 highlights the key amino acid residues involved in the binding.

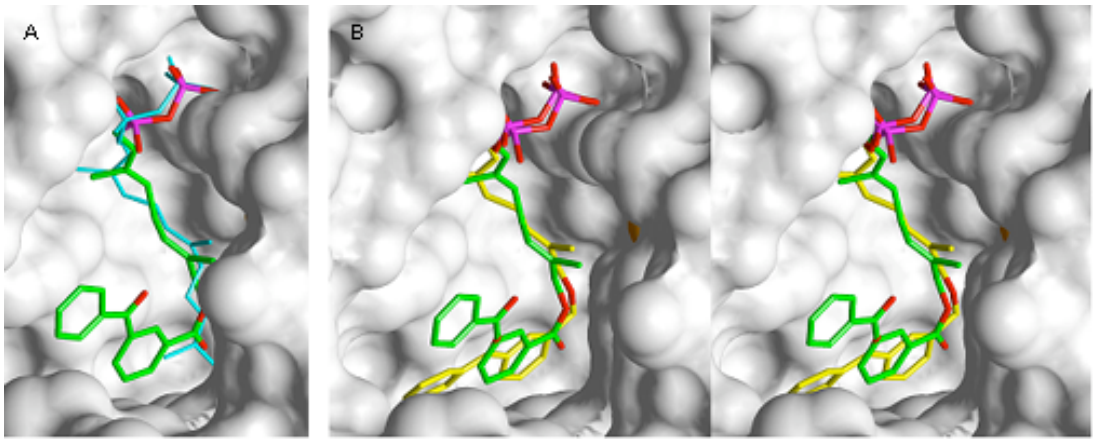

Figure 2.3. Crystallographic Analysis of Analogue **3** bound to rPFTase. A (left image): Superposition of **3** and FPP bound to PFTase. B (center and right images): Stereoview of a superposition of **3** and a related diphosphate analogue **2**. Analogue **3** is shown in green (carbon), red (oxygen) and purple (phosphorous). FPP is shown in blue. Analogue **2** is shown in yellow (carbon), red (oxygen) and purple (phosphorous). The solvent accessible protein surface is white with the Zn atom shown in red.

Electron density maps clearly show that **3** is bound in the rPFTase active site cavity. The presence of the higher molecular weight phosphate atoms in the molecule provides

helpful information in defining the binding mode. Comparison of the protein in the structure of the rPFTase:**3** complex and the rPFTase:FPP:SCH66336 ternary complex shows a 0.2 Å r.m.s. deviation for all protein atoms, indicating that no significant movement of the protein side-chains has occurred.[34, 35] Interestingly, the two phosphate P atoms from FPP and those from **3** are essentially superimposable suggesting that the phosphonophosphate substitution present in the analogue is not deleterious. Due to the absence of the intervening oxygen atom in **3** (the oxygen attached to C-1 in FPP) and the presence of the bulky benzophenone group, there small are perturbations in the structure of the isoprenoidal portion of the analogue; the average r.m.s. deviation for all atoms in the diphosphate unit and the first two isoprene units is 0.8 Å. However, these changes are in general small, indicating close complementarity between the natural substrate, FPP, and **3**. A superposition of **3** and **2**, a related diphosphate-based analogue with an ether-linked benzophenone, is shown in Figure 2.3, panel B. As was observed above with FPP, there is substantial overlap between these two structures particularly in the diphosphate unit and the first two isoprene units. However, there is a significant difference in the position of the benzophenone group in **3** relative to **2**. Clearly, the presence of the more conformationally restricted ester linkage in **3** alters the orientation of the benzophenone compared to that of the more flexible ether-linked analogue **2**. This structural difference may account for the greater inhibitory potency observed with **2** compared with **3**. Nevertheless, it can be concluded that beyond the greater size of the benzophenone groups that causes them to protrude beyond the FPP binding site, analogues such as **3** are good mimics of FPP and that the use of a phosphonophosphate group does not cause any significant changes in the mode of binding to PFTase.

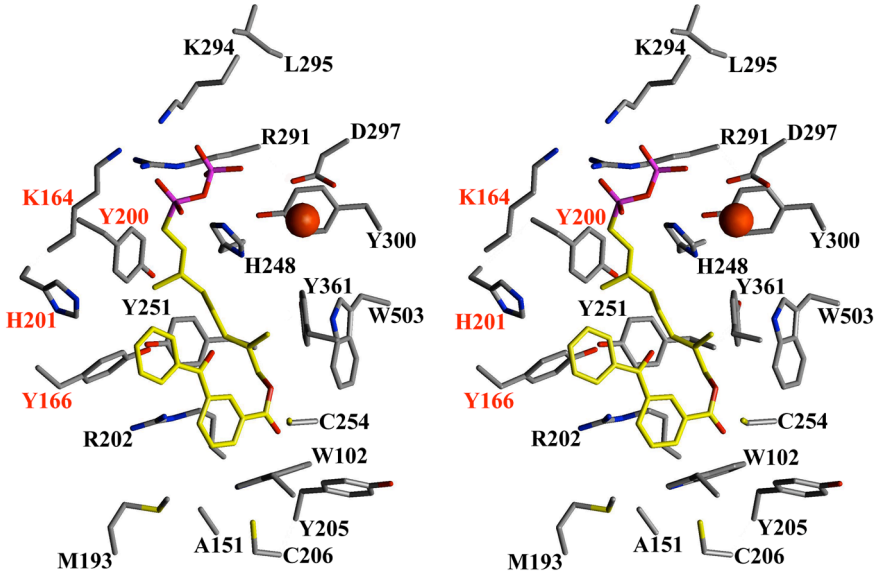

Figure 2.4. Stereoview of **3** bound to rPFTase. Residues highlighted in red are from the α subunit; black are from the β subunit. The catalytic zinc is shown as a red sphere.

2.3.2.3 Photoaffinity Labeling

To verify the ability of phosphonophosphate **3** to act as a photoaffinity label of prenyltransferase enzymes, the radiolabeled analogue [^{32}P]**3** was synthesized using a method developed by Bartlett and co-workers[36], adapted to incorporation of a radiolabel, and purified using a method previously described.[37] Photolysis of protein prenyltransferases with [^{32}P]**3** at a concentration 10-fold higher than the IC_{50} value determined for PFTase was performed with 300-400 nm light[26] for 2 hours. Preferential labeling of the β subunit was observed for both PFTase and PGGTase-I (Figure 2.5: PFTase and [^{32}P]**3** and Figure 2.6: PGGTase-I and [^{32}P]**3**; lane 2' in each). Upon addition of the natural substrate (FPP for PFTase, GGPP for PGGTase-I) in the photolysis reactions containing [^{32}P]**3**, protection from labeling was observed (Figure 2.5: PFTase

and [^{32}P]**3** and Figure 2.6: PGGTase-I and [^{32}P]**3**; lane 3' in each). Phosphorimaging analysis was used to quantify the relative labeling efficiencies of each subunit for each enzyme. For PFTase, the β subunit was labeled 4.8-fold over the α subunit. Inclusion of the natural substrate FPP, 1, in the photolysis reaction resulted in a substantial (2.3-fold) decrease in β subunit labeling. In the case of PGGTase-I photolabeling by [^{32}P]**3**, the β subunit was labeled 24-fold over the α subunit, while inclusion of the physiologically relevant substrate GGPP resulted in a substantial decrease in β subunit labeling (8.7-fold). The observed labeling specificity is in agreement with results obtained from other photoactive analogues with PFTase and PGGTase-I, all implicating β subunit involvement in prenyl group recognition.[19, 24]

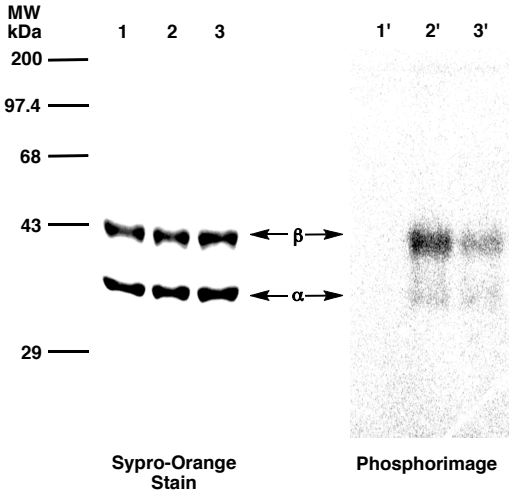

Figure 2.5. Analysis of photolabeling of pure PFTase with [^{32}P]**3** by SDS-PAGE. Lanes 1 and 1'contain samples of PFTase and [^{32}P]**3** that were not irradiated. Lanes 2 and 2' contain samples of PFTase and [^{32}P]**3** irradiated at 350 nm. Lanes 3 and 3' contain samples of PFTase and [^{32}P]**3** irradiated in the presence of FPP. Lanes 1, 2 and 3 show proteins identified with Sypro-Orange staining. Lanes 1', 2' and 3' show the radiolabeled proteins identified with phosphorimaging.

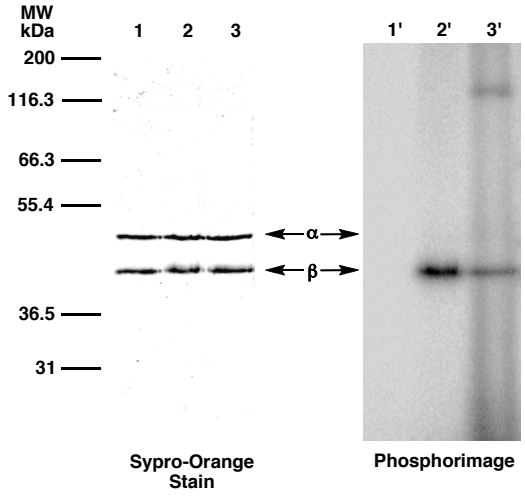

Figure 2.6. Analysis of photolabeling of pure PGGTase-I with [^{32}P]**3** by SDS-PAGE. Lanes 1 and 1'contain samples of PGGTase-I and [^{32}P]**3** that were not irradiated. Lanes 2 and 2' contain samples of PGGTase-I and [^{32}P]**3** irradiated at 350 nm. Lanes 3 and 3' contain samples of PGGTase-I and [^{32}P]**3** irradiated in the presence of GGPP. Lanes 1, 2 and 3 show proteins identified with Sypro®-Orange staining. Lanes 1', 2' and 3' show the radiolabeled proteins identified with phosphorimaging.

The applicability of this probe for labeling specific targets in a mixture of proteins was demonstrated by the photolysis of a partially purified sample of PGGTase-I with [^{32}P]**3**. Of the crude mixture of proteins, the β subunit is the major labeled species, while no labeling of the α subunit is observed (Figure 2.7). In this crude mixture, a large number of proteins are clearly visible by Sypro-orange staining. Interestingly, the phosphorimage (Fig. 2.7, lane 1') reveals three major labeled species with the β subunit of PGGTase-I as the most intensely labeled protein. Thus, although **3** is not absolutely specific for PGGTase-I, it obviously manifests substantial selectivity in this complex mixture. Based on the promising results obtained with **3** labeling in crude extracts, we decided to explore the ability of this probe to identify an unknown target.

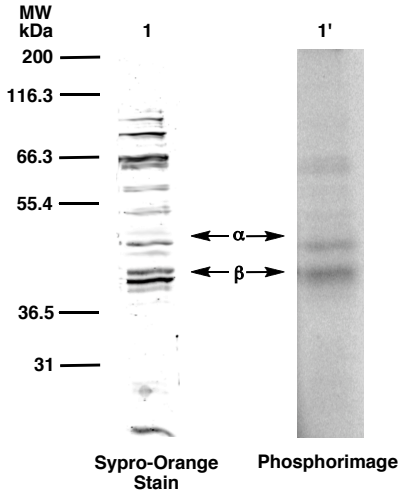

Figure 2.7. Analysis of crude PGGTase-I with [^{32}P]**3** by SDS-PAGE. Lanes 1 and 1' contain samples of crude cell lysate after ion-exchange chromatography, irradiated at 350 nm in the presence of [^{32}P]**3**. Lane 1 shows protein identified with Sypro-orange staining. Lane 1'shows radiolabeled protein identified with phosphorimaging.

2.3.3.Studies with *Hevea brasiliensis* washed rubber particles

2.3.3.1 Photoaffinity Labeling

Photolysis of suspensions of WRPs containing 10 μM [^{32}P]**3** was performed for 6 hours. Electrophoretic separation of the reaction mixture and visualization of the proteins indicated the presence of a wide range of species. The WRPs from *H. brasiliensis* are clearly a complex mixture. Interestingly, phosphorimaging analysis of the photolysis mixture gave a very different picture. Two major labeled species were observed as well as several minor bands (Figure 2.8, Lane 1'). The presence of FPP during the labeling reaction reduced the amount of radiolabel throughout the gel (Figure 2.8, Lane 2').

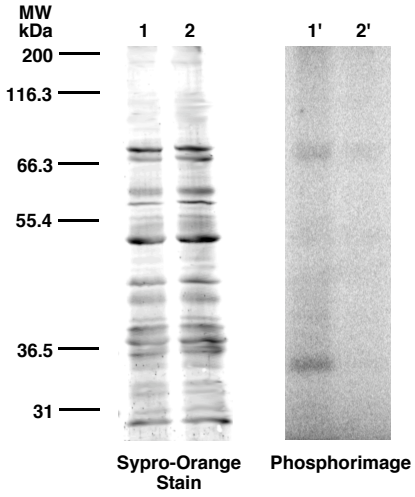

Figure 2.8. Analysis of photolabeling of *H. brasiliensis* washed rubber particles with [^{32}P]**3** by SDS-PAGE. Lanes 1 and 1' contain samples of WRPs and **[^{32}P]**3 irradiated at 350 nm. Lanes 2 and 2' contain samples of WRPs and [^{32}P]**3** irradiated in the presence of FPP. Lanes 1 and 2 show proteins identified with Sypro-orange staining. Lanes 1'and 2' show radiolabeled proteins identified with phosphorimaging.

2.3.3.2 Mass spectrometry of labeled proteins

The identify of the cross-linked proteins from the photolabeling of *H. brasiliensis* WRPs with [^{32}P]**3** was determined by performing a second set of photolysis reactions. Samples were fractionated by isoelectric focusing followed by SDS-PAGE. Surprisingly, the higher molecular weight proteins shown to be labeled previously were not observed. Instead, a series of proteins (10-20 kDa) appeared to be labeled (Figure 2.9).

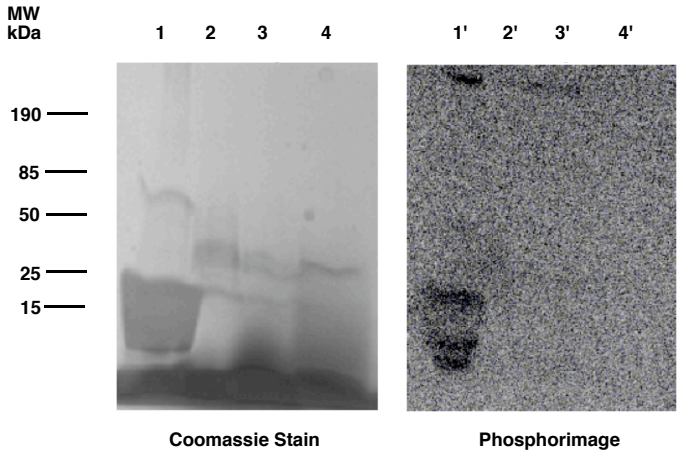

Figure 2.9. Analysis of photolabeling of *H. brasiliensis* washed rubber particles with [^{32}P]**3** by SDS-PAGE. Lanes 1-4 contain samples of WRPs and [^{32}P]**3** irradiated at 350 nm that have been separated by isoelectric focusing. Lane 1: pH 4.6-5.4 Lanes 2: pH 5.4-6.2 Lane 3: pH 6.2-7.0 Lane 4: pH 7.0-10.0. Left image shows proteins identified with Coomassie staining. Right image shows radiolabeled proteins identified with phosphorimaging.

These labeled protein bands were extracted from the gel, subjected to tryptic digestion, and analyzed by MALDI-MS/MS. A peak list of the data was then generated and searched using the MASCOT database. A 14.6 kDa protein, Rubber Elongation Factor, was identified (Table 2.2) based on the masses of eight different peptides. Together these represent approximately 69% of the complete primary sequence.

Table 2.2. Tryptic peptides determined by MS/MS Analysis

Amino acid residues	Calculated Mass	Observed Mass	Sequence	Confidence Interval (%)
17-40	2689.3547	2689.3516	YLGFVQDAATYAVTTFSNVYLFAK	100.000
41-58	1849.0065	1849.0023	DKSGPLQPGVDIIEGPVK	100.000
43-58	1605.8846	1605.8828	SGPLQPGVDIIEGPVK	100.000
68-77	1109.599	1109.6146	FSYIPNGALK	99.999
78-92	1621.8795	1621.8759	FVDSTVVASVTIIDR	82.268
93-99	753.4869	753.4849	SLPPIVK	99.591
100-110	1158.6477	1158.6460	DASIQVVSAIR	100.000
118-128	1088.5946	1088.5912	SLASSLPGQTK	97.974

Rubber Elongation Factor (REF), also known as the latex allergen Hev b1[38], is a known constituent in *H. brasiliensis* latex compromising 10-60% of the total protein.[39] While it is possible that REF can exist as carrier or binding partner in rubber biosynthesis, it has been directly implicated in playing a larger role. A study done by Dennis and coworkers showed that treatments of WRPs to either hydrolyze or remove REF completely abolishes prenyltransferase activity. However, attempts to reconstitute rubber biosynthesis in REF depleted WRPs with solubilized REF were unsuccessful, making the exact role of REF in rubber biosynthesis uncertain.[40] In our experiments, the cross-linking of REF in WRP suspensions with a photoactivatible analogue of FPP suggests that REF can interact with

isoprenoid diphosphates. This interaction may be key for rubber biosynthesis. However, even if this is the case, it is unlikely that REF is the sole protein responsible for rubber synthesis.

It is important to point out the apparent contradiction in the observed labeled proteins between separation techniques. With 1-D separation of the WRP proteins, the predominately labeled species were of 35 and 70 kDa apparent weight (as shown in Figure 2.8). Because of this, a second 1-D protein separation was performed and the 35 and 70 kDa proteins were isolated, subjected to tryptic digestion, and analyzed by MALDI-MS/MS. Upon searching of the MASCOT database, it was found that both the 35 kDa and the 70 kDa proteins could be attributed to REF. The appearance of the 14.6 kDa REF protein at these higher molecular weights is most likely due to contamination given that the most abundant protein in the rubber particle is REF.[39, 41] Further work is needed to efficiently isolate the labeled proteins from any contaminating REF for accurate identification.

2.4 Conclusions and Future Directions

Compound **3** is a photoactive phosphonophosphate-containing analogue of FPP. Kinetic and structural studies with **3** and PFTase or PGGTase-I demonstrate that this probe is a good mimic of isoprenoid diphosphates. The greater stability of **3** has allowed us to use it to label and identify a specific protein in rubber biosynthesis, REF. Current efforts are focused on utilizing a biotinylated version of **3** (Figure 2.10) to selectively enrich for the photo cross-linked proteins. The biotinylated proteins can be isolated from

those not labeled using immobilized Streptavidin chromatography. Subsequent elution from the resin, or tryptic digestion of proteins directly on resin, would allow for mass spectral analysis of the labeled proteins.

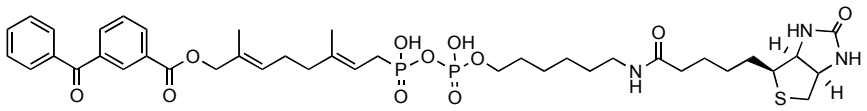

Figure 2.10. Biotinylated probe **3**.

2.5 Experimental

2.5.1 Acid Stability Study of GPP

500 μL of 1.0 mM solution of GPP in 50:50 25 mM NH_4HCO_3/CH_3CN containing 0.2 % TFA was allowed to sit at rt. 50 μL aliquots were removed at prescribed intervals (h) and analyzed by reverse-phase HPLC. A gradient of solvent A (25mM NH_4HCO_3) and solvent B (CH_3CN) and detecting at 214 nm (flow rate, 0.7 mL/min) was employed. Elution was performed by a 40 min linear gradient of 20-80% B. Integration of the peak corresponding to GPP was performed using HPLC software. Hydrolysis half life was determined from a plot of remaining starting material (%) as a function of time.

2.5.2 Acid Stability Study of 3

The same procedure as described for GPP was performed with a 0.30 mM solution of **3** in in 50:50 25 mM NH_4HCO_3/CH_3CN containing 0.2 % TFA.

2.5.3 Purification of PFTase and PGGTase-I

PFTase was purified as described by Mayer et al.[42] and published in our earlier work.[19] PGGTase-I was purified using modifications of published procedures.[23, 43, 44]

2.5.4 Enzyme Inhibition Experiments

The concentration of **3** was varied (0, 0.4, 0.6, 1.5, 3, 4.5, 6 μM) while the natural susbtrate, **1**, and PFTase were maintained at a fixed concentrations (10 μM and 11 nM). Enzymatic rates were obtained from linear regression analysis of the time-dependent fluorescence emission data using the fluorimeter software and the IC_{50} was calculated from a plot of the enzymatic rate versus concentration of **3**.

2.5.5 X-Ray Crystallography Studies

Crystals of the PFTase:**3** complex was prepared by soaking **3** into preformed crystals using methods previously described.[34] X-ray diffraction data for the PFTase:**3** complex was collected on a Rigaku rotating anode generator equipped with osmic mirrors and a Raxis-IV image plate detector. With the detector set at 150 mm, data were collected in 323 contiguous 0.30° oscillation images each exposed for 8 minutes. The data extend to 2.2 Å resolution and have a R_{merge} of 4.6% with a 5.8-fold multiplicity . The structure was refined using CNX2002 (Accelrys Inc.) to an R_{factor} of 18.3% and an R_{free} of 21.9%.

2.5.5 Photolysis Reaction of Protein Prenyltransferases with [^{32}P]3

All reactions (100 μL) were performed in siliconized quartz test tubes (10 x 75 mm) and contained 52 mM Tris-HCl (pH 7.5), 5.8 mM DTT, 12 mM $MgCl_2$, 12 μM $ZnCl_2$, 25 mM NH_4HCO_3, 10 μM [^{32}P]**3** (~10 fold above IC_{50} value) and 400 nM pure enzyme (PFTase, PGGTase-I) or 21.2 μg of partially purified (after ion-exchange FPLC) protein sample containing PGGTase-I. For substrate protection experiments, FPP or GGPP was added to a final concentration of 100 μM. Reactions were photolyzed for 2 h at 4 ºC using a Rayonet Mini-Reactor fitted with 6X 350 nm bulbs and a spinning platform. Samples were spun to ensure an even exposure to the light. Loading buffer (100 μL) was then added to each sample and samples were heated to 100 ºC for 3 min followed by analysis with 12% Tris-Glycine SDS-polyacrylamide gel electrophoresis. Gels were stained with Sypro®-orange and subjected to ^{32}P-phosphorimaging at rt.

2.5.6 Preparation of *Hevea Brasiliensis* Washed Rubber Particles

H. brasiliensis WRPs used in this study were prepared as previously described by R. Krishnakumar et al.[46] and Cornish et al.[47]

2.5.7 Photolysis Reaction of *Hevea Brasiliensis* Washed Rubber Particles with [^{32}P]3

All reactions (~100 μL) were performed in siliconized quartz test tubes (10 x 75 mm) and contained 0.1 M Tris-HCl (pH 7.5), 1.25 mM $MgSO_4$, 5 mM DTT, 10 μM [^{32}P]**3** and

one *H. brasiliensis* WRP (35-40 μL/particle, 4.51 μg protein/μL). For substrate protection experiments, FPP was added to a final concentration of 100 μM. Reactions were photolyzed for 6 h using the apparatus described above. Loading buffer (50 μL) was then added to each sample and samples were heated to 100 ºC for 3 min followed by gel analysis as described above.

2.5.8 Tryptic Digest of Labeled Proteins from Photolysis Reaction of *Hevea Brasiliensis* Washed Rubber Particles with [^{32}P]3

Proteins from previously described photolysis reaction (no SDS-PAGE analysis) were extracted with 5 mL of sequential extraction reagent (5.0 M urea, 2.0 M thiourea, 2.0% CHAPS, 2% SB-3-10, 40 mM Tris, and 0.2% Bio-Lyte 3 to 10 ampholyte). Samples were incubated in this buffer for 1 h at rt with constant rocking, and then centrifuged at max speed in a microcentrifuge for 15 min. The supernatant was then transferred to 50 mL conical tube and 4 volumes of cold acetone were added. Acetone precipitated protein pellets were washed twice with 80% acetone in water. Pellets were dried under N_2 and prepared for fractionation using the ZOOM IEF fractionator according to manufacturer's instructions. After IEF fractionation, samples from the different pH ranges were acetone precipitated as described above. Samples were then dissolved in 45 μL Laemmli sample buffer (0.06 M Tris-HCl pH 6.8, 0.01% bromophenol blue, 1.5% SDS, 10% glycerol) and analyzed by SDS-PAGE using 4-20% gradient gel. Gels were stained with Coomassie and subjected to ^{32}P-phosphorimaging at rt. Radiolabeled protein bands were excised using pipette tip (3 spots from each band). For tryptic digestion of proteins, samples were

reduced and alkylated using 10 mM dithiothreitol and 100 mM iodoacetamide in water, then digested with 100 ng of trypsin in 25mM NH_4HCO_3.

2.5.9 Mass Spectral Analysis of Labeled Proteins

Samples from tryptic digestion were spotted onto a MALDI target and eluted with 70% CH_3CN, 0.2% formic acid containing 5 mg/mL MALDI matrix (α-cyano-4-hydroxycinnamic acid). A 0.5 μL drop was then spotted onto the MALDI target. Analysis was performed using an Applied Biosystems 4700 Proteomics Analyzer with TOF/TOF Optics. MALDI-MS data was acquired in reflector mode from a mass range of 700 – 4000 Daltons and 1250 laser shots were averaged for each mass spectrum. Each sample was internally calibrated using the trypsin autolysis products (m/z of 842.51 and 2211.10) as internal standards. The eight most intense ions from the MS spectrum were then subjected to MS/MS analysis. The mass range was 70 to precursor ion with a precursor window of -1 to 3 Daltons with an average 5000 laser shots for each spectrum. A peak list was created by GPS Explorer software (Applied Biosystems) from the raw data based on signal to noise filtering and included de-isotoping. The resulting file was then searched by MASCOT (Matrix Science) using user specified databases. A tolerance of 20 ppm was used if the sample was internally calibrated and 200 ppm tolerance if the default calibration was applied. Protein identification was validated by the following criteria: greater than 20 ppm mass accuracy on all MS ions and all ions in at least two MS/MS spectra, which were not modified, had to be accounted for.

2.6 References

1. Backhaus, R. A., Rubber formation in plants - a mini-review. *Isr. J. Bot.* **1985,** *34*, 283-293.

2. Bonner, J., Effects of temperature on rubber accumulation by the guayule plant. *Bot. Gaz.* **1943,** *105*, 233-243.

3. Madhavan, S.; Greenblatt, G. A.; Foster, M. A.; Benedict, C. R., Stimulation of isopentenyl pyrophosphate incorporation into polyisoprene in extracts from guayule plants (Parthenium argentatum Gray) by low temperature and 2-(3,4-dichlorophenoxy)triethylamine. *Plant Physiol.* **1989,** *89*, 506-511.

4. Whitworth, J. W. W., E.E., *Guayule natural rubber: a technical publication with emphasis on recent findings*. Office of Arid Land Studies, The University of Arizona Tucson, Arizona, **1991**; p 445.

5. Veatch, M. E.; Ray, D. T.; Mau, C. J. D.; Cornish, K., Growth, rubber, and resin evaluation of two-year-old transgenic guayule. *Ind. Crops Prod.* **2005,** *22*, 65-74.

6. Cornish, K. C., J.; Chapman, M.H., *Membrane-bound cis-prenyltransferase activity: regulation and substrate specificity*. Wiley-VCH-Verlag: **1998**; p 316-323.

7. Tanaka, Y., Structural characterization of natural polyisoprenes: solve the mystery of natural rubber based on structural study. *Rubber Chem. Technol.* **2001,** *74*, 355-375.

8. Walsh, C., *Enzymatic Reaction Mechanisms*. **1979**; p 978.

9. Archer, B. L.; Audley, B. G., Biosynthesis of rubber. *Adv. Enzymol. Relat. Subj. Biochem.* **1967,** *29*, 221-257.

10. Light, D. R.; Dennis, M. S., Purification of a prenyltransferase that elongates cis-polyisoprene rubber from the latex of *Hevea brasiliensis*. *J. Biol. Chem.* **1989,** *264*, 18589-18597.

11. Archer, B. L. A., B.G., New aspects of rubber biosynthesis. *Bot. J. Linn. Soc.* **1987,** *94*, 181-196.

12. Tanaka, Y., Structure and biosynthesis mechanism of natural polyisoprene. *Prog. Polym. Sci.* **1989,** *14*, 339-371.

13. Tanaka, Y.; Aik-Hwee, E.; Ohya, N.; Nishiyama, N.; Tangpakdee, J.; Kawahara, S.; Wititsuwannakul, R., Initiation of rubber biosynthesis in *Hevea brasiliensis*: characterization of initiating species by structural analysis. *Phytochemistry* **1996,** *41*, 1501-1505.

14. Cornish, K., Similarities and differences in rubber biochemistry among plant species. *Phytochemistry* **2001,** *57*, 1123-1134.

15. Cornish, K., Biochemistry of natural rubber, a vital raw material, emphasizing biosynthetic rate, molecular weight and compartmentalization, in evolutionarily divergent plant species (1963 to 2000). *Nat. Prod. Rep.* **2001,** *18*, 182-189.

16. Cornish, K. S., D.J.; Grosjean, O-K.; Goodman, N., Fundamental similarities in rubber particle architecture and function in three evolutionarily divergent plant species. *J. Nat. Rubb. Res.* **1993,** *8*, 275-285.

17. Webb, Y.; Zhou, X.; Ngo, L.; Cornish, V.; Stahl, J.; Erdjument-Bromage, H.; Tempst, P.; Rifkind, R. A.; Marks, P. A.; Breslow, R.; Richon, V. M., Photoaffinity labeling and mass spectrometry identify ribosomal protein S3 as a potential target for hybrid polar cytodifferentiation agents. *J. Biol. Chem.* **1999,** *274*, 14280-14287.

18. Zhang, C. X.; Chang, P. V.; Lippard, S. J., Identification of nuclear proteins that interact with platinum-modified DNA by photoaffinity labeling. *J. Am. Chem. Soc.* **2004,** *126*, 6536-6537.

19. Gaon, I.; Turek, T. C.; Weller, V. A.; Edelstein, R. L.; Singh, S. K.; Distefano, M. D., Photoactive analogs of farnesyl pyrophosphate containing benzoylbenzoate esters: synthesis and application to photoaffinity labeling of yeast protein farnesyltransferase. *J. Org. Chem.* **1996,** *61*, 7738-7745.

20. Turek, T. C.; Gaon, I.; Gamache, D.; Distefano, M. D., Synthesis and evaluation of benzophenone-based photoaffinity labeling analogs of prenyl pyrophosphates containing stable amide linkages. *Bioorg. Med. Chem. Lett.* **1997,** *7*, 2125-2130.

21. Turek-Etienne, T. C.; Strickland, C. L.; Distefano, M. D., Biochemical and structural studies with prenyl diphosphate analogues provide insights into isoprenoid recognition by protein farnesyl transferase. *Biochemistry* **2003,** *42*, 3716-3724.

22. Gaon, I.; Turek, T. C.; Distefano, M. D., Farnesyl and geranylgeranyl pyrophosphate analogs incorporating benzoylbenzyl ethers: synthesis and inhibition of yeast protein farnesyltransferase. *Tet. Lett.* **1996,** *37*, 8833-8836.

23. Omer, C. A.; Kral, A. M.; Diehl, R. E.; Prendergast, G. C.; Powers, S.; Allen, C. M.; Gibbs, J. B.; Kohl, N. E., Characterization of recombinant human farnesyl-protein transferase: cloning, expression, farnesyl diphosphate binding, and functional homology with yeast prenyl-protein transferases. *Biochemistry* **1993,** *32*, 5167-5176.

24. Turek, T. C.; Gaon, I.; Distefano, M. D.; Strickland, C. L., Synthesis of farnesyl diphosphate analogues containing ether-linked photoactive benzophenones and their application in studies of protein prenyltransferases. *J. Org. Chem.* **2001,** *66*, 3253-3264.

25. Yokoyama, K.; McGeady, P.; Gelb, M. H., Mammalian protein geranylgeranyltransferase-I: substrate specificity, kinetic mechanism, metal requirements, and affinity labeling. *Biochemistry* **1995,** *34*, 1344-1354.

26. Dorman, G.; Prestwich, G. D., Benzophenone photophores in biochemistry. *Biochemistry* **1994,** *33*, 5661-5673.

27. Marecak, D. M.; Horiuchi, Y.; Arai, H.; Shimonaga, M.; Maki, Y.; Koyama, T.; Ogura, K.; Prestwich, G. D., Benzoylphenoxy analogs of isoprenoid diphosphates as photoactivatable substrates for bacterial prenyltransferases. *Bioorg. Med. Chem. Lett.* **1997,** *7*, 1973-1978.

28. Zhang, Y. W.; Koyama, T.; Marecak, D. M.; Prestwich, G. D.; Maki, Y.; Ogura, K., Two subunits of heptaprenyl diphosphate synthase of *Bacillus subtilis* form a catalytically active complex. *Biochemistry* **1998,** *37*, 13411-13420.

29. Blau, N. F. W., T.S.; Buess, C.M., Potential Inhibitors of cholesterol biosynthesis. Phosphonates derived from geraniol and congeners. *J. Chem. Eng. Data* **1970,** *15*, 206-208.

30. Popjak, G.; Hadley, C., Inhibition of liver prenyltransferase by citronellyl and geranyl phosphonate and phosphonylphosphate. *J. Lipid Res.* **1985,** *26*, 1151-1159.

31. Zgani, I.; Menut, C.; Seman, M.; Gallois, V.; Laffont, V.; Liautard, J.; Liautard, J.-P.; Criton, M.; Montero, J.-L., Synthesis of prenyl pyrophosphonates as new potent phosphoantigens inducing selective activation of human Vg9Vd2 T lymphocytes. *J. Med. Chem.* **2004,** *47*, 4600-4612.

32. Bartlett, D. L.; King, C. H. R.; Poulter, C. D., An affinity column for the purification of prenyltransferases. *Anal. Biochem.* **1985,** *149*, 507-515.

33. Sagami, H.; Morita, Y.; Ogura, K., Purification and properties of geranylgeranyl-diphosphate synthase from bovine brain. *J. Biol. Chem.* **1994,** *269*, 20561-20566.

34. Strickland, C. L.; Weber, P. C.; Windsor, W. T.; Wu, Z.; Le, H. V.; Albanese, M. M.; Alvarez, C. S.; Cesarz, D.; del Rosario, J.; Deskus, J.; Mallams, A. K.; Njoroge, F. G.; Piwinski, J. J.; Remiszewski, S.; Rossman, R. R.; Taveras, A. G.; Vibulbhan, B.; Doll, R. J.; Girijavallabhan, V. M.; Ganguly, A. K., Tricyclic farnesyl protein transferase inhibitors: crystallographic and calorimetric studies of structure-activity relationships. *J. Med. Chem.* **1999,** *42*, 2125-2135.

35. Strickland, C. L.; Windsor, W. T.; Syto, R.; Wang, L.; Bond, R.; Wu, Z.; Schwartz, J.; Le, H. V.; Beese, L. S.; Weber, P. C., Crystal structure of farnesyl protein transferase complexed with a CaaX peptide and farnesyl diphosphate analogue. *Biochemistry* **1998,** *37*, 16601-16611.

36. Bartlett, D. L.; King, C. H.; Poulter, C. D., Purification of farnesylpyrophosphate synthetase by affinity chromatography. *Methods Enzymol.* **1985,** *110*, 171-184.

37. Turek, T. C.; Gaon, I.; Distefano, M. D., Synthesis and rapid purification of 32P-labeled photoactive analogs of farnesyl pyrophosphate. *J. Labelled Comp. Radiopharm.* **1997,** *39*, 139-146.

38. Yeang, H. Y.; Cheong, K. F.; Sunderasan, E.; Hamzah, S.; Chew, N. P.; Hamid, S.; Hamilton, R. G.; Cardosa, M. J., The 14.6 kd rubber elongation factor (Hev b 1) and 24 kd (Hev b 3) rubber particle proteins are recognized by IgE from patients with spina bifida and latex allergy. *J. Allergy Clin. Immun.* **1996,** *98*, 628-639.

39. Dennis, M. S.; Light, D. R., Rubber elongation factor from *Hevea brasiliensis*. Identification, characterization, and role in rubber biosynthesis. *J. Biol. Chem.* **1989,** *264*, 18608-18617.

40. Durauer, A.; Csaszar, E.; Mechtler, K.; Jungbauer, A.; Schmid, E., Characterisation of the rubber elongation factor from ammoniated latex by electrophoresis and mass spectrometry. *J. Chrom. A* **2000,** *890*, 145-158.

41. Dennis, M. S.; Henzel, W. J.; Bell, J.; Kohr, W.; Light, D. R., Amino acid sequence of rubber elongation factor protein associated with rubber particles in Hevea latex. *J. Biol. Chem.* **1989,** *264*, 18618-18626.

42. Mayer, M. P.; Prestwich, G. D.; Dolence, J. M.; Bond, P. D.; Wu, H. Y.; Poulter, C. D., Protein farnesyltransferase: production in Escherichia coli and immunoaffinity purification of the heterodimer from *Saccharomyces cerevisiae*. *Gene* **1993,** *132*, 41-47.

43. Stirtan, W. G.; Poulter, C. D., Yeast protein geranylgeranyltransferase type-I: overproduction, purification, and characterization. *Arch. Biochem. Biophys.* **1995,** *321*, 182-190.

44. Zhang, F. L.; Diehl, R. E.; Kohl, N. E.; Gibbs, J. B.; Giros, B.; Casey, P. J.; Omer, C. A., cDNA cloning and expression of rat and human protein geranylgeranyltransferase type-I. *J. Biol. Chem.* **1994,** *269*, 3175-3180.

Chapter 3. Caged substrate analogues as tools to study the mechanism and in vivo consequences of protein prenylation

3.1 Introduction

Mutated Ras proteins have been implicated in 30% of all human cancers, with the highest frequencies being K-Ras in pancreatic (90%), colorectal (50%), and lung (30%) cancer.[1] Farnesylation of Ras proteins is essential for communication with its downstream effectors and hence, its oncogenic properties[2]. The geranylgeranylated Rho proteins have also been implicated in malignant transformation[3] thus prompting the creation of PGGTase-I inhibitors.[4] Following these discoveries, research efforts focused on developing inhibitors of PFTase in an attempt to thwart Ras-induced cancer as well as inhibitors of PGGTase-I. To date, there are two RPFTase inhibitors in phase II clinical trials and one in phase III, which show modest results[5]. Part of this lack of efficacy is due to the fact that K-Ras is an alternative substrate for PGGTase-I. Upon blocking the farnesylation of K-Ras, it is alternatively geranylgeranylated thus rescuing its oncogenic activity.[6-8] While inhibition of farnesylation is fairly non-toxic, dual inhibition of PGGTase-I and RPFTase is quite toxic.[9]

Another interesting discovery is that, despite being designed for cancers expressing mutated Ras, PFTase inhibitors are also effective in cancers expressing normal Ras[10]. In order to comprehend this interesting phenomenon, a greater understanding of the

prenylation reaction as well as the *in vivo* consequences of protein prenylation is needed. Such knowledge should facilitate the creation of more potent and selective inhibitors.

Photoactivatable, or caged, enzymes and enzyme substrates are well-established tools for the investigation of biological function and catalytic mechanism[11-16]. Using a photocleavable yeast peptide pheromone (α-factor, WHWLQLKPGQPMY), Parker et al. recently demonstrated that the arrest of MATa cells at the G1 stage of division is possible with brief exposure to light[17]. Such control allows for synchronizing yeast cell cultures and investigating signaling processes related to morphogenesis and transcription. Rather and coworkers were able to reversibly inactivate the bacterial Sssl DNA methyltransferase by incorporating a dimethoxynitrobenzyl photolabile group onto an active site cysteine residue[18]. This caged enzyme may be useful for controlling DNA methylation patterns as well as time-resolved structure analysis. One of the earliest examples of the use of a caged enzyme substrate for time-resolved x-ray crystallography is from the work of Schlichting and coworkers[19]. Crystals of H-Ras p21 with nitrophenethyl-caged GTP were used to investigate the conformational changes of p21 upon GTP hydrolysis. Using Laue diffraction methods, they were able to observe the short-lived p21:GTP complex as well as structural changes that occurred in the regions of the enzyme believed to interact with the GTPase-activating protein.

3.2 Research Objectives

To achieve temporal control of prenyltransferase activity, similar to the examples reported above, we have designed a series of photoactivatable substrate analogues.

Described here is the characterization of the first generation of caged protein farnesyltransferase analogues which contain a nitrobenzyl-based photolabile group incorporated at the distal phosphate of the isoprenoid diphosphate substrate or the sulfhydryl side-chain of the cysteine residue in a CAAX peptide substrate.

3.3 Results and Discussion

3.3.1 Caged Isoprenoid Diphosphates

3.3.1.1 Photolysis kinetics

The *o*-nitrobenzyl (NBz) or the dimethoxynitrophenethyl (DMNPE) caging group was installed on the distal phosphate of farnesyl diphosphate (FPP) as described in DeGraw et. al (see Figure 3.1 for structures)[20].

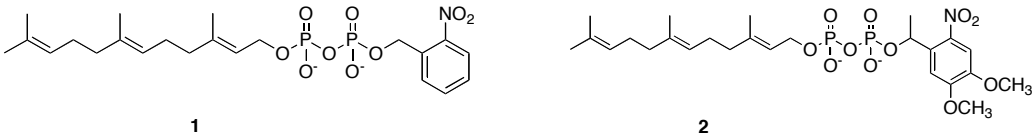

1 **2**

Figure 3.1. Structures of caged isoprenoid diphosphates

Irradiation of **1** and **2** stock solutions with 300-400 nm (λ_{max} = 350nm) light lead to the release of farnesyl diphosphate. The time course of this reaction was followed by RP-HPLC analysis of aliquots removed at varying intervals. The single-photon uncaging efficiencies, Q_{u1}, were determined from the following relationship: $Q_{u1} = (I\sigma t_{90\%})^{-1}$, where I is the irradiation intensity of the setup used in ein•cm^{-2}•s^{-1} (determined by potassium

ferrioxalate actinometry), σ is the decadic extinction coefficient (10^3 ε, molar extinction coefficient) in $cm^{-2} \bullet mol^{-1}$, and $t_{90\%}$ is the irradiation time in seconds for 90% conversion to product. These data are summarized in Table 3.1.

Table 3.1. Photochemical properties of caged analogues described here and related compounds.

Caged Compound	λ_{irrad}	Q_{u1}	**Uncaging Rate (sec)$^{-1}$**
NBz-FPP (**1**)	350	0.70	25.8
DMNPE-FPP (**2**)	350	0.08	7.20
KKKSKTKC(CNBz)VIM (**8**)	350	0.16	0.14
DMNPE-ATP[12]	350	0.07	18.0
DMNPE-Doxycycline[21]	347	0.01	NR
DMNBz-TRβ agonist[22]	366	NR	0.03

λ_{irrad}, wavelength data was obtained at; Q_{u1}, quantum efficiency; NR, not reported; NBz, nitrobenzyl; DMNPE, dimethoxynitrophenethyl; CNBz, α-carboxy-nitrobenzyl; DMNBz, dimethoxynitrobenzyl;

It should be noted that the values for **1** and **2** are comparable to those previously reported for other caged molecules that have been employed in biochemical studies; additionally, our results are also consistent with the previously noted observation that compounds with the nitrobenzyl photolabile group have a greater quantum yield and uncage faster (**1**, k = 0.43 min^{-1}, Q_{u1} = 0.70) than identical compounds incorporating a dimethoxy-nitrophenethyl caging group[14] (**2**, k = 0.12 min^{-1}, Q_{u1} = 0.08).

3.3.1.2 Substrate studies

The specific activity of the yeast PFTase (yPFTase) in the presence of **1** or **2** and their photolysis products was evaluated using a continuous fluorescence assay developed by Pompliano and coworkers[23] to assess their compatibility. Table 3.2 shows the rate of enzymatic prenylation (μM/min) is approximately 14% of its rate with FPP when only **1** is present as the isoprenoid substrate. Once **1** was irradiated for 12 min (~3 times the half-life for uncaging), saturating amounts of FPP were released, based on the total return in enzymatic activity. This result also demonstrates that the byproducts of the photolysis reaction do not interfere with catalysis in any way. Similar results were observed with derivative **2**, although this analogue appears to be a poorer substrate prior to uncaging (7.6% compared with FPP). Substrate reactions were also analyzed by HPLC (see supporting information). The yPFTase catalyzed prenylation resulted in the same prenylated product regardless of whether the FPP source was pure FPP or the product of photolysis of **1** or **2**.

Table 3.2. Activity[a] of yPFTase in the presence of compounds NBz-FPP (**1**) and DMNPE-FPP (**2**).

Substrate	Enzyme activity (μM/min)	Normalized activity (%)
FPP	0.765 + 0.007	100
Compound **1**	0.104 + 0.006	14
Irradiated Compound **1**	0.681 + 0.012	89
Compound **2**	0.058 + 0.001	7.6
Irradiated Compound **2**	0.557 + 0.006	73

[a] When present, FPP and/or caged FPP were each at 10 μM. Given the rate of photolysis, the irradiated samples would be expected to contain 10 μM free FPP and side products. The CAAX peptide substrate is *N*-Dansyl-GCVIA.

There are a number of characteristics that make a caged compound suitable for studying a particular enzyme. It is preferable to perform the photocleavage at wavelengths above 300 nm in order to minimize enzyme inactivation[11]. Additionally, the photochemical byproducts should not interfere with photolysis nor enzyme catalysis. Finally, the caged substrate must be soluble in aqueous media[12]. Caged isoprenoid diphosphates **1** and **2** meet these criteria. In addition, their uncaging kinetics are comparable to many other commercially available and previously reported caged enzyme substrates/inhibitors and signaling molecules (see Table 3.1)[21, 22, 24-27]. Caged ATP (Molecular Probes) has been widely used to study the mechanism of ATPases[25, 26] and the molecular basis of skeletal muscle fiber contraction[24, 27]. Cambridge et. al. developed a dimethoxynitrophenethyl-caged analogue of doxycycline, a known analogue of the

tetracycline gene activation system, and demonstrated its efficacy in spatially restricted photoactivated gene expression[21].

One requirement for caged compounds is that they are truly inactive as substrates for the target enzyme. While analogues **1** and **2** are considerably slower substrates than FPP, they are still processed by the enzyme at measurable rates (14% and 7.6% respectively relative to FPP) thus limiting their utility. As noted above, analogue **1** is a better substrate than compound **2** indicating that rate decreases with increasing steric bulk on the diphosphate moiety. This suggests that it may be possible to further decrease the rate of processing of isoprenoids caged on the diphosphate by employing larger caging groups including 3',5'-dimethoxybenzoin[28], bromohydroxy quinoline[29, 30], or bromohydroxy coumarin[31]; such experiments are currently underway. Nevertheless, these caged FPP analogues may be useful for studies with other FPP-utilizing enzymes or FPP binding proteins. For example, recent work by Das and coworkers has implicated FPP as a transcriptional activator of the thyroid hormone nuclear receptor-β (TRβ)[32]. A photo-caged thyroid hormone receptor analogue, a known agonist of TRβ, has been applied to time-dependent gene expression profiling[22]. Similar experiments with caged-FPP could be used to gain a better understanding of FPP as TRβ agonist. The quantum efficiency and rates of photolysis of caged FPP analogues **1** and **2** are quite comparable to these aforementioned probes, showing their applicability towards a number of biochemical applications including experiments performed in live cells.

3.3.2 Caged CAAX Peptides

Alkylation of the cysteine's thiol group within the CAAX peptide with a nitrobenzyl-based photolabile group offers an alternative means of creating a catalytically caged prenyltransferase substrate. The kinetics of uncaging these substrates were investigated and their interactions with rat PFTase (rPFTase) were studied by a variety of enzymatic assays and x-ray crystallography.

3.3.2.1 Synthesis

Peptides **5** and **6** (Scheme 3.1) were synthesized on resin using an ABI Peptide Synthesizer employing DIC, HOBt coupling chemistry.

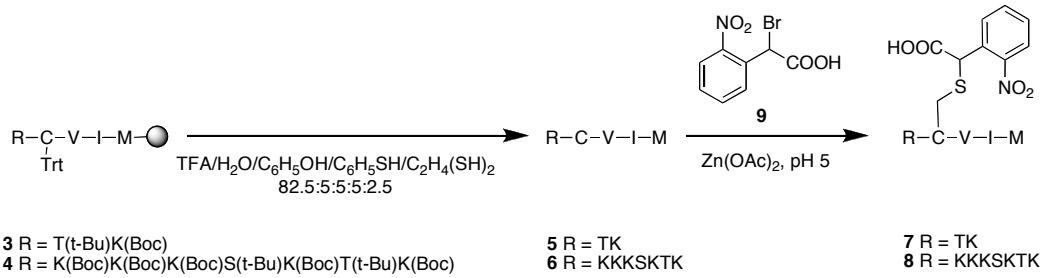

Scheme 3.1. Synthesis of caged peptide substrates.

This peptide sequence was chosen because it is the C-terminal sequence of K-Ras4B, a naturally prenylated mammalian protein implicated in oncogenesis[33]. Upon cleavage from the resin, the cysteine thiol was alkylated with **9** under acidic conditions to form the desired caged analogues **7** and **8**.[34] Stock solutions were made by dissolving in 20 mM Tris-HCl, 10 mM EDTA and stored in the dark at -20°C to minimize oxidation and photodecomposition.

3.3.2.2 Photolysis kinetics

RP-HPLC analysis of an irradiated stock solution of **8** with 300-400 nm light (λ_{max} = 350) at increasing time intervals showed the production of **6**, the parent peptide. A plot of the remaining caged peptide (determined by integration of the peak area in the chromatogram) as a function of irradiation time is shown in Figure 3.2. Non-linear regression analysis using a first-order kinetic model gave a rate constant of 0.14 min^{-1}. Q_{u1}, the corresponding quantum efficiency of uncaging was 0.16 mol*ein^{-1} (Table 3.1).

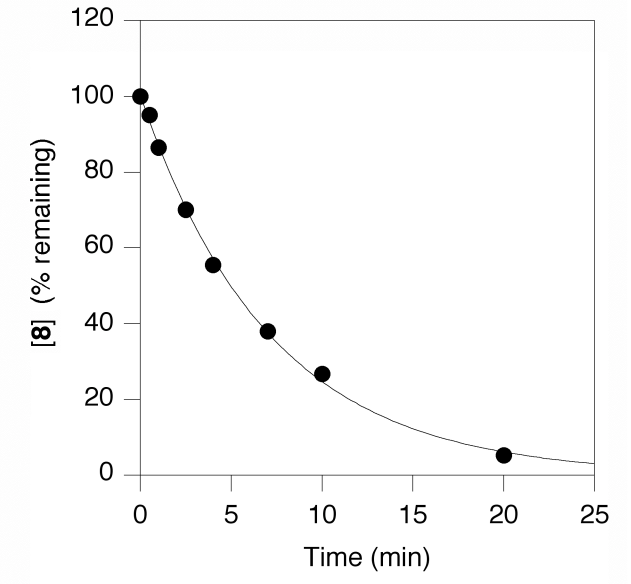

Figure 3.2. Photolysis rate determination for **8**.

3.3.2.3 Substrate studies

A filter binding assay, where the positively-charged amino acids upstream of the CAAX sequence will bind to p81 phosphocellulose paper (Whatman) and incorporation of a prenyl group onto that peptide can be detected through a radiolabel on the isoprenoid

chain[35], was used to evaluate the ability of **8** to act as a rPFTase substrate before and after photolysis. Prior to irradiation with 350 nm light, there is no enzyme catalyzed prenylation of **8** with radiolabeled FPP (Figure 3.3, bottom of bar graph). The amount of tritiated isoprenoid incorporated into the photoreleased peptide is comparable to the amount incorporated into the pure CAAX peptide, **6** (Figure 3.3, top and middle of bar graph).

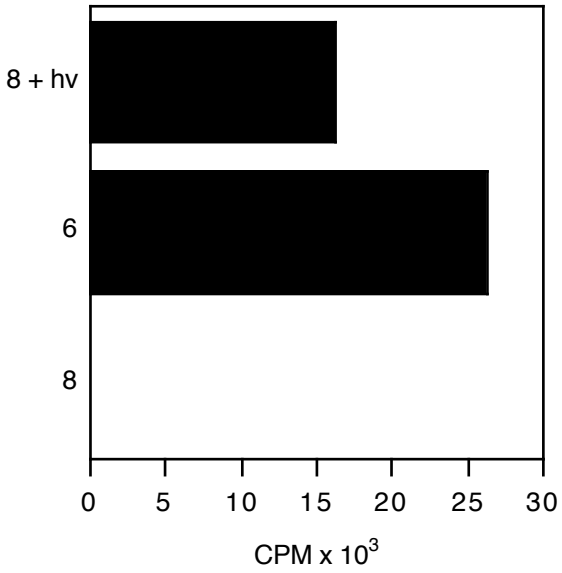

Figure 3.3. PFTase catalyzed prenylation of **8** before and after photolysis with ^{3}H-FPP.

Binding of a caged enzyme substrate prior to photolysis is crucial for time-resolved enzyme experiments. If the caged substrate does not bind, the rate of enzyme reaction initiation is severely limited by diffusion of the released substrate and binding to the active site; in the solid state (i.e. protein crystals) this could be quite slow. Initially, the continuous fluorescence assay using *N*-Dansyl-GCVLS and FPP as the substrates was used to evaluate the ability of **8** to bind to rPFTase. An IC_{50} value of 4.7 $\pm$ 1.8 μM was calculated (Figure 3.4), as compared to 165 nM for the tetrapeptide CVIM[36].

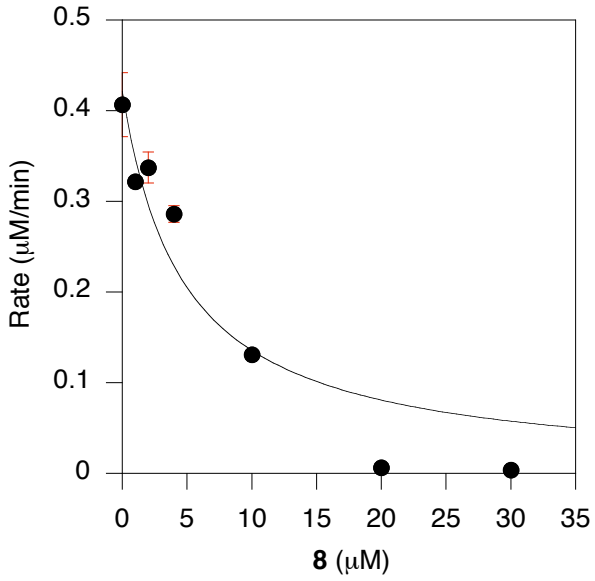

Figure 3.4. Inhibition of PFTase by caged CAAX peptide **8**.

3.3.2.4 X-ray crystallography

While there is a significant decrease in binding ability, the caged CAAX peptide **8** is able to bind the enzyme active site. Next, X-ray crystallography was employed to determine if the isoprenoid diphosphate substrate was able to bind simultaneously with the caged CAAX peptide. Because the upstream residues of the caged CAAX peptide were not critical for obtaining co-crystal of caged CAAX peptide and rPFTase, analogue **7** was utilized for crystallography experiments due to availability. The structure of the rPFTase:FPP:**7** complex was solved at a resolution of 2.7 Å, and is shown in Figure 3.5; a superposition with an uncaged CAAX peptide is shown (panel B) for comparison.

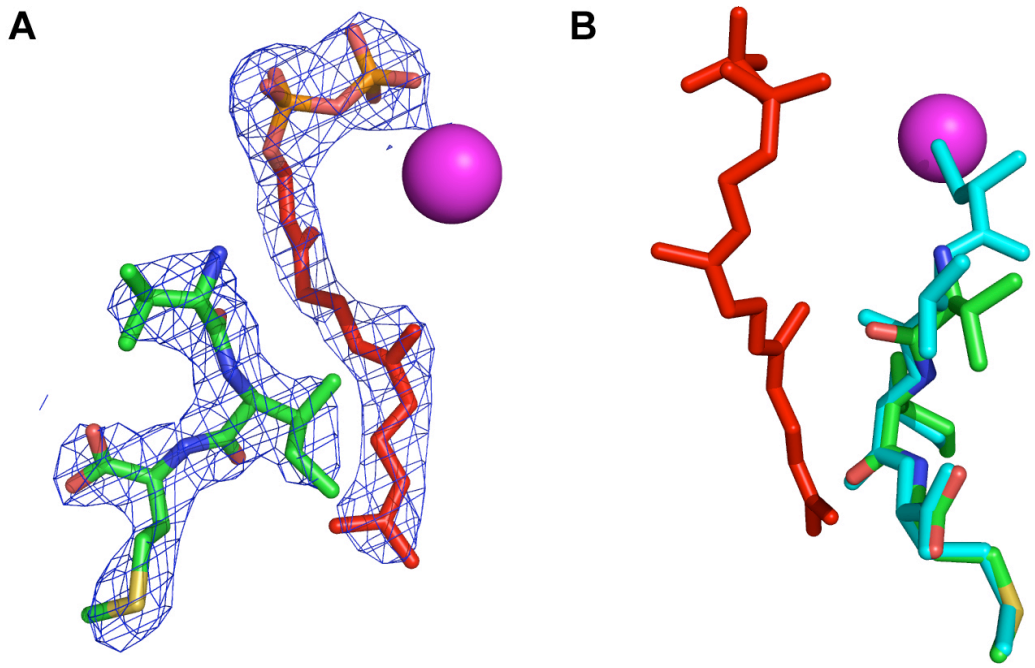

Figure 3.5. Crystallographic analysis of analogue **7** and FPP bound to rPFTase. (A, left image): 2Fo-Fe electron density map of **7** and FPP contoured at 1.5σ. (B, right image): Superposition of **7** and VIM peptide. Analogue **7** is shown in green (carbon), red (oxygen), blue (nitrogen), and yellow (sulfur). **7** is shown in red. The CVIM peptide is shown in cyan. The Zn atom in the enzyme active site is in pink.

The electron density map clearly indicates that both **7** and FPP are bound in the enzyme active site (Figure 3.5, panel A). Comparison of the protein structures from rPFTase:FPP:**7** and rPFTase:FPT-II:CVIM (PDB 1D8D) complexes shows a 0.174 Å rms deviation. Focusing in on an 8 Å sphere surrounding the substrate binding pocket, the rms deviation increases to 0.203 Å. Taken together, these data indicate that no significant movement of the protein side chains, including those needed for catalysis, has occurred. The VIM residues of **7** are essentially superimposable with those in the ternary complex (PDB 1D8D), demonstrating that the alkylation of the cysteine residue with the carboxynitrobenzyl caging group does not affect the position of the C-terminal residues.

The N-terminal residues of **7**, including the caged cysteine, are disordered and thus not visible in the electron density map. This suggests that **7** can adopt many different binding conformations due to the loss of the strong thiolate-Zn interaction (due to S-alkylation) that normally restricts movement of the cysteine residue within the substrate peptide. The FPP that is bound in the presence of **7** occupies the isoprenoid binding pocket of the active site. The first isoprene unit of FPP is slightly rotated (0.546 Å rms deviation calculated over all FPP atoms, PDB 1KZO), while the diphosphate and second two isoprene units are superimposable. In conclusion, the incorporation of a caging moiety at the cysteine residue of the CAAX peptide does not invoke major changes in the binding capacity or conformation of either enzyme substrate or the protein itself.

Alkylation of the thiol present in peptide **5** with a α-carboxy-nitrobenzyl group yielded a caged molecule (**7**) that was not processed by the enzyme at any detectable level although it retained the ability to bind to the enzyme. The tripeptide substructure VIM of **7** bound in a manner indistinguishable from the unmodified peptide CVIM. However, based on the IC_{50} value for **8** compared to that for the unalkylated precursor CVIM, the caged molecule binds approximately 30-fold less. Thus, the caged substrates **7** and **8** and related analogues possess all the requisite features necessary for a variety of investigations where temporal control of initiation of the reaction catalyzed by rPFTase is required including time-resolved x-ray crystallography and analysis of prenylation reactions in living cells.

3.4 Conclusions and Future Directions

The molecules described here are the first examples of caged forms of isoprenoid diphosphates as well as the first documented caged substrate for a bisubstrate enzyme that is capable of binding simultaneously with the other substrate. Kinetic studies of caged isoprenoid diphosphates NBz-FPP (**1**) and DMNPE-FPP (**2**) demonstrated that they are poor substrates for yPFTase but efficiently release FPP upon irradiation that can be utilized for catalysis. Given the plethora of enzymes that use FPP as a substrate, including the diverse family of sesquiterpene cyclases, these probes should be useful for a variety of studies. The caged CAAX peptide (**7** or **8)** photoreleases the parent peptide with similar kinetics to the caged isoprenoid diphosphates **1** and **2**. While caged, the CAAX peptide does not function as a substrate, but is able to bind with efficient capacity and nearly identical conformation as compared to the photoreleased peptide and does not interfere with the binding of the isoprenoid diphosphate substrate. These results open the door to a wide variety of experiments where temporal control is necessary. A number of such experiments are currently underway in the Distefano laboratory.

3.5 Experimental

3.5.1 Photolysis rate and quantum efficiency of NBz-FPP (1) and DMNPE-FPP (2)

A solution of **1** (0.1 mM in 25 mM NH_4HCO_3) in siliconized quartz tubes (10 x 75 mm) was irradiated with 350 nm light from a UV Rayonet mini-reactor (8 x 4 watt bulbs with spectral distributions from 300-400 nm, λ_{max} 350nm) fitted with a spinning platform, holding samples 1 cm from bulbs. The duration of irradiation ranged from 0.25 to 16 min.

After each period of irradiation, a 300 μL aliquot of the solution was removed for analysis by RP-HPLC. Aliquots were flash frozen in liquid N_2 and stored at -20°C until analyzed. The compound was eluted with a gradient of 25 mM NH_4HCO_3 in H_2O and CH_3CN (gradient 0.3%/mL, flow rate 1 mL/min). Absorbance was detected at 248 nm. Photodecomposition curves were plotted in Kaleidagraph 3.0 and analyzed by non-linear regressional analysis (first-order kinetics). Quantum efficiency, Q_{u1} were determined from the relationship $Q_{u1} = (I\sigma t_{90\%})^{-1}$, where I is the irradiation intensity in ein•cm^{-2}•s^{-1}, σ is the decadic extinction coefficient (10^3 times ε, molar extinction coefficient) in cm^2•mol^{-1}, and $t_{90\%}$ is the irradiation time in seconds for 90% conversion to product[30]. The UV intensity of the lamps in the mini-reactor was measured using potassium ferrioxalate actinometry using the same apparatus[37]. The same procedure was used for DMNPE-FPP, **2**.

3.5.2 Purification of yPFTase

yPFTase was purified as described by Mayer et al.[38] and published in our earlier work[39]

3.5.3 yPFTase substrate studies with NBz-FPP (1)

Photolysis of a 100 μL solution of **1** (230 μM) and yPFTase (550 nM in) in a siliconized quartz test tube (10 x 75mm) was conducted for 12 min (~3 times the half-life, $t_{1/2}$ = 3.60 min) at 4 ºC in a UV Rayonet mini-reactor fitted with six RMR-3500Å lamps and a circulating platform. The sample was spun to ensure equal distribution of

irradiation. The yPFTase catalysis rates were determined using a continuous fluorescence assay[23, 40]. A solution containing *N*-Dansyl-GCVIA was prepared by dissolving solid peptide in buffer (20 mM Tris-HCl, pH 7.0 and 10 mM EDTA) and its concentration was determined by UV absorbance at 340 nm using *N*-Dansyl glycine as a standard. FPP was prepared either by diluting a purchased solution (Aldrich) in 7:3 25mM NH_4OH:MeOH or obtained from photolysis reactions. yPFTase was prepared by diluting purified enzyme with buffer (52 mM Tris-HCl, pH 7.0, 5.8 mM DTT, 12 mM $MgCl_2$, 12 μM $ZnCl_2$) containing **1** mg/mL bovine serum albumin. Assay solutions contained 50 mM Tris-HCl, pH 7.5, 10 mM $MgCl_2$, 10 μM $ZnCl_2$, 5.0 mM DTT, 0.04% (w/v) *n*-dodecyl-β-D-maltoside, 2.4 μM *N*-Dansyl-GCVIA, and FPP (10 μM) or 1 (12.7 μL of 0.29 mM stock solution or 22.7 μL of irradiated **1** + yPFTase solution). The assay solution was placed in a quartz cuvette, equilibrated at 30 ºC for 5 min, initiated by the addition of yPFTase or irradiated **1** + yPFTase, and monitored spectrofluorimetrically (340 nm excitation and 505 nm emission, 10 nm slit widths). Enzymatic rates were obtained from linear regression analysis of the time-dependent fluorescence emission data using the fluorimeter software.

3.5.4 yPFTase substrate studies with DMNPE-FPP (2)

A similar procedure as described for **1** was employed, except for the following: Photolysis of a 100 μL solution of **2** (190 μM) and yPFTase (550 nM) in a siliconized quartz test tube (10 x 75mm) was conducted for 15 min (~3 times the half-life, $t_{1/2}$ = 5.82 min). Assay solutions contained 50 mM Tris-HCl, pH 7.5, 10 mM $MgCl_2$, 10 μM $ZnCl_2$,

5.0 mM DTT, 0.04% (w/v) *n*-dodecyl-β-D-maltoside, 2.4 μM *N*-Dansyl-GCVIA, and FPP (10 μM) or **2** (17.5 μL of 0.40 mM stock solution or 27.5 μL of irradiated **2** + yPFTase solution).

3.5.5 Construction of *r*FPTase *E. coli* expression vector, pRFT529

We have designed a new *E. coli* expression construct for production of recombinant rPFTase using the pCDF-Duet1 vector (Novagen). pCDF-Duet1 is ideal for robust co-expression of heterodimeric proteins or protein complexes, as it contains two multiple cloning sites (MCSI and II) under the control of separate IPTG-inducible T7 promoters. The gene encoding the alpha subunit of rPFTase was excised from a pUC13-rPFTalpha construct (American Type Culture Collection) using EcoRI and HindIII restriction enzymes (all restriction enzymes were obtained from New England Biolabs) and subcloned into MCSI of pCDF-Duet1 at the same restriction sites. The vector encodes an N-terminal His_6 tag at this MCS, and the Stratagene Quikchange site-directed mutagenesis kit was used to bring the ligated insert in-frame with the His_6 tag. Mutagenesis primer sequences were 5'-ATCACCATCATCACCACAAGCCAGGATCCGAATTC-3' and 5'-GAATTCGGATCCTGGCTTGTGGTGATGATGGTGAT-3'. The resulting affinity tag and linker amino acid sequence N-terminal to the wild-type rPFTase alpha subunit sequence is MGSSHHHHHHKPGSEFELAPADGGE. The beta subunit of rPFTase was amplified using the high fidelity Platinum *Pfx* DNA polymerase (Invitrogen) according to the manufacturer's suggested protocol from a pAlter-Ex2 construct containing the gene

that was a kind gift of Dr. Patrick Casey's laboratory at Duke University[41]. The rPFT beta forward primer sequence including an NdeI restriction site (underlined) was 5'-GACCTGATACATATGGCTTCTTCGAGTTCCTTCACCTATTATTGTCC-3', and the reverse primer sequence including the AvrII restriction site (underlined) 5'-GTAAGCCCTAGGGCTAGTCAGTGGCAGGATCTGAGGTCACC-3'. The insert was then subcloned into MCSII of pCDF-Duet1 using the NdeI and AvrII restriction sites. All DNA sequencing to confirm the error-free construction of the rPFTase expression vector was performed by the Duke University Medical Center DNA Analysis Facility.

3.5.6 Purification of rPFTase

Competent BL21(DE3) *E. coli*. (Novabiochem) were transformed with the pRFT529 according to manufacturers protocol, using streptomycin (50 μg/mL) as the selection antibiotic. A single colony was used to inoculate 100 mL LB media containing 50 μg/mL streptomycin. Cells were grown at 37 °C for 18 h, shaking at 250 rpm. 10 mL of the overnight culture was used to inoculate 1 L of LB media containing 50 μg/mL streptomycin. Cells were grown at 37 °C (250 rpm shaking) until an OD_{600} of 1.3 was reached. IPTG at a final concentration of 1.0 mM and 0.5 mM $ZnSO_4$ were added to induce rPFTase expression. Cells were grown for an additional 4 h at 37 °C (250 rpm shaking) and harvested by centrifugation at 5,000 × *g* (4 °C) for 10 min. The cell pellet from 1 L of growth (~15 g) was resuspended in 100 mL of lysis buffer containing 50 mM Tris pH 7.7, 200 mM NaCl, 5.0 μM $ZnCl_2$, 5.0 mM $MgCl_2$, 20 mM imidazole, 1.0 mM β-mercaptoethanol, and Sigma protease inhibitor cocktail (EDTA free). Cells were lysed by

sonication for 5 min (10 sec on, 10 sec off). Cell debris was removed by centrifugation at 26,000 × *g* (4 °C) for 1 h. Supernatant was loaded onto a Ni-NTA chelating column (15 mL resin bed) pre-equilibrated in 50 mM Tris pH 7.7, 200 mM NaCl, 5.0 μM $ZnCl_2$, 5.0 mM $MgCl_2$, 20 mM imidazole and 1.0 mM β-mercaptoethanol. The column was washed with a solution of 50 mM Tris pH 7.7, 200 mM NaCl, 5.0 uM $ZnCl_2$, 5.0 mM $MgCl_2$, 20 mM imidazole and 1.0 mM β-mercaptoethanol and monitored by absorbance at 280 nm. Bound proteins were then eluted with 50 mM Tris pH 7.7, 200 mM NaCl, 5.0 μM $ZnCl_2$, 5.0 mM $MgCl_2$, 250 mM imidazole and 1.0 mM β-mercaptoethanol. Fractions containing active enzyme (determined with a continuous fluorescence assay[23, 40]) were pooled and the salt concentration was adjusted by adding an equivalent volume of 20 mM Tris-HCl pH 7.7, 1.0 M $(NH_4)_2SO_4$, 5.0 μM $ZnCl_2$, and 1.0 mM DTT slowly (over 5 min) while stirring. The solution was left to incubate at 4 °C for 15 min without stirring. The solution was then filtered (0.45 μM filter) and applied to a Phenyl Sepharose column (15 mL resin bed) pre-equilibrated in 20 mM Tris-HCl pH 7.7, 500 mM $(NH_4)_2SO_4$, 5.0 μM $ZnCl_2$, and 1.0 mM DTT (Buffer A). Enzyme was then eluted from the column using a linear gradient of 0-100% Buffer B (20 mM Tris-HCl pH 7.7, 5.0 uM $ZnCl_2$, and 1.0 mM DTT). Active enzyme eluted at 100% B. Active fractions (based on continuous fluorescence assay[23, 40]) were then pooled and concentrated used Millipore Centricon centrifuge tubes (10 kDa MWCO) and centrifugation at 4,000 × *g* for 70 min. Glycerol was added to a final concentration of 40% (v/v) to stabilize the enzyme for long term storage at -80 °C.

3.5.7 General procedure for peptide synthesis

The linear sequences were assembled by automated Fmoc SPPS, starting with Wang resin, using an ABI 430 synthesizer. DIC and HOBt were used for coupling to avoid racemization of cysteine[42]. The peptide was cleaved with Reagent K[43] (TFA, phenol, thioanisole, water, ethanedithiol 82.5:5:5:5:2.5) for 2 h, precipitated with Et_2O, and centrifuged to form a pellet, which was washed with Et_2O. The crude peptide was purified by RP-HPLC.

3.5.7.1 TKCVIM (5)

Yield 200 mg. Purity >95% by RP-HPLC. Deconvoluted ESI-MS calcd 694.4; found 694.4.

3.5.7.2 KKKSKTKCVIM (6)

Yield 130 mg. Purity >95% by RP-HPLC. Deconvoluted ESI-MS calcd 1293.8; found 1293.7.

3.5.8 General procedure for cysteine alkylation

Peptide (1.0 eq) and $Zn(OAc)_2 \cdot 2H_2O$ (5.0 eq) were dissolved in MeOH/0.1 M NaOAc pH 5 (4:1, v/v) (2.0 mL solvent per 1.0 mg peptide). Carboxynitrobenzyl bromide[44] (5.0

eq) was then added. The reaction was monitored by RP-HPLC, and once judged complete (typically 24 h), was filtered, and purified by RP-HPLC.

3.5.8.1 TKC(CNBz)VIM (7)

Reaction scale: 100 mg peptide. Yield: ~7 mg. Purity >95% by RP-HPLC. Deconvoluted ESI-MS calcd 873.4; found 873.3.

3.5.8.2 KKKSKTKC(CNBz)VIM (8)

Reaction scale: 100 mg peptide. Yield ~9 mg. Purity >90% by RP-HPLC. Deconvoluted ESI-MS calcd 1472.8; found 1472.6.

3.5.9 Photolysis rate and quantum efficiency of KKKSKTKC(CNBz)VIM (8)

A solution of **8** (1 mM in 20 mM NH_4HCO_3, 10 mM EDTA) in siliconized quartz tubes (10 x 75 mm) was irradiated with 350 nm light from a UV Rayonet reactor (16 x 14 watt bulbs with spectral distributions from 300-400 nm, λ_{max} 350nm) fitted with a spinning platform, holding sample 1 cm from bulbs. The duration of irradiation ranged from 0.5 to 20 min. After each period of irradiation, a 150 μL aliquot of the solution was removed for analysis by RP-HPLC. Aliquots were flash frozen in $N_2(l)$ and stored at -20 °C until analyzed. The compound was eluted with a gradient of 0.1% TFA in H_2O and 0.1% TFA in CH_3CN (gradient 1%/mL, flow rate 1 mL/min). Absorbance was detected at 220 nm.

Photodecomposition curves were plotted in Kaleidagraph 3.0 and analyzed by non-linear regressional analysis (first-order kinetics). Quantum efficiency, Q_{u1}, was determined as described for **1**.

3.5.10 rPFTase substrate studies with KKKSKTKC(CNBz)VIM (8)

A solution containing **8** or **6** (KKKSKTKCVIM) was prepared by dissolving solid peptide in buffer (20 mM Tris-HCl, pH 7.0 and 10 mM EDTA) and its concentration was estimated by mass. Photolysis of a 20 μL solution of **8** (10 μM) in a siliconized quartz test tube (10 x 75mm) was conducted for 15 min (~3 times the half-life, $t_{1/2}$ = 4.9 min) at 4 ºC in a UV Rayonet mini-reactor fitted with sixteen RPR-3500Å lamps and a circulating platform. The sample was spun to ensure equal distribution of irradiation. ^{3}H-FPP was used as purchased from American Radiolabeled Chemicals (25 μM in 70% EtOH/25 mM aqueous NH_4HCO_3, 20 Ci/mmol). Assay solutions contained 50 mM Tris-HCl, pH 7.5, 10 mM $MgCl_2$, 10 μM $ZnCl_2$, 5.0 mM DTT, 4 μM ^{3}H-FPP, and **8** (2.0 μM), irradiated **8** (2.0 μM), or **6** (2.0 μM). The reaction was initiated by addition of rPFTase (4 mg/mL) and incubated at 35 °C for 60 min. Eppendorf tubes containing reaction mixture were kept on ice for 2 min, centrifuged (10 s at 1,000 rpm), and the total reaction mixture was spotted onto p81 phosphocellulose paper (Whatman). After 10 min of air drying, each paper was placed on a Millipore 1225 Sampling Manifold and washed first with 1.0% aqueous trichloroacetic acid solution (2 x 5 mL) then distilled water (3 x 5 mL). The wet papers were put into scintillation vials containing 5.0 mL scintillation fluid (Cyto-scint) and the radioactivity associated with the ^{3}H-farnesylated peptide was

determined by scintillation counting. Each reaction was performed in triplicate using a solution containing no peptide as a control.

3.5.11 Inhibition of rPFTase by KKKSKTKC(CNBz)VIM (8)

Inhibition of rPFTase was evaluated using the same previously described continuous fluorescence assay (see substrate studies with **1**). Assay solutions contained 50 mM Tris-HCl, pH 7.5, 10 mM $MgCl_2$, 10 μM $ZnCl_2$, 5.0 mM DTT, 0.2% (w/v) octylglucopyranoside, 1.0 μM *N*-Dansyl-GCVLS, FPP (10 μM), and **8** (0, 2, 4, 6, 10, 20, 30 μM). The assay solution was placed in a quartz cuvette, equilibrated at 30 ºC for 5 min, initiated by the addition of rPFTase (5 ng/mL) and monitored spectrofluorimetrically (340 nm excitation and 505 nm emission, 10 nm slit widths). Enzymatic rates were obtained from linear regression analysis of the time-dependent fluorescence emission data using the fluorimeter software.

3.5.12 X-ray crystallography studies with TKC(CNBz)VIM (7)

Untagged rPFTase was prepared as described[45] using a baculovirus/SF9 expression system. Crystals of the enzyme containing a farnesylated KKKSKTKCVIM peptide were prepared as described[46]. To form a ternary complex with FPP and **7**, the farnesylated product complex was displaced from RPFTase crystals as described by soaking in a stabilizing solution containing 300 μM **7** and 150 μM FPP for one week[47]. Crystals were cryoprotected as described[46] and X-ray diffraction data were collected at

the Southeast Regional Collaborative Access Team (SER-CAT) 22-BM beamline at the Advanced Photon Source, Argonne National Laboratory. The crystal diffracted to 2.70 Å resolution, with an overall merging R factor of 7.9% and 99% completeness of data in the highest resolution bin. Data were reduced and scaled with HKL2000[48], and phases were determined using molecular replacement as implemented by PHASER[49] with the PDB file 1D8D as the search model with ligands removed to reduce model bias. Iterative model building and refinement were carried out in COOT[50] and REFMAC5[51], respectively. The final R_{cryst}/R_{free} was 21.6/25.3. PYMOL was used to perform the superpositions, calculate rmsd values, and prepare Figure 3.5. The structure was deposited to the PDB with accession code 3DPY.

3.6 References

1. Ohkanda, J.; Knowles, D. B.; Blaskovich, M. A.; Sebti, S. M.; Hamilton, A. D., Inhibitors of protein farnesyltransferase as novel anticancer agents. *Curr. Top. Med. Chem.* **2002,** *2*, 303-323.

2. Crul, M.; de Klerk, G. J.; Beijnen, J. H.; Schellens, J. H., Ras biochemistry and farnesyl transferase inhibitors: a literature survey. *Anti-cancer drugs* **2001,** *12*, 163-84.

3. Jaffe, A. B.; Hall, A., Rho GTPases in transformation and metastasis. *Adv. Cancer Res.* **2002,** *84*, 57-80.

4. Sebti, S. M.; Hamilton, A. D., Inhibition of Rho GTPases using protein geranylgeranyltransferase I inhibitors. *Methods Enzymol.* **2000,** *325*, 381-388.

5. Bell, I. M., Inhibitors of farnesyltransferase: A rational approach to cancer chemotherapy? *J. Med. Chem.* **2004,** *47*, 1869-1878.

6. Whyte, D. B.; Kirschmeier, P.; Hockenberry, T. N.; Nunez-Oliva, I.; James, L.; Catino, J. J.; Bishop, W. R.; Pai, J. K., K- and N-Ras are geranylgeranylated in cells treated with farnesyl protein transferase inhibitors. *J. Biol. Chem.* **1997,** *272*, 14459-14464.

7. Rowell, C. A.; Kowalczyk, J. J.; Lewis, M. D.; Garcia, A. M., Direct demonstration of geranylgeranylation and farnesylation of Ki-Ras in vivo. *J. Biol. Chem.* **1997,** *272*, 14093-14097.

8. Lerner, E. C.; Zhang, T. T.; Knowles, D. B.; Qian, Y.; Hamilton, A. D.; Sebti, S. M., Inhibition of the prenylation of K-Ras, but not H- or N-Ras, is highly resistant to CAAX peptidomimetics and requires both a farnesyltransferase and a geranylgeranyltransferase I inhibitor in human tumor cell lines. *Oncogene* **1997,** *15*, 1283-1288.

9. Sousa, S. F.; Fernandes, P. A.; Ramos, M. J., Farnesyltransferase inhibitors: a detailed chemical view on an elusive biological problem. *Curr. Med. Chem.* **2008,** *15*, 1478-1492.

10. Rowinsky, E. K., Lately, it occurs to me what a long, strange trip it's been for the farnesyltransferase inhibitors. *J. Clin. Oncol.* **2006,** *24*, 2981-2984.

11. Young, D. D.; Deiters, A., Photochemical control of biological processes. *Org. Biomol. Chem.* **2007,** *5*, 999-1005.

12. Ellis-Davies, G. C., Caged compounds: photorelease technology for control of cellular chemistry and physiology. *Nat. Methods* **2007,** *4*, 619-628.

13. Mayer, G.; Heckel, A., Biologically active molecules with a "light switch". *Angew. Chem. Int. Ed.* **2006,** *45*, 4900-4921.

14. Pelliccioli, A. P.; Wirz, J., Photoremovable protecting groups: reaction mechanisms and applications. *Photochem. Photobiol. Sci.* **2002,** *1*, 441-458.

15. Curley, K.; Lawrence, D. S., Caged regulators of signaling pathways. *Pharmacol. Ther.* **1999,** *82*, 347-354.

16. Adams, S. R.; Tsien, R. Y., Controlling cell chemistry with caged compounds. *Annu. Rev. Physiol.* **1993,** *55*, 755-784.

17. Parker, L. L.; Kurutz, J. W.; Kent, S. B.; Kron, S. J., Control of the yeast cell cycle with a photocleavable alpha-factor analogue. *Angew. Chem. Int. Ed.* **2006,** *45*, 6322-6325.

18. Rathert, P.; Rasko, T.; Roth, M.; Slaska-Kiss, K.; Pingoud, A.; Kiss, A.; Jeltsch, A., Reversible inactivation of the CG specific SssI DNA (cytosine-C5)-methyltransferase with a photocleavable protecting group. *Chembiochem* **2007,** *8*, 202-207.

19. Schlichting, I.; Rapp, G.; John, J.; Wittinghofer, A.; Pai, E. F.; Goody, R. S., Biochemical and crystallographic characterization of a complex of c-Ha-ras p21 and caged GTP with flash photolysis. *Proc. Natl. Acad. Sci. U. S. A.* **1989,** *86*, 7687-7690.

20. DeGraw, A. J.; Hast, M. A.; Xu, J.; Mullen, D.; Beese, L. S.; Barany, G.; Distefano, M. D., Caged protein prenyltransferase substrates: tools for understanding protein prenylation. *Chem. Biol. Drug. Des.* **2008,** *72*, 171-181.

21. Cambridge, S. B.; Geissler, D.; Keller, S.; Curten, B., A caged doxycycline analogue for photoactivated gene expression. *Angew. Chem. Int. Ed.* **2006,** 45, 2229-2231.

22. Link, K. H.; Cruz, F. G.; Ye, H. F.; O'Reilly K, E.; Dowdell, S.; Koh, J. T., Photo-caged agonists of the nuclear receptors RARgamma and TRbeta provide unique time-dependent gene expression profiles for light-activated gene patterning. *Bioorg. Med. Chem.* **2004,** *12*, 5949-5959.

23. Pompliano, D. L.; Gomez, R. P.; Anthony, N. J., Intramolecular fluorescence enhancement: a continuous assay of Ras farnesyl:protein transferase. *J. Am. Chem. Soc.* **1992,** 114, 7945-7946.

24. He, Z.; Stienen, G. J.; Barends, J. P.; Ferenczi, M. A., Rate of phosphate release after photoliberation of adenosine 5'-triphosphate in slow and fast skeletal muscle fibers. *Biophys. J.* **1998,** *75*, 2389-2401.

25. Hartung, K.; Froehlich, J. P.; Fendler, K., Time-resolved charge translocation by the Ca-ATPase from sarcoplasmic reticulum after an ATP concentration jump. *Biophys. J.* **1997,** *72*, 2503-2514.

26. Gropp, T.; Cornelius, F.; Fendler, K., K+-dependence of electrogenic transport by the NaK-ATPase. *Biochim. Biophys. Acta.* **1998,** *1368*, 184-200.

27. Allen, D. G.; Lannergren, J.; Westerblad, H., The use of caged adenine nucleotides and caged phosphate in intact skeletal muscle fibres of the mouse. *Acta. Physiol. Scand.* **1999,** *166*, 341-347.

28. Corrie, J. E. T.; Trentham, D. R., Synthetic, Mechanistic and Photochemical Studies of Phosphate Esters of Substituted Benzoins. *J. Chem. Soc. Perkin Trans.* **1992**, 2409-2417.

29. Zhu, Y.; Pavlos, C. M.; Toscano, J. P.; Dore, T. M., 8-Bromo-7-hydroxyquinoline as a photoremovable protecting group for physiological use: mechanism and scope. *J. Am. Chem. Soc.* **2006,** *128*, 4267-4276.

30. Fedoryak, O. D.; Dore, T. M., Brominated hydroxyquinoline as a photolabile protecting group with sensitivity to multiphoton excitation. *Org. Lett.* **2002,** *4*, 3419-3422.

31. Furuta, T.; Takeuchi, H.; Isozaki, M.; Takahashi, Y.; Kanehara, M.; Sugimoto, M.; Watanabe, T.; Noguchi, K.; Dore, T. M.; Kurahashi, T.; Iwamura, M.; Tsien, R. Y., Bhc-cNMPs as either water-soluble or membrane-permeant photoreleasable cyclic nucleotides for both one- and two-photon excitation. *Chembiochem* **2004,** *5*, 1119-1128.

32. Das, S.; Schapira, M.; Tomic-Canic, M.; Goyanka, R.; Cardozo, T.; Samuels, H. H., Farnesyl pyrophosphate is a novel transcriptional activator for a subset of nuclear hormone receptors. *Mol. Endocrinol.* **2007,** *21*, 2676-2686.

33. Lowy, D. R.; Willumsen, B. M., Function and regulation of ras. *Annu. Rev. Biochem.* **1993,** *62*, 851-891.

34. Xue, C. B. B., J.M.; Naider, F., Efficient regioselective isoprenylation of peptides in acidic aqueous solution using zinc acetate as a catalyst. *Tet. Lett.* **1992,** *33*, 1435-1438.

35. Khan, S. G.; Mukhtar, H.; Agarwal, R., A rapid and convenient filter-binding assay for ras p21 processing enzyme farnesyltransferase. *J. Biochem. Biophys. Methods* **1995,** *30*, 133-144.

36. Graham, S. L.; deSolms, S. J.; Giuliani, E. A.; Kohl, N. E.; Mosser, S. D.; Oliff, A. I.; Pompliano, D. L.; Rands, E.; Breslin, M. J.; Deana, A. A.; et al., Pseudopeptide inhibitors of Ras farnesyl-protein transferase. *J. Med. Chem.* **1994,** *37*, 725-732.

37. Hatchard, C. G.; Parker, C. A., A new sensitive chemical actinometer. II. Potassium ferrioxalate as a standard chemical actinometer. *Proc. Roy. Soc.* **1956,** *A235*, 518-536.

38. Mayer, M. P.; Prestwich, G. D.; Dolence, J. M.; Bond, P. D.; Wu, H. Y.; Poulter, C. D., Protein farnesyltransferase: production in *Escherichia coli* and immunoaffinity purification of the heterodimer from *Saccharomyces cerevisiae*. *Gene* **1993,** *132*, 41-47.

39. Gaon, I.; Turek, T. C.; Weller, V. A.; Edelstein, R. L.; Singh, S. K.; Distefano, M. D., Photoactive analogs of farnesyl pyrophosphate containing benzoylbenzoate esters: synthesis and application to photoaffinity labeling of yeast protein farnesyltransferase. *J. Org. Chem.* **1996,** *61*, 7738-7745.

40. Cassidy, P. B.; Dolence, J. M.; Poulter, C. D., Continuous fluorescence assay for protein prenyltransferases. *Methods Enzymol.* **1995,** *250*, 30-43.

41. Fu, H. W.; Moomaw, J. F.; Moomaw, C. R.; Casey, P. J., Identification of a cysteine residue essential for activity of protein farnesyltransferase. Cys299 is exposed only upon removal of zinc from the enzyme. *J. Biol. Chem.* **1996,** *271*, 28541-28548.

42. Han, Y.; Albericio, F.; Barany, G., Occurrence and minimization of cysteine racemization during stepwise solid-phase peptide synthesis. *J. Org. Chem.* **1997,** *62*, 4307-4312.

43. King, D. S.; Fields, C. G.; Fields, G. B., A cleavage method which minimizes side reactions following Fmoc solid phase peptide synthesis. *Int. J. Pept. Protein. Res.* **1990,** *36*, 255-266.

44. Grewer, C.; Jager, J.; Carpenter, B. K.; Hess, G. P., A new photolabile precursor of glycine with improved properties: A tool for chemical kinetic investigations of the glycine receptor. *Biochemistry* **2000,** *39*, 2063-2070.

45. Chen, W. J.; Moomaw, J. F.; Overton, L.; Kost, T. A.; Casey, P. J., High level expression of mammalian protein farnesyltransferase in a baculovirus system. The purified protein contains zinc. *J. Biol. Chem.* **1993,** *268*, 9675-9680.

46. Long, S. B.; Casey, P. J.; Beese, L. S., The basis for K-Ras4B binding specificity to protein farnesyltransferase revealed by 2Å resolution ternary complex structures. *Structure* **2000,** *8*, 209-222.

47. Reid, T. S.; Terry, K. L.; Casey, P. J.; Beese, L. S., Crystallographic analysis of CaaX prenyltransferases complexed with substrates defines rules of protein substrate selectivity. *J. Mol. Biol.* **2004,** *343*, 417-433.

48. Otwinowski, Z.; Minor, W., Processing of x-ray diffraction data collected in oscillation mode. *Methods Enzymol.* **1997,** *276*, 307-326.

49. McCoy, A. J.; Grosse-Kunstleve, R. W.; Adams, P. D.; Winn, M. D.; Storoni, L. C.; Read, R. J., Phaser crystallographic software. *J. Appl. Crystallogr.* **2007,** *40*, 658-674.

50. Emsley, P.; Cowtan, K., Coot: model-building tools for molecular graphics. *Acta. Crystallogr. D Biol. Crystallogr.* **2004,** *60*, 2126-2132.

51. Murshudov, G. N.; Vagin, A. A.; Dodson, E. J., Refinement of macromolecular structures by the maximum-likelihood method. *Acta. Crystallogr. D Biol. Crystallogr.* **1997,** *53*, 240-255.

Chapter 4. Azide- and alkyne-modified analogues of isoprenoids as chemical reporters of protein prenylation

4.1 Introduction

The inhibition of protein farnesylation has been a target for disease intervention for the past two decades. Protein farnesyltransferase inhibitors (FTIs) have been evaluated as chemotherapeutics for certain forms of cancer, anti-parasitic agents to treat malaria and Chagas disease, and tools to ameliorate the symptoms of Hutchinson-Gilford progeria syndrome. Protein geranylgeranyltransferase inhibitors (GGTIs) are also in development.[1, 2] Despite copious amounts of research, much still remains unclear about protein prenylation and its inhibition. For example, the driving force behind FTI development for cancer therapy has focused on the oncogenic Ras proteins, since they must be farnesylated to be active.[3] During pre-clinical studies with these inhibitors, antiproliferative and pro-apoptotic activity were observed in cases where oncogenic Ras was not present, suggesting that other downstream effectors contributing to the anti-cancer activity of FTIs.[4].

A number of studies point towards the inhibition of RhoB farnesylation and subsequent accumulation in geranylgeranylated RhoB as the mechanism of action for FTIs.[5-8] Inhibition of H-Ras and Rheb farnesylation block the activation of the PI3K/Akt and mTor pathways, respectively, both of which appear to contribute to FTIs' antiproliferative and proapoptotic activity in cancer cell lines.[9-13] Although FTIs have been shown to induce accumulation at prometaphase during mitosis, whether or not this

proceeds through blocking the farnesylation of two centromere-associated proteins (CENPs), CENP-E and CENP-F, is a matter of debate.[14, 15] Some GGTIs have been shown to arrest cells in the G1 phase of the cell division cycle through inhibition of geranylgeranylated RhoA.[16, 17]

Despite these extensive studies, the mechanism by which FTIs and GGTIs inhibit tumor growth and induce apoptosis in human cancer cell lines where the aforementioned pathways do not play a role is yet to be determined. While a number of prenylated proteins have been proposed to be targets of FTIs, direct evidence of the inhibition of these proteins, or another yet undiscovered prenylated protein, is severely lacking.[18, 19] Determination of the protein farnesyltransferase (PFTase) and/or protein geranylgeranyltransferase type I (PGGTase-I) substrates affected by the inhibition of these enzymes is critical for enhancing our knowledge of the mechanism of action of FTIs and GGTIs. It is interesting to note that inhibition of protein geranylgeranyltransferase type II (PGGTase-II) catalyzed prenylation may also contribute to antiproliferative and proapoptotic affects of prenylation inhibitors. A recent study demonstrated that certain FTIs that are potent inducers of apoptosis directly inhibit PGGTase-II, and this activity was mimicked by PGGTase-II knockdown.[20] Only a fraction of prenylated proteins have been observed experimentally despite the hundreds predicted by bioinformatics approaches.[21, 22] Clearly, a comprehensive experimental technique designed to study the post-translational modification of proteins with isoprenoids by protein prenyltransferases is needed. Such a technique would help us to better understand the mechanism(s) of action of FTIs and GGTIs, as well as create more potent and selective compounds.

Mass spectrometry is often the tool of choice for the study of the cellular proteome, but significant barriers remain for applying high-throughput proteomics techniques towards the analysis of protein post-translational modifications (PTMs).[23, 24] Identifying and studying PTMs is particularly challenging in that there is often high background signal from unmodified proteins. However, a relatively new technology, chemical proteomics, selectively enriches post-translationally modified protein from abundant background proteins. The principle steps underlying this technique for the study of protein PTMs are outlined in Figure 1.[25]

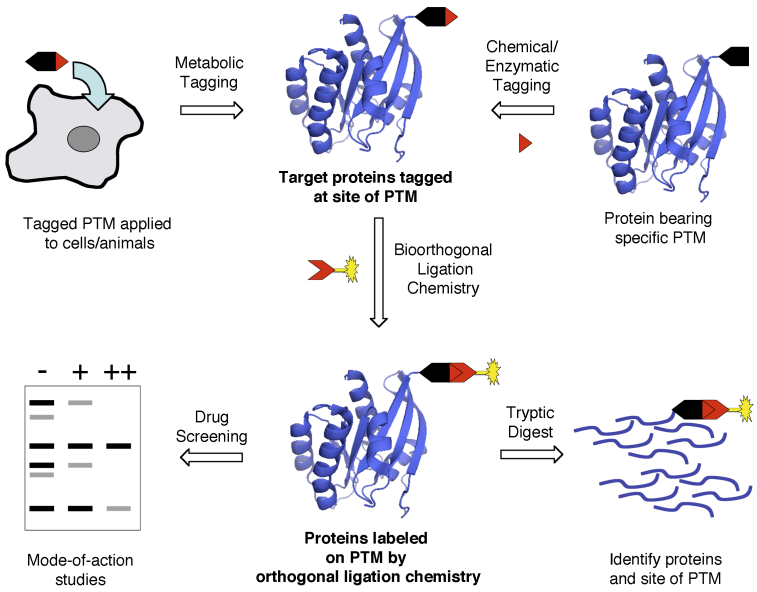

Figure 4.1 An overview of the chemical proteomics method for studying protein post-translational modifications (Adapted from Tate[25]).

In chemical proteomics, the proteins of interest are first labeled with a small chemical tag at the site of the PTM. This can be done by exploiting the cells own machinery to label the proteins *in situ* with a tagged analogue of the PTM, or by post-lysis modification of the PTM by chemical or enzymatic means. If the tag is incorporated via metabolic

means, it is critical that the tag be functionally silent and not interfere with wild-type activity of the modified proteins. The next step involves performing a bioorthogonal chemical ligation reaction with a capture reagent. A number of such reagents have been created bearing affinity labels (i.e.; biotin, FLAG, etc.), reporter dyes, radiolabels, oligonucleotide tags, and stable isotope tags. The choice of capture reagent depends on the downstream application. Reporter dyes are utilized to visualize the post-translational proteome of interest as a whole, while affinity labels are applied for enrichment of the modified proteins for subsequent clean-up and identification via mass spectrometry.

There are a number of ligation chemistries that can be employed for selective modification of protein PTMs. As previously stated, it is critical that the PTM tag be functionally silent, but it is also important for the conjugation reaction to proceed *selectively* in the presence of a plethora of reactive groups (amines, alcohols, sulfhydryls, etc.) in biological systems. Table 4.1 contains a summary of common reactions used for the modification of protein PTMs. For a complete examination of all types of bioorthogonal chemistry and their applications, see the review by Sletten and Bertozzi.[26]

Table 4.1 Summary of commonly used bioorthogonal reactions in chemical proteomics

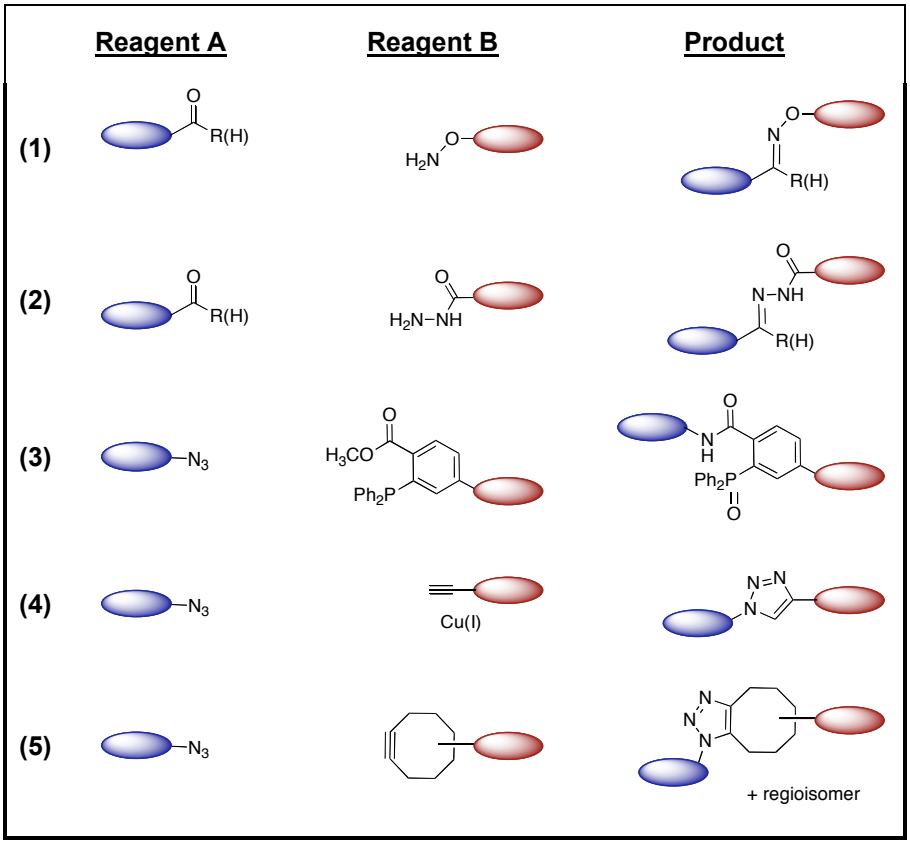

Reactions **1** and **2** are based on the condensation of ketones or aldehydes with aminooxy (Table 4.1, Reaction **1**) or hydrazide (Table 4.1, Reaction **2**) compounds, which form oxime and hydrazone linkages, respectively. These reactions are not optimal for labeling biomolecules inside cells or within live organisms due to competing endogenous aldehydes and ketones, but have shown applicability in labeling of cell surface proteins.[27, 28] Unlike aldehydes and ketones, azides are completely absent from biological systems. Azides are also small in size and, therefore, only minimally perturb a modified susbtrate. The Staudinger ligation (Table 4.1, Reaction **3**) is a variation of the Staudinger reaction between azides and triphenylphosphines.[29] Despite the potential cross-reactivity of azides and phosphines with thiols and disulfides, the Staudinger

ligation has been used to probe biomolecules in many cellular environments.[29-31] The Staudinger ligation does have its limitations in that it suffers from relatively slow reaction kinetics ($k \sim 10^{-3}$ $M^{-1} \bullet s^{-1}$), and efforts to improve on this rate have not been successful.[26, 32] As a result, there has been considerable interest in faster reactions with azides.

The Sharpless and Meldal labs found that the Huisgen 1,3-dipolar cycloaddition of azides and alkynes[33] could be efficiently catalyzed using copper under mild, biocompatible conditions (Table 4.1, Reaction **4**).[34, 35] Addition of specific ligands for copper provided further enhancement ($k \sim 10^{-1}$ $M^{-1} \bullet s^{-1}$).[36] The copper-catalyzed 1,3-dipolar cycloaddition of azides and alkynes has all the properties of a click reaction as defined by Sharpless and coworkers[37] and, because of its widespread use in bioconjgation[38-40], has been coined the "the click reaction". Despite the large number of applications the click reaction has proven useful for, its use in living systems is hindered by the toxicity of Cu(I).[26] This lead to the creation of alkyne molecules activated by ring strain, as pioneered by the Bertozzi lab.[41] By incorporating electron-withdrawing fluorine atoms at the propargylic position, they were able to create a difluorinated-cyclooctyne (DIFO) molecule that underwent addition with azides under similar kinetics to the copper-catalyzed click reaction.[42, 43] Additionally, a dibenzo-cycloctyne was created by Boons and coworkers, which has reaction kinetics similar to DIFO. [44] Chemoselective ligation with these strained-ring alkynes is often referred to as "copper-free click chemistry".

Post-translational proteomics using the chemical approaches described above offer a number of advantages over traditional techniques.[25] Because these techniques are applied post-genomically, these methods are transferable between different classes of organisms.

When compared to the limited range and specificity of current affinity-column based enrichment strategies, the chemical tagging of the PTM offers enhanced selectivity and efficiency in capture of the modified proteins. To date, chemical proteomics have been applied towards the study of a number of post-translational modifications including glycosylation,[45-49] phosphorylation,[50, 51] myristoylation,[52-54] palmitoylation,[53, 55-57] and prenylation.[58-60]

The Tamanoi lab, in collaboration with the Zhao lab, was the first to explore using chemical proteomics to catalogue the spectrum of farnesylated proteins using a technique they called "tagging-via-substrate" technology.[59] Through incorporation of an azide moiety on the farnesyl chain (Figure 4.2, **1**), they were able to selectively label farnesylated proteins *in vivo* by incubating COS cells in media containing **1**. This work not only demonstrated that probe **1** could be metabolically incorporated onto proteins, but also that cells treated with the alcohol precursor (**2**) where able to phoshoporylate the probe, thus making it a substrate for the PFTase enzyme. By using a biotinylated phosphine capture reagent with Staudinger ligation chemistry (Table 4.1 Reaction **3**), they were able to selectively enrich for a number of prenylated proteins and subsequently identify them by mass spectrometry. A total of 18 prenylated proteins were identified. The majority of these proteins were known farnesylated proteins including the nuclear lamins and the H-, N-, and K-isoforms of the Ras protein. The geranylgeranylated protein CDC42 was also identified, which they postulated was from the *in vivo* conversion of the C15-azide probe (**1**) being converted to the C20-azide, which could then be used by the PGGTase-I enzyme as a substrate. Despite the elegant nature of this study, there were no novel prenylated proteins observed except for Annexin A2, which contains an

unprecedented CAAXX motif. Because the prenylated peptide remains attached to the capture reagent, their technique was not amendable to identification of the labeled peptides, making subsequent confirmation of the enriched proteins not possible.

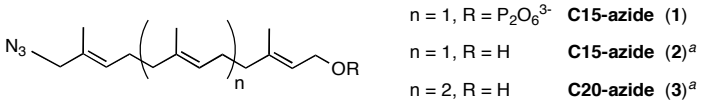

Figure 4.2 Azide-isoprenoid analogues used as chemical proteomics probes for protein prenylation. [a]Probes now commercially available from Invitrogen

In collaboration with Invitrogen, Corp., the Tamanoi lab continued their pursuit of studying and identifying prenylated proteins.[58] A C20 azide probe was created (Figure 4.2, **3**) and incubated with MCF and Jurkat cells. Using the Cu(I)-catalyzed click reaction (Table 4.1, Reaction **4**), they selectively labeled proteins with an alkyne-functionalized tetramethylcarboxyrhodamine (TAMRA) fluorophore, which were visualized by SDS-PAGE and in-gel fluorescence scanning. Identification of these labeled proteins was accomplished by pre-fractionation of the proteins by pH, separation of each fraction by a narrow pH range 2-D gel electrophoresis, and in-gel digestion of the fluorescent protein bands. A total of 10 proteins were identified, 9 from the Rab protein family and the novel Rap2C protein, a member of the Ras family. While it was demonstrated that the C15-azide (Figure 4.2, **2)** and C20-azide (Figure 4.2, **3**) probes can be used to study prenylation of specific proteins, this method still lacks a means for identification of the labeled peptides for protein PTM confirmation.

Applying the allylic azide probes used by the Tamanoi lab towards the identification of the specific peptide that is prenylated in a protein proves problematic. Allylic azides can

spontaneously undergo isomerization in solution (Scheme 4.1).[61, 62] Because both azides can undergo 1,3-dipolar cycloaddition with an activated alkyne or Staudinger ligation with a phosphine reagent, the chromatographic separation of labeled peptides is convoluted, making proper identification of the peptide sequence difficult.[62]

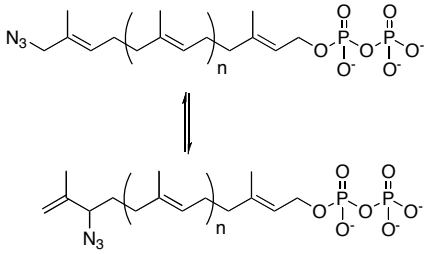

Scheme 4.1 Isomerization of allylic azide-isoprenoid analogues

The Distefano lab has also created azide-based isoprenoid analogues for the study of protein prenylation.[62, 63] These analogues (Figure 4.3, **4** and **5**) have a dihydro-bond at the terminal isoprene unit which prevents the isomerization of the azide group. The rate of enzymatic prenylation of a CAAX peptide by PFTase with analogue **5** was found to be approximately 3-times slower than with the natural substrate FPP,[63] suggesting that this probe performs equally as well as the C15-azide probe (**1**).

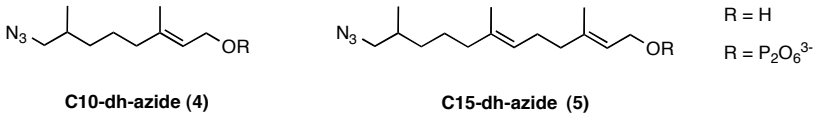

Figure 4.3 Azide-modified probes created by the Distefano lab

Isoprenoid analogues (Figure 4.4, **6** and **7**) that contain a propargyl-group at the terminal isoprene unit have also been created by the Distefano lab. The kinetics of

PFTase-catalyzed prenylation of a peptide with **6** was poor (~ 12-fold slower) as compared to the natural substrate FPP.[61, 64] Analogue **7** was tested as a dual substrate for PFTase and PGGTase-I. As compared to their natural substrates, FPP and GGPP respectively, **7** is incorporated into the respective peptide substrates at comparable concentrations and rates.[65] Interestingly, incubation of **7** in the presence of both PFTase and PGGTase-I peptide substrates, and the corresponding prenyltransferase enzymes, resulted in both peptides being prenylated highlighting, its true dual substrate nature.

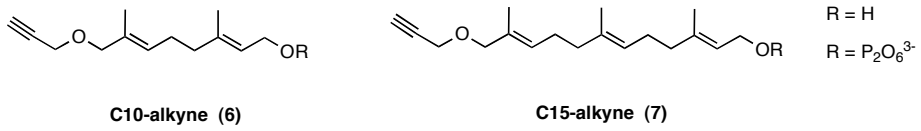

Figure 4.4 Alkyne-modified probes created by the Distefano lab

Analogues **6** and **7** can be labeled with an azide-based capture reagent using Cu(I)-catalyzed click chemistry. This reversal of click chemistry reagents offers an added benefit over the traditional incorporation of the azide on the isoprenoid and reaction with an alkyne-based capture reagent. Previous reports have shown that reacting azides with excess alkyne-reagent results in a higher degree of non-specific protein labeling as compared to the reaction of alkynes with excess azide.[64, 66] The source of background labeling is believed to result from the first intermediate in the proposed catalytic mechanism for the Cu(I)-catalyzed click reaction (Scheme 4.2), which is an alkyne-copper coordinated species with enhanced reactivity as compared to the uncoordinated alkyne. When applying the click reaction towards the analysis of the protein prenylome,

excess background labeling could prove problematic given the small percentage of prenylated proteins within the proteome.[22]

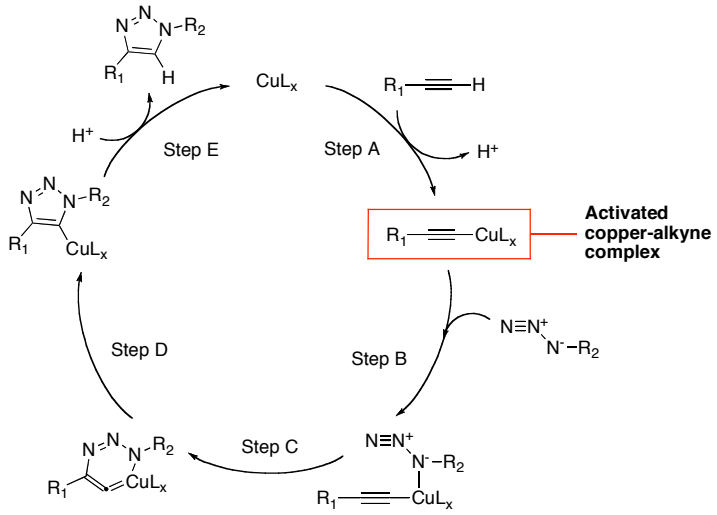

Scheme 4.2 Proposed catalytic mechanism of the Cu(I)-catalyzed click reaction

4.2 Research Objectives

The goal of this work was to apply our azide- and alkyne-modified isoprenoid analogues towards the analysis and characterization of the mammalian protein prenylome. Cells are treated with either the diphosphate isoprenoid analogue or the alcohol version, which is converted into the diphosphate by cellular kinases. These analogues were then appended onto prenylated proteins and through Cu(I)-catalyzed cycloaddition with a corresponding azide- or alkyne-modified fluorophore, direct visualization of prenylated proteins could be accomplished. Application of this same reaction with a biotinylated capture reagent allowed for enrichment of the modified proteins and subsequent identification by liquid chromatography-tandem mass spectrometry.

4.3 Results and Discussion

4.3.1 Comparison of azide- and alkyne-modified isoprenoid analogues for studying the protein prenylome

HeLa cells were treated with the C10-alkyne probe (**6,** R = H), the C15-alkyne probe (**7**, R = H) or the C15-dh-azide probe (**5**, R = H) to compare the amount of background labeling observed upon reaction with excess azide or alkyne capture reagent. The cells' endogenous prenyltransferase enzymes labeled their cognate proteins with the probes. Co-treatment of the cells with lovastatin, which shuts down the biosynthesis of FPP and GGPP, ensured that the isoprenoid analogues would be utilized as substrates. Cells that were left untreated or were treated with probe were lysed and reacted with excess azido- or propargyl-labeled tetramethylcarboxyrhodamine (TAMRA) fluorophore via the Cu(I)-catalyzed click reaction. Separation of the proteins was accomplished by SDS-PAGE and the labeled proteins were visualized by in-gel fluorescence.

Labeling of specific proteins in the crude cell lysate was accomplished with probes **5**, **6**, and **7** and is shown in Figure 4.5. Lanes 1 through 3 contain lysates treated with excess TAMRA-azide, while lanes 4 and 5 contain lysates treated with excess TAMRA-alkyne. Despite equal amounts of proteins being loaded in each lane, significant background labeling was observed in cell lysate not treated with any isoprenoid analogues and reacted with excess TAMRA-alkyne (Lane 4'). Remarkebly, lysate not treated with isoprenoid analogues and reacted with excess TAMRA-azide show no background labeling (Lane 1').

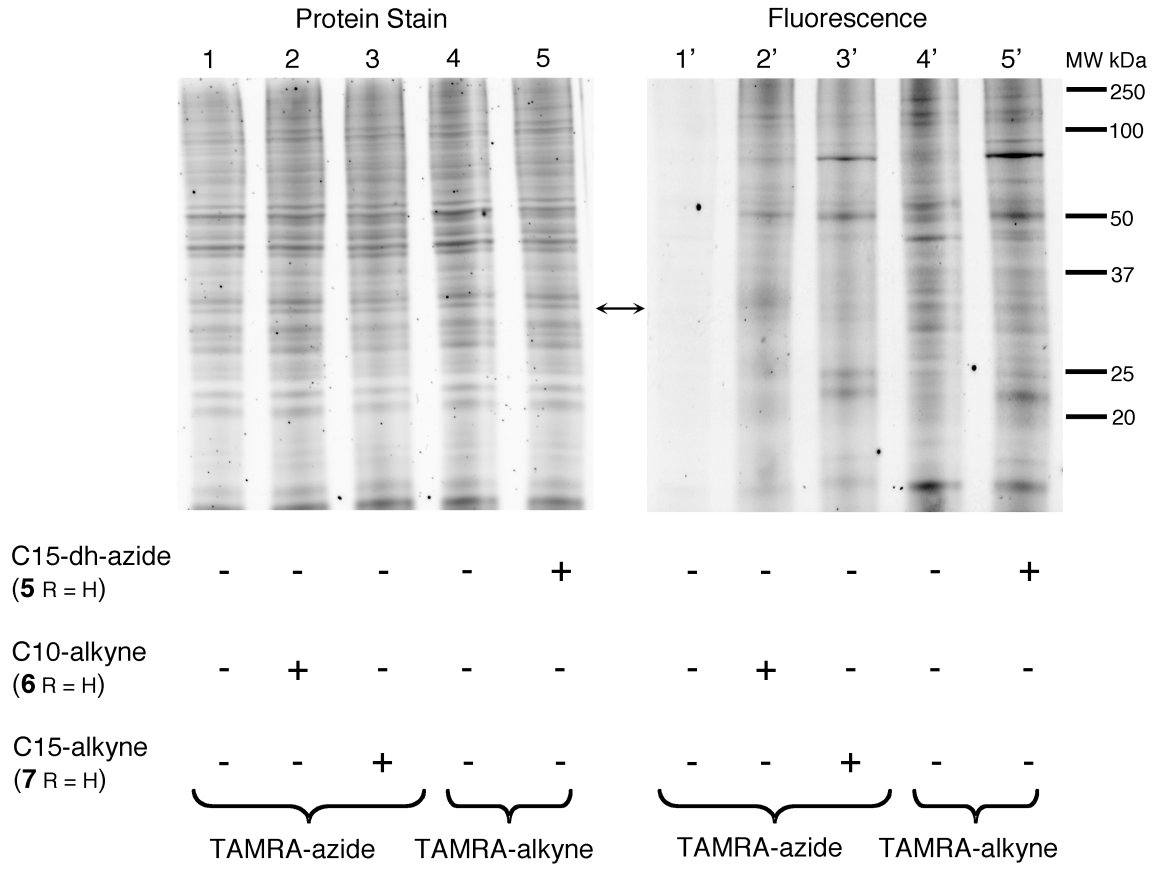

Figure 4.5. Analysis of labeled proteins in crude HeLa cell lysates by Cu(I)-catalyzed click chemistry. Lanes 1-5 show proteins stained with Sypro Ruby. Lanes 1'-5' shown fluorescently labeled proteins. Lanes 1/1' and 4/4' contain lysate from cells not treated with isoprenoid analogue. Lanes 2/2' and 3/3' contain lysate from cells treated with analogues **5** and **6** respectively. Lane 5/5' contains lysate from cells treated with analogue **4.** Lanes 1/1' through 3/3' were reacted with TAMRA-azide while lanes 4/4' and 5/5' were reacted with TAMRA-alkyne.

It is interesting to note that the labeling patterns observed with each probe is slightly different, suggesting that endogenous prenyltransferase enzymes prefer one probe over another for the labeling of certain proteins (Figure 4.5: Compare lanes 2', 3' and 5'). Taken together these results suggest that, despite the significant amount of background labeling observed upon reaction with excess TAMRA-alkyne, separate treatment of cells

with both azide- and alkyne-based isoprenoid analogues may be required to obtain full coverage of the protein prenylome during analysis.

4.3.2 Visualizing prenylated proteins across various cell lines and changes in prenylation status upon exposure to protein prenyltransferase inhibitors

Because protein prenylation varies between different organism and cell types, our analogues were applied towards the analysis of protein prenylation in a number of cultured mammalian cell lines. Through simultaneous treatment with either an FTI or GGTI, the targets and specificity of these inhibitors could also be observed. HeLa cells, an immortal cell line derived from cervical cancer, were treated with C15-dh-azide probe (**5**, R = H) or C15-alkyne probe (**7**, R = $P_2O_6^{3-}$), reacted with the corresponding TAMRA capture reagent and subjected to in-gel fluorescence analysis (Figure 4.6). Proteins at molecular weights from 15 to 100 kDa were labeled with **5** (Figure 4.6: panel A, lane 2)**.** Treatment with the FTI (Figure 4.6: panel A, lane 3) resulted in diminished labeling of one labeled protein at ~ 70 kDa while treatment with the GGTI (Figure 4.6: panel A, lane 4) did not affect the labeling pattern. Interestingly, the labeled protein at ~ 30 kDa appeared to be labeled more in the presence of the FTI. The alkyne probe **7** manifests a very different labeling pattern with only a few proteins being labeled (Figure 4.6: panel B, lane 2) from ~ 20-30 kDa and ~ 40-70 kDa. As seen in HeLa cells treated with probe **5**, little change is observed upon treatment with the GGTI (Figure 4.6: panel B, lane 4) while the protein at ~ 70 kDa is diminished with the protein at ~ 30 kDa was enhanced up treatment with the FTI, as evidenced by the increase in fluorescence (Figure 4.6: panel B, lane 3).

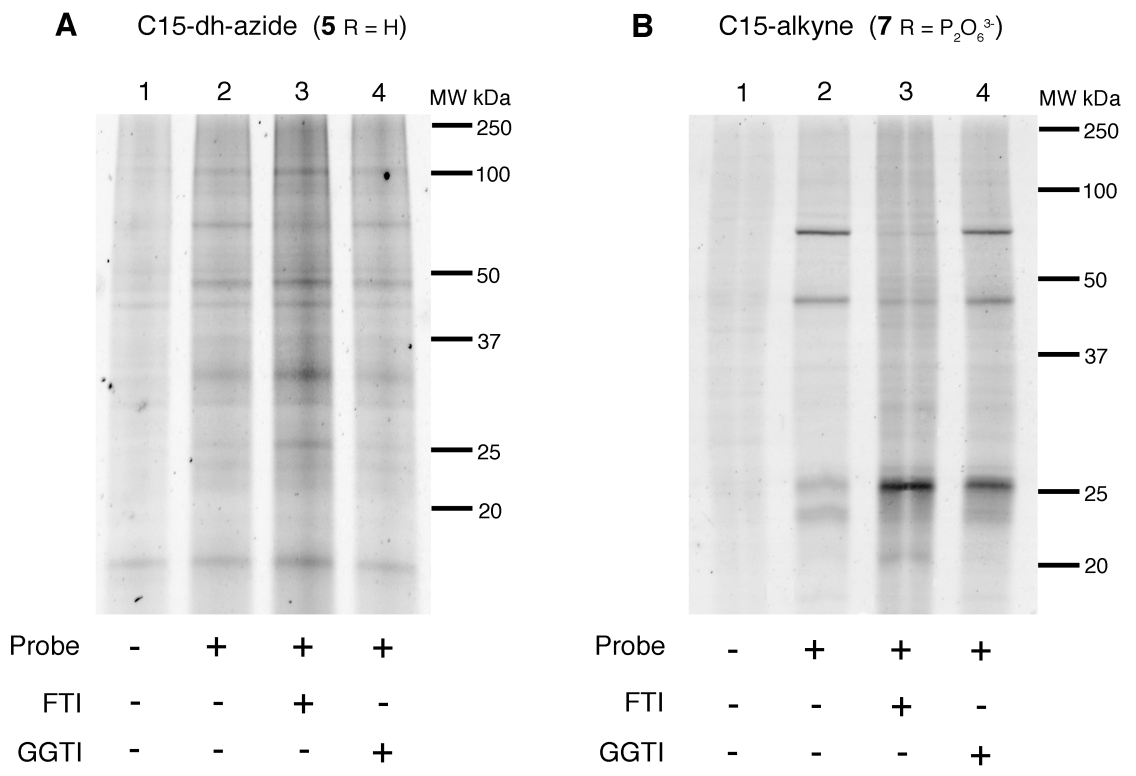

Figure 4.6 In-gel fluorescence analysis of prenylated proteins in HeLa cells. A: Treatment with C15-dh-azide (**4**) isoprenoid analogue and reacted with TAMRA-alkyne. B: Treatment with C15-alkyne (**6**) isoprenoid analogue and reacted with TAMRA-azide. 1 = no treatment control, 2 = treatment with isoprenoid analogue only, 3 = treatment with analogue and FTI, 4 = treatment with analogue and GGTI.

MCF10A cells, a non-tumorigenic epithelial cell line, were treated with C15-dh-azide probe (**4**, R = H) or C15-alkyne probe (**6**, R = $P_2O_6^{3-}$) and analyzed to see how cancerous and non-cancerous derived cell lines vary in prenylation levels (Figure 4.7). A significantly different labeling pattern is observed in cells treated with azide probe **4**. Two proteins in particular (one just under 50 kDa in molecular weight, the other above) appear to be predominantly. (Figure 4.7: panel A, lane 2). Interestingly, neither of these proteins, or any of the other proteins in MCF10A cells are affected by treatment with the FTI or the GGTI (Figure 4.7: panel A, lanes 3 and 4). Treatment with the alkyne probe **6**

showed a pattern very similar to that observed in HeLa cells, including the proteins affected by treatment with the FTI (Figure 4.7: panel B).

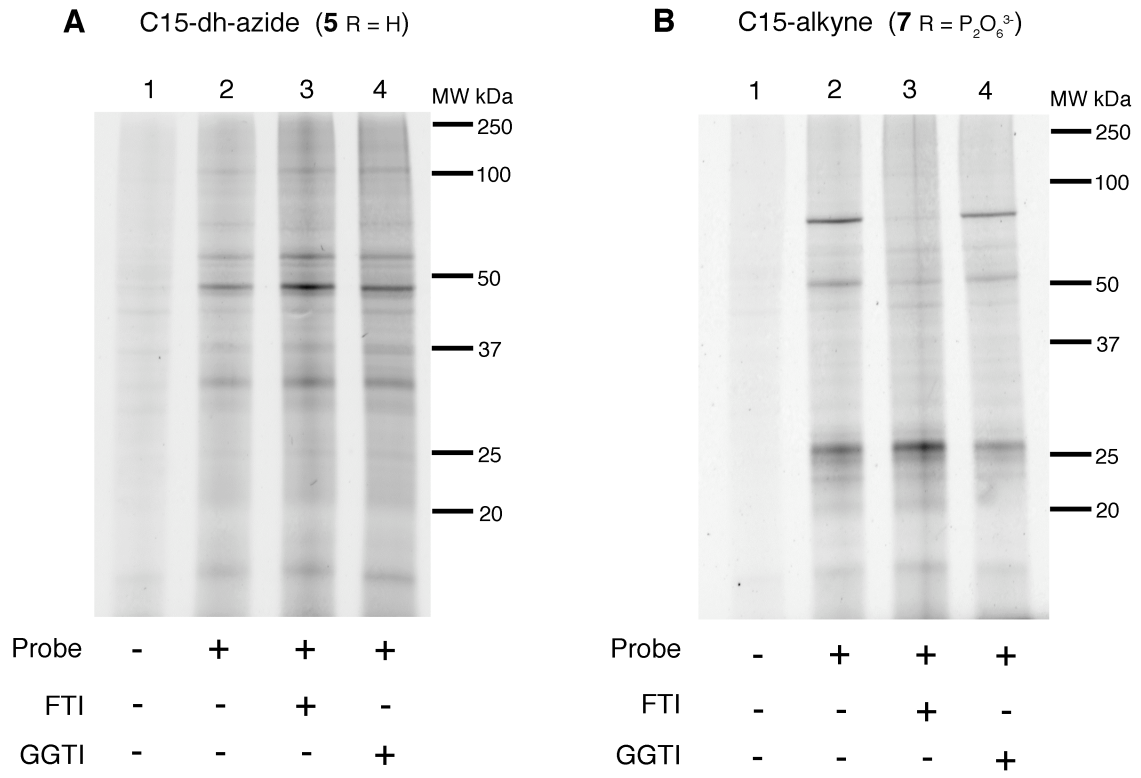

Figure 4.7 In-gel fluorescence analysis of prenylated proteins in MCF10A cells. A: Treatment with C15-dh-azide (**4**) isoprenoid analogue and reacted with TAMRA-alkyne. B: Treatment with C15-alkyne (**6**) isoprenoid analogue and reacted with TAMRA-azide. 1 = no treatment control, 2 = treatment with isoprenoid analogue only, 3 = treatment with analogue and FTI, 4 = treatment with analogue and GGTI.

While isoprenoids are believed to play a role in Alzheimer's disease (AD) given their elevated levels[67], a recent study point towards the involvement of a yet unknown prenylated protein in AD neuropathophysiology.[68] To explore the applicability of our probes towards the study of prenylated proteins in brain cells, we treated astrocytes with C15-dh-azide probe (**4**, R = H) or C15-alkyne probe (**6**, R = $P_2O_6^{3-}$). Astrocytes are cells found in the brain and spinal cord that serve a variety of functions.[69] The labeling patterns

observed upon treatment with either probe are similar to those observed in the HeLa cell line (Figure 4.8).

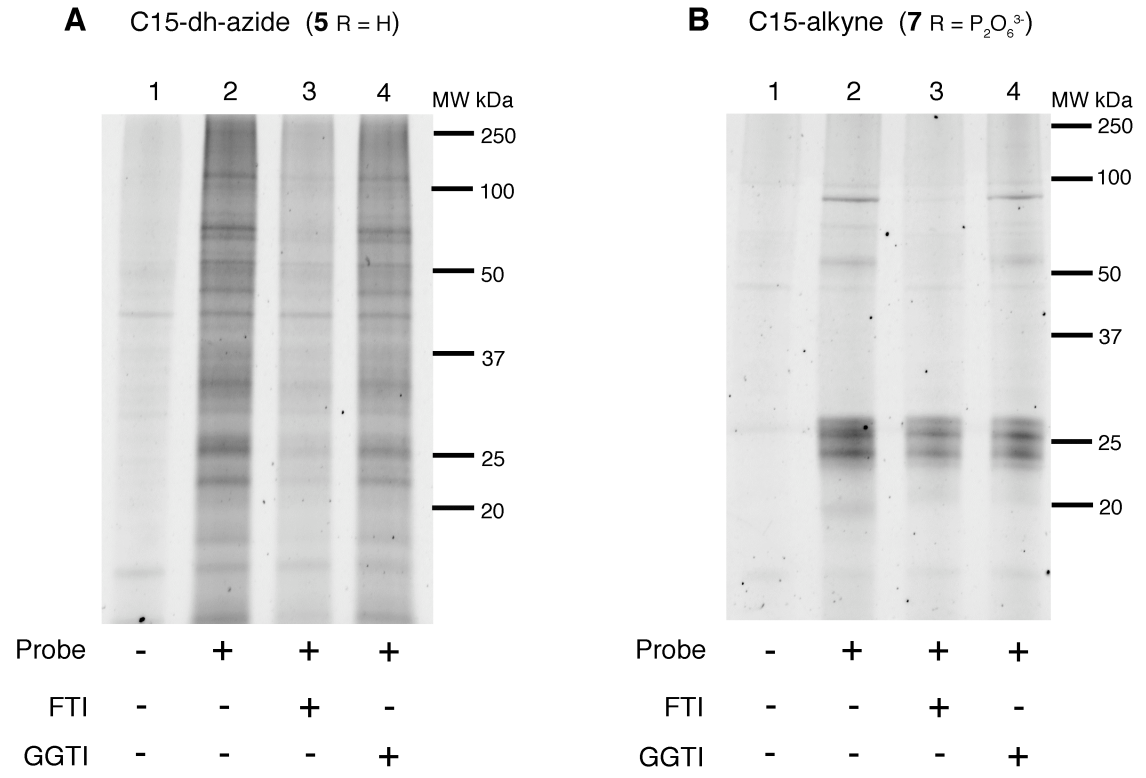

Figure 4.8 In-gel fluorescence analysis of prenylated proteins in astrocytes. A: Treatment with C15-dh-azide (**4**) isoprenoid analogue and reacted with TAMRA-alkyne. B: Treatment with C15-alkyne (**6**) isoprenoid analogue and reacted with TAMRA-azide. 1 = no treatment control, 2 = treatment with isoprenoid analogue only, 3 = treatment with analogue and FTI, 4 = treatment with analogue and GGTI.

Upon treatment with the C15-dh-azide (**4**), a variety of proteins ranging from ~ 15 to 100 kDa in molecular weight were labeled (Figure 4.8: panel A, lane 2). While treatment with the GGTI had no effect on the labeling (Figure 4.8: panel A, lane 4), treatment with the FTI results in significant diminishment in labeling of nearly every protein (Figure 4.8: panel A, lane 3). This decrease in labeling, however, was not observed in the HeLa cell line, suggesting that prenyltransferases found in astrocytes are particularly sensitive to the FTI. Only proteins from ~ 20-30 kDa and ~ 50-100 kDa were labeled with the C15-

alkyne (**6**) (Figure 4.8: panel B, lane 2), as was observed in the other cell lines tested. Additionally, proteins from ~ 50-100 kDa were affected by FTI treatment (Figure 4.8: panel B, lane 3) while none of the proteins were affected by treatment with the GGTI (Figure 4.8: panel B, lane 4).

4.3.3 Enrichment of prenylated proteins from a COS cell line and identification via mass spectrometry

Both our azide- and alkyne-isoprenoid analogues showed applicability towards the analysis of prenylated proteins in a variety of cell lines by in-gel fluorescence experiments. Such studies provide a broad overview of the protein prenylome and a qualitative look as to which proteins are affected by prenyltransferase inhibitors. In order to truly characterize the protein prenylome and examine which proteins are targeted by FTIs and GGTIs, one must be able to identify the prenylated proteins.

In order to identify the labeled proteins, COS cells were treated with either C15-dh-azide probe (**5**, R = H) or C15-alkyne probe (**7**, R = $P_2O_6^{3-}$), lysed, and reacted with a biotinylated azide- or alkyne-capture reagent. Upon enrichment of the labeled proteins with immobilized streptavidin, tryptic digestion on resin and liquid chromatography with tandem mass spectrometry (LC-MSMS) of the peptides were performed. The Protein Pilot software (Applied Biosystems) was used to ascertain the protein identities. A depiction of the experimental procedure is shown in Figure 4.9.

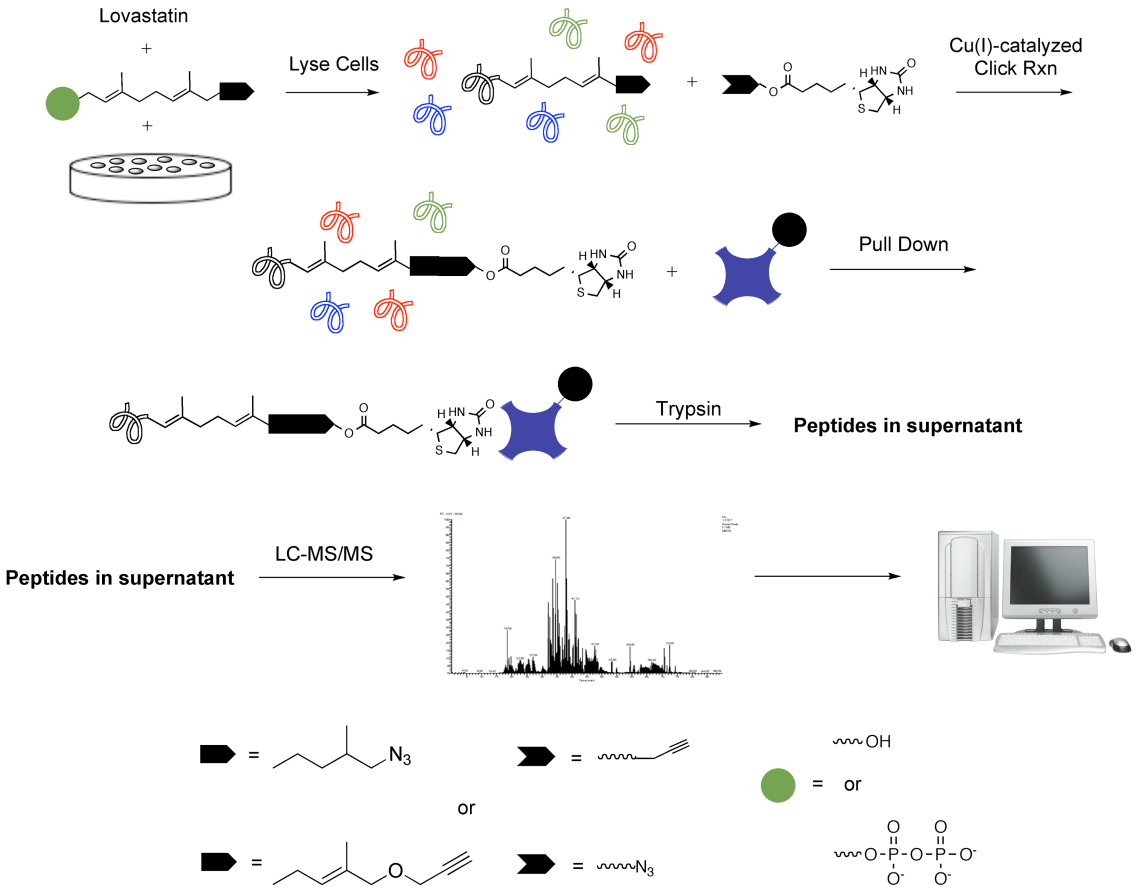

Figure 4.9 Chemical prenylomics procedure for the enrichment and identification of prenylated proteins

Despite multiple runs, no protein IDs were made at greater than 95% confidence with either probe. Upon lowering the percent confidence threshold to 90%, two IDs were made from cells treated with C15-alkyne probe (**6**, R = $P_2O_6^{3-}$) (Table 4.2). The first protein, Annexin A2, was previously identified by the Tamanoi group using the C15-azide probe (Figure 4.2, **1**)[59]. Regardless of the identification via chemical proteomic methods, Annexin A2 has never been experimentally verified as a substrate for protein prenyltransferases. Given that it contains a C-terminal sequence not known to signal prenylation (-CGGDD), further studies are needed for confirmation. The second protein identified, Rab21, is a member of the Ras oncogene family. This protein has been

previously identified using the azide-isoprenoid probe (**2**).[58, 59] The C-terminal sequence, CCSSG is interesting in that it could potentially be a substrate for PFTase as it contains the CAAX consensus sequence, or it could be a substrate for PGGTase-II as it contains two adjacent cysteine residues.[70, 71]

Table 4.2 Proteins identified by chemical prenylomics

Probe used for enrichment	Protein Name	C-terminal sequence	% Coverage
C15-alkyne (**6**, R = $P_2O_6^{3-}$)	Annexin A2	YLCGGDD	7.4
C15-alkyne (**6**, R = $P_2O_6^{3-}$)	Rab21	GGCCSSG	16

Based on the lack of substantial results, further refinement in our enrichment procedure is required. Because one of the limiting factors in LC-MS/MS is dynamic range, pre-fractionation of tryptic digest peptides by strong cation exchange (SCX) may be beneficial. For instance, when performing large-scale profiling of the protein palmitoylome using chemical proteomics, Cravatt and coworkers applied a version of LC-MS/MS known as MudPIT to maximize the probability of protein identification[56]. MudPIT, or Multidimensional Protein Identification Technology, uses columns consisting of SCX material back-to-back with reversed phase (RP) material inside fused silica capillaries. The chromatography proceeds in cycles, each comprising an increase in salt concentration to "bump" peptides off of the SCX followed by a gradient of increasing hydrophobicity to progressively elute peptides from the RP into the ion source.[70] Increasing the amount of crude cell lysate prior to enrichment may also prove to be beneficial.[25]

4.4 Conclusions and Future Directions

The Distefano lab has created a second generation of isoprenoid analogues for the chemical proteomic analysis of protein prenylation. The benefit of these analogues over others previously developed is two-fold. First, the azide-isoprenoid probe (Figure 4.3) does not suffer from isomerization of the azido-tag, which could convolute chromatographic separation of labeled peptides. Second, less non-specific labeling occurs in lysates from cells treated with the alkyne-isoprenoids (Figure 4.4) and subsequently reacted with azido-capture reagents. The applicability of our probes towards the global analysis of protein prenylation and its inhibition across a number of cell lines has been demonstrated. Analysis of other PFTase and PGGTase-I inhibitors, as well inhibitors of PGGTase-II in other tumorigenic cell lines is currently underway. Future work will involve refinement of the prenylated protein enrichment and identification procedure. Adjustments will include starting with larger amounts of crude cell lysate and performing a 2-D separation of peptides prior to the tandem mass spectrometry analysis.

A major driving force behind the development of chemical proteomic tools for the analysis of protein prenylation was the necessity to identify and study the targets of protein prenyltransferase inhibitors *in vivo*. Given the added benefits of our probes over the commercially available probes, we would like to apply them towards the identification of the labeled peptides from prenylated proteins. Methods have been developed by the Cravatt lab for the identification of modified proteins in activity-based protein profiling[72, 73], which should be readily amendable towards the study of protein post-translational modification sites. Quantitative proteomic methods, such as iTRAQ,

are becoming the technique of choice for the quantification of changes within a proteome, particularly upon exposure to an inhibitor.[74-78] The key component in a quantitative proteomic experiment is identification of the tagged-peptide. By coupling our probes with a tandem orthogonal proteolysis technique in which there is an isobaric tag incorporated into the capture reagent[79], we could potentially identify and quantify the targets of protein prenyltransferase inhibitors, which would be essential in the classification of prenyltransferase inhibitor mechanism of action.

4.5 Experimental

4.5.1 General cell growth and lysis for in-gel fluorescence experiments

Cells (40-50% confluence) were grown in DMEM supplemented with 10% FBS, 25 μM lovastatin, and 50 μM **5** (R = H) or 50 μM **6** (R = H) or 50 μM **7** (R = H) or 50 μM **7** (R = $P_2O_6^{3-}$). In some cases, the PFTase inhibitor L-778,834 at 10 μM (FTI) or the PGGTase-I inhibitor GGTI-286 (GGTI) at 5 μM were included in the cell media. The cells were allowed to reach 80-90% confluence (~ 24 h) and then washed with PBS. Cells were then suspended in PBS, placed in 1.5 mL microcentrifuge tube, and pelleted by centrifugation at 2,000 × *g*, 4 °C, for 5 min. After discarding the supernatant, a PBS solution containing 0.1% SDS, 0.2% Triton X-100, protease inhibitor cocktail (Sigma Aldrich), benzonase (Sigma Aldrich) and 2.4 μM PMSF was added to the cell pellet. After vigorous vortexing, cell lysate was harvested by sonicating 4 times for 10 sec each with 20 sec intervals between sonications. The concentration of protein in the lysate was determined using BioRad's DC protein assay.

4.5.2 Comparison of azide- and alkyne-modified isoprenoid analogues

To 100 μg (0.83 mg/mL) of HeLa lysate protein was added 25, 50, or 100 μM TAMRA-azide (Invitrogen) or TAMRA-alkyne (Invitrogen), 50 mM TCEP (Sigma), and 100 μM TBTA (Sigma Aldrich). After vortexing, 1 mM $CuSO_4$ was added and the reaction was allowed to proceed at rt for 1 h. Excess reagents were removed by protein preciption with Calbiochem's ProteoExtract protein precipitation kit. Protein pellets were suspended in 1x Laemmli SDS-PAGE loading buffer and sonicated in a water bath for 20 min to ensure dissolution. A 12% acrylamide gel was loaded with 15 μg of protein for in-gel fluorescence scanning and visualized on a BioRad FX Molecular Imager.

4.5.3 Analyzing changes in protein prenylation upon exposure to an inhibitor

To the cell lysate (1-2 mg/mL of protein) from one 60 mm dish of cells was added 50 μM TAMRA-azide (Invitrogen) or TAMRA-alkyne (Invitrogen), 50 mM TCEP (Sigma Aldrich), and 100 μM TBTA (Sigma Aldrich). After vortexing, 1 mM $CuSO_4$ was added and the reaction was allowed to proceed at rt for 1 h. Excess reagents were removed by protein preciption with Calbiochem's ProteoExtract protein precipitation kit. Protein pellets (200-300 μg of total protein) were suspended in 1X Laemmli SDS-PAGE loading buffer and sonicated in a water bath for 20 min to ensure dissolution. A 12% acrylamide gel was loaded with ~ 10 μg of protein for in-gel fluorescence scanning and visualized on a BioRad FX Molecular Imager.

4.5.4 COS cell growth and lysis for identification of labeled and enriched proteins

COS cells (40-50% confluence) were grown in DMEM supplemented with 10% FBS, 25 μM lovastatin, and 50 μM **4** (R = H) or 50 μM **6** (R = $P_2O_6^{3-}$). The cells were allowed to reach 80-90% confluence (~ 24 h) then washed with PBS. Cells were then suspended in PBS, placed in 15 mL centrifuge tube, and pelleted by centrifugation at 2,000 × *g*, 4°C, for 5 min. A PBS solution containing 0.1% SDS, 0.2% Triton X-100, protease inhibitor cocktail (Sigma), and 2.4 μM PMSF was added to the cell pellet. After vigorous vortexing, cell lysate was harvested by sonicating 4 times for 10 sec each with 20 sec intervals between sonications. The concentration of protein in the lysate was determined using BioRad's DC protein assay.

4.5.5 Enrichment of prenylated proteins from COS cells

To the COS cell lysate (1-2 mg/mL of protein, ~2 mg total protein) was added 50 μM Biotin-azide (Invitrogen) or Biotin-alkyne (Invitrogen), 50 mM TCEP (Sigma), and 100 μM TBTA (Sigma Aldrich). After vortexing, 1 mM $CuSO_4$ was added and the reaction was left to mix at rt for 1 h. Excess reagents were removed by protein precipitation with Calbiochem's ProteoExtract protein precipitation kit. Protein pellets (1-2 mg of total protein) from reaction with Biotin-azide or Biotin-alkyne were suspended in PBS containing 1.2% SDS, sonicated until solubilized, and then diluted 6X with PBS. Neutravidn-agarose beads (Thermo Scientific) were added and the samples were rotated for 2 h at rt, then washed 3X with 10 mL of PBS containing 0.2% SDS, 3X with 10 mL of PBS, and 1X with 10 mL of 50 mM NH_4HCO_3. Resin was then incubated with 0.04% SDS in 50 mM NH_4HCO_3, reduced with 1 mM TCEP for 1 hr at 60 °C, and alkylated

with 4 mM methyl methanethiosulfonate for 10 min at rt. Next, the solution was adjusted to contain 1 mM $CaCl_2$ and the samples were digested with sequence-grade trypsin (Applied Biosystems) overnight at 37 °C. Supernatants were collected the following day, acidified with 10% formic acid, and vacufuged to dryness. The resulting pellet was dissolved in nanopure H_2O containing 0.1% formic acid, and solid phase extraction with an MCX cartridge (Waters) was used to desalt the peptides. First, peptides were bound to the column, then washed with 5% MeOH in H_2O containing 0.1% formic acid and 100% MeOH. The peptides were then eluted with 1.4 % NH_4OH in MeOH and vacufuged to dryness.

4.5.6 LC-MS/MS analysis of prenylated proteins enriched from COS cells

Dried MCX eluent was reconstituted with reversed-phase load buffer (98:2 water/acetonitrile, 0.1% formic acid) and injected onto an Agilent 1100 series capillary HPLC system online with a 4000 Q-Trap MS/MS system (Applied Biosystems/MDS Sciex, Concord, ON, Canada). Peptides were loaded onto a LC Packings (Dionex Company) μ-precolumn™ cartridge (PepMap C18 5 μm, 0.3 mm internal diameter x 5 mm length) for desalting prior to loading onto a 0.075 x 100 mm fused silica column (IntegraFrit CAPILLARY, New Objective, Woburn, MA), packed in house with C18 packing material (5 mm particle size, 200 Å pore size; Michrom BioResources, Auburn, CA)[79]. The peptides were eluted with a linear gradient from 3% to 75% B over 15 min then 75% to 90% B over 5 min or with a longer gradient from 2% to 35% B over 60 min then 35% to 80% B over 15 min. Solvent B was 2:95 water/acetonitrile, 0.1% formic acid and solvent A was the same as load buffer above. MS/MS spectra were collected in

information-dependent acquisition (IDA) mode which included continuous cycles of one enhanced MS (EMS) scan from *m/z* 400 to 2400 (0.5 s), one enhanced resolution (ER) scan (0.5 s) to determine charge state and four product ion scans from *m/z* 50 to 2,000 (2 s each). Analyst™ software selected precursor *m/z* values (top 4 most intense ions) from a peak list automatically generated from the EMS scan during acquisition. ProteinPilot™ 3.0 software (Applied Biosystems) with the Paragon Algorithm[80] was used for the protein identification. Tandem mass spectrometry data were searched against the NCBI reference sequence mammalian protein database v20080307 (318899 proteins) plus common contaminants (179 proteins). The search parameters were ≥95% confidence for protein identification threshold, trypsin as enzyme, methylmethanethiosulfonate-labeled cysteines as fixed modification and thorough ID as search method. Greater than 150 variable modifications, such as oxidation of methionine and deamidation of asparagines, were included in the selection of the biological modifications parameter. MS/MS spectra were also searched against the above database using Mascot® software.

4.6 References

1. Sebti, S. M.; Hamilton, A. D., Inhibition of Rho GTPases using protein geranylgeranyltransferase I inhibitors. *Methods Enzymol.* **2000,** *325*, 381-388.

2. Sebti, S. M.; Hamilton, A. D., Farnesyltransferase and geranylgeranyltransferase I inhibitors and cancer therapy: lessons from mechanism and bench-to-bedside translational studies. *Oncogene* **2000,** *19*, 6584-6593.

3. Crul, M.; de Klerk, G. J.; Beijnen, J. H.; Schellens, J. H., Ras biochemistry and farnesyl transferase inhibitors: a literature survey. *Anti-cancer drugs* **2001,** *12*, 163-184.

4. End, D. W. M., L.; Angibaud, P., Farnesyl protein transferase inhibitors: medicinal chemistry, molecular mechanisms, and progress in the Clinic. *Top. Med. Chem.* **2007,** *1*, 133-168.

5. Du, W.; Lebowitz, P. F.; Prendergast, G. C., Cell growth inhibition by farnesyltransferase inhibitors is mediated by gain of geranylgeranylated RhoB. *Mol. Cell. Biol.* **1999,** *19*, 1831-40.

6. Du, W.; Prendergast, G. C., Geranylgeranylated RhoB mediates suppression of human tumor cell growth by farnesyltransferase inhibitors. *Cancer Res.* **1999,** *59*, 5492-5496.

7. Lebowitz, P. F.; Casey, P. J.; Prendergast, G. C.; Thissen, J. A., Farnesyltransferase inhibitors alter the prenylation and growth-stimulating function of RhoB. *J. Biol. Chem.* **1997,** *272*, 15591-15594.

8. van Golen, K. L.; Bao, L.; DiVito, M. M.; Wu, Z.; Prendergast, G. C.; Merajver, S. D., Reversion of RhoC GTPase-induced inflammatory breast cancer phenotype by treatment with a farnesyl transferase inhibitor. *Mol. Cancer Ther.* **2002,** *1*, 575-583.

9. Castro, A. F.; Rebhun, J. F.; Clark, G. J.; Quilliam, L. A., Rheb binds tuberous sclerosis complex 2 (TSC2) and promotes S6 kinase activation in a rapamycin- and farnesylation-dependent manner. *J. Biol. Chem.* **2003,** *278,* 32493-32496.

10. Jiang, K.; Coppola, D.; Crespo, N. C.; Nicosia, S. V.; Hamilton, A. D.; Sebti, S. M.; Cheng, J. Q., The phosphoinositide 3-OH kinase/AKT2 pathway as a critical target for farnesyltransferase inhibitor-induced apoptosis. *Mol. Cell. Biol.* **2000,** 20, 139-148.

11. Law, B. K.; Norgaard, P.; Moses, H. L., Farnesyltransferase inhibitor induces rapid growth arrest and blocks p70s6k activation by multiple stimuli. *J. Biol. Chem.* **2000,** *275*, 10796-10801.

12. Liu, A.; Prendergast, G. C., Geranylgeranylated RhoB is sufficient to mediate tissue-specific suppression of Akt kinase activity by farnesyltransferase inhibitors. *FEBS Lett.* **2000,** *481*, 205-208.

13. Tamanoi, F.; Kato-Stankiewicz, J.; Jiang, C.; Machado, I.; Thapar, N., Farnesylated proteins and cell cycle progression. *J. Cell. Biochem. Suppl.* **2001,** *37*, 64-70.

14. Ashar, H. R.; James, L.; Gray, K.; Carr, D.; Black, S.; Armstrong, L.; Bishop, W. R.; Kirschmeier, P., Farnesyl transferase inhibitors block the farnesylation of CENP-E and CENP-F and alter the association of CENP-E with the microtubules. *J. Biol. Chem.* **2000,** *275*, 30451-30457.

15. Crespo, N. C.; Ohkanda, J.; Yen, T. J.; Hamilton, A. D.; Sebti, S. M., The farnesyltransferase inhibitor, FTI-2153, blocks bipolar spindle formation and chromosome alignment and causes prometaphase accumulation during mitosis of human lung cancer cells. *J. Biol. Chem.* **2001,** *276*, 16161-16167.

16. Adnane, J.; Bizouarn, F. A.; Qian, Y.; Hamilton, A. D.; Sebti, S. M., p21(WAF1/CIP1) is upregulated by the geranylgeranyltransferase I inhibitor GGTI-298 through a transforming growth factor beta- and Sp1-responsive element: involvement of the small GTPase rhoA. *Mol. Cell. Biol.* **1998,** *18*, 6962-6970.

17. Vogt, A.; Sun, J.; Qian, Y.; Hamilton, A. D.; Sebti, S. M., The geranylgeranyltransferase-I inhibitor GGTI-298 arrests human tumor cells in G0/G1 and

induces p21(WAF1/CIP1/SDI1) in a p53-independent manner. *J. Biol. Chem.* **1997,** *272*, 27224-27229.

18. Prendergast, G. C., Actin' up: RhoB in cancer and apoptosis. *Nat. Rev. Cancer* **2001,** *1*, 162-168.

19. Sebti, S. M.; Der, C. J., Opinion: Searching for the elusive targets of farnesyltransferase inhibitors. *Nat. Rev. Cancer* **2003,** *3*, 945-951.

20. Lackner, M. R.; Kindt, R. M.; Carroll, P. M.; Brown, K.; Cancilla, M. R.; Chen, C.; de Silva, H.; Franke, Y.; Guan, B.; Heuer, T.; Hung, T.; Keegan, K.; Lee, J. M.; Manne, V.; O'Brien, C.; Parry, D.; Perez-Villar, J. J.; Reddy, R. K.; Xiao, H.; Zhan, H.; Cockett, M.; Plowman, G.; Fitzgerald, K.; Costa, M.; Ross-Macdonald, P., Chemical genetics identifies Rab geranylgeranyl transferase as an apoptotic target of farnesyl transferase inhibitors. *Cancer Cell* **2005,** *7*, 325-336.

21. Sebti, S. M., Protein farnesylation: implications for normal physiology, malignant transformation, and cancer therapy. *Cancer Cell* **2005,** *7*, 297-300.

22. Maurer-Stroh, S.; Koranda, M.; Benetka, W.; Schneider, G.; Sirota, F. L.; Eisenhaber, F., Towards complete sets of farnesylated and geranylgeranylated proteins. *PLoS Comput. Biol.* **2007,** *3*, e66.

23. Kislinger, T.; Emili, A., Multidimensional protein identification technology: current status and future prospects. *Expert Rev. Proteomics* **2005,** *2*, 27-39.

24. Reinders, J.; Lewandrowski, U.; Moebius, J.; Wagner, Y.; Sickmann, A., Challenges in mass spectrometry-based proteomics. *Proteomics* **2004,** *4*, 3686-3703.

25. Tate, E. W., Recent advances in chemical proteomics: exploring the post-translational proteome. *J. Biol. Chem.* **2008,** *1*, 17-26.

26. Sletten, E. M. and Bertozzi, C.R., Bioorthogonal chemistry: fishing for selectivity in a sea of functionality. *Angew. Chem. Int. Ed.* **2009,** *48*, 6974-6998.

27. Mahal, L. K. Y., K.J.; Bertozzi, C.R., Engineering chemical reactivity on cell surfaces through oligosaccharide biosynthesis. *Science* **1997,** *276*, 1125-1128.

28. Hang, H. C., Bertozzi, C. R., Ketone Isosteres of 2-N-Acetamidosugars as substrates for metabolic cell surface engineering. *J. Am. Chem. Soc.* **2001,** *123*, 1242-1243.

29. Saxon, E. a. B., C.R., Cell surface engineering by a modified Staudinger reaction. *Science* **2000,** *287*, 2007-2010.

30. Saxon, E. L., S. J.; Hang, H. C.; Yu, C.; Lee, S. C.; Bertozzi, C. R., Investigating cellular metabolism of synthetic azidosugars using the Staudinger ligation. *J. Am. Chem. Soc.* **2002,** *124*, 14893-14902.

31. Prescher, J. A. D., D. H.; Bertozzi, C. R., Chemical remodelling of cell surfaces in living animals. *Nature* **2004,** *430*, 873-877.

32. Lin, F., Hoyt, H. M.; van Halbeek, H.; Bergman, R. G.; Bertozzi, C. R., Mechanistic investigation of the Staudinger ligation. *J. Am. Chem. Soc.* **2005,** *127*, 2686-2695.

33. Huisgen, R., Kinetics and mechanism of 1,3-dipolar cycloaddition. *Angew. Chem. Int. Ed.* **1963,** *2*, 633-645.

34. Tornoe, C. W.; Christensen, C.; Meldal, M., Peptidotriazoles on solid phase: [1,2,3]-triazoles by regiospecific copper(I)-catalyzed 1,3-dipolar cycloadditions of terminal alkynes to azides. *J. Org. Chem.* **2002,** *67*, 3057-3064.

35. Rostovtsev, V. V.; Green, L. G.; Fokin, V. V.; Sharpless, K. B., A stepwise huisgen cycloaddition process: copper(I)-catalyzed regioselective "ligation" of azides and terminal alkynes. *Angew. Chem. Int. Ed.* **2002,** *41*, 2596-2599.

36. Chan, T. R.; Hilgraf, R.; Sharpless, K. B.; Fokin, V. V., Polytriazoles as copper(I)-stabilizing ligands in catalysis. *Org. Lett.* **2004,** *6*, 2853-2855.

37. Kolb, H. C.; Finn, M. G.; Sharpless, K. B., Click chemistry: diverse chemical function from a few good reactions. *Angew. Chem. Int. Ed.* **2001,** *40*, 2004-2021.

38. Fokin, V. V., Click imaging of biochemical processes in living systems. *ACS Chem. Biol.* **2007,** *2*, 775-778.

39. Dieterich, D. C.; Lee, J. J.; Link, A. J.; Graumann, J.; Tirrell, D. A.; Schuman, E. M., Labeling, detection and identification of newly synthesized proteomes with bioorthogonal non-canonical amino-acid tagging. *Nat. Protoc.* **2007,** *2*, 532-540.

40. Breinbauer, R.; Kohn, M., Azide-alkyne coupling: a powerful reaction for bioconjugate chemistry. *Chembiochem* **2003,** *4*, 1147-1149.

41. Agard, N. J.; Prescher, J. A.; Bertozzi, C. R., A strain-promoted [3 + 2] azide-alkyne cycloaddition for covalent modification of biomolecules in living systems. *J. Am. Chem. Soc.* **2004,** *126*, 15046-15047.

42. Baskin, J. M.; Prescher, J. A.; Laughlin, S. T.; Agard, N. J.; Chang, P. V.; Miller, I. A.; Lo, A.; Codelli, J. A.; Bertozzi, C. R., Copper-free click chemistry for dynamic in vivo imaging. *Proc. Natl. Acad. Sci. U. S. A.* **2007,** *104*, 16793-16797.

43. Codelli, J. A.; Baskin, J. M.; Agard, N. J.; Bertozzi, C. R., Second-generation difluorinated cyclooctynes for copper-free click chemistry. *J. Am. Chem. Soc.* **2008,** *130*, 11486-11493.

44. Ning, X.; Guo, J.; Wolfert, M. A.; Boons, G. J., Visualizing metabolically labeled glycoconjugates of living cells by copper-free and fast huisgen cycloadditions. *Angew. Chem. Int. Ed.* **2008,** *47*, 2253-2255.

45. Bertozzi, C. R.; Kiessling, L. L., Chemical glycobiology. *Science* **2001,** *291*, 2357-2364.

46. Gama, C. I.; Hsieh-Wilson, L. C., Chemical approaches to deciphering the glycosaminoglycan code. *Curr. Opin. Chem. Biol.* **2005,** *9*, 609-619.

47. Laughlin, S. T.; Bertozzi, C. R., Metabolic labeling of glycans with azido sugars and subsequent glycan-profiling and visualization via Staudinger ligation. *Nat. Protoc.* **2007,** *2*, 2930-44.

48. Luchansky, S. J.; Argade, S.; Hayes, B. K.; Bertozzi, C. R., Metabolic functionalization of recombinant glycoproteins. *Biochemistry* **2004,** *43*, 12358-12366.

49. Sprung, R.; Nandi, A.; Chen, Y.; Kim, S. C.; Barma, D.; Falck, J. R.; Zhao, Y., Tagging-via-substrate strategy for probing O-GlcNAc modified proteins. *J. Proteome Res.* **2005,** *4*, 950-957.

50. Warthaka, M.; Karwowska-Desaulniers, P.; Pflum, M. K., Phosphopeptide modification and enrichment by oxidation-reduction condensation. *ACS Chem. Biol.* **2006,** *1*, 697-701.

51. Zhou, H.; Watts, J. D.; Aebersold, R., A systematic approach to the analysis of protein phosphorylation. *Nat. Biotechnol.* **2001,** *19*, 375-378.

52. Charron, G.; Zhang, M. M.; Yount, J. S.; Wilson, J.; Raghavan, A. S.; Shamir, E.; Hang, H. C., Robust fluorescent detection of protein fatty-acylation with chemical reporters. *J. Am. Chem. Soc.* **2009,** 131, 4967-4975.

53. Hang, H. C.; Geutjes, E. J.; Grotenbreg, G.; Pollington, A. M.; Bijlmakers, M. J.; Ploegh, H. L., Chemical probes for the rapid detection of Fatty-acylated proteins in Mammalian cells. *J. Am. Chem. Soc.* **2007,** *129*, 2744-2745.

54. Heal, W. P.; Wickramasinghe, S. R.; Bowyer, P. W.; Holder, A. A.; Smith, D. F.; Leatherbarrow, R. J.; Tate, E. W., Site-specific N-terminal labeling of proteins in vitro and in vivo using N-myristoyl transferase and bioorthogonal ligation chemistry. *Chem. Commun.* **2008**, *4*, 480-482.

55. Kostiuk, M. A.; Corvi, M. M.; Keller, B. O.; Plummer, G.; Prescher, J. A.; Hangauer, M. J.; Bertozzi, C. R.; Rajaiah, G.; Falck, J. R.; Berthiaume, L. G., Identification of palmitoylated mitochondrial proteins using a bio-orthogonal azido-palmitate analogue. *Faseb J.* **2008,** *22*, 721-732.

56. Martin, B. R.; Cravatt, B. F., Large-scale profiling of protein palmitoylation in mammalian cells. *Nat Methods* **2009,** *6*, 135-138.

57. Roth, A. F.; Wan, J.; Green, W. N.; Yates, J. R.; Davis, N. G., Proteomic identification of palmitoylated proteins. *Methods* **2006,** *40*, 135-142.

58. Chan, L. N.; Hart, C.; Guo, L.; Nyberg, T.; Davies, B. S.; Fong, L. G.; Young, S. G.; Agnew, B. J.; Tamanoi, F., A novel approach to tag and identify geranylgeranylated proteins. *Electrophoresis* **2009,** *30*, 3598-3606.

59. Kho, Y.; Kim, S. C.; Jiang, C.; Barma, D.; Kwon, S. W.; Cheng, J.; Jaunbergs, J.; Weinbaum, C.; Tamanoi, F.; Falck, J.; Zhao, Y., A tagging-via-substrate technology for detection and proteomics of farnesylated proteins. *Proc. Natl. Acad. Sci. U. S. A.* **2004,** *101*, 12479-12484.

60. Nguyen, U. T.; Guo, Z.; Delon, C.; Wu, Y.; Deraeve, C.; Franzel, B.; Bon, R. S.; Blankenfeldt, W.; Goody, R. S.; Waldmann, H.; Wolters, D.; Alexandrov, K., Analysis of the eukaryotic prenylome by isoprenoid affinity tagging. *Nat. Chem. Biol.* **2009,** *5*, 227-235.

61. Labadie, G. R.; Viswanathan, R.; Poulter, C. D., Farnesyl diphosphate analogues with omega-bioorthogonal azide and alkyne functional groups for protein farnesyl transferase-catalyzed ligation reactions. *J. Org. Chem.* **2007,** *72*, 9291-9297.

62. Xu, J.; Degraw, A. J.; Duckworth, B. P.; Lenevich, S.; Tann, C. M.; Jenson, E. C.; Gruber, S. J.; Barany, G.; Distefano, M. D., Synthesis and reactivity of 6,7-dihydrogeranylazides: reagents for primary azide incorporation into peptides and subsequent staudinger ligation. *Chem. Biol. Drug Des.* **2006,** *68*, 85-96.

63. Duckworth, B. P.; Xu, J.; Taton, T. A.; Guo, A.; Distefano, M. D., Site-specific, covalent attachment of proteins to a solid surface. *Bioconjugate Chem.* **2006,** *17*, 967-974.

64. Duckworth, B. P.; Zhang, Z.; Hosokawa, A.; Distefano, M. D., Selective labeling of proteins by using protein farnesyltransferase. *Chembiochem* **2007,** *8*, 98-105.

65. Hosokawa, A. W., J.W.; Zhang, Z.; Chen, L.; Barany, G.; Distefano, M.D., Evaluation of an alkyne-containing analogue of farnesyldiphosphate as a dual substrate for protein-prenyltransferases. *Int. J. Pep. Res. Ther.* **2007,** *13*, 345-354.

66. Speers, A. E.; Cravatt, B. F., Profiling enzyme activities in vivo using click chemistry methods. *Chem. Biol.* **2004,** *11*, 535-546.

67. Cole, S. L. V., R., Isoprenoids and Alzheimer's disease: A complex relationship. *Neurobiol. Dis.* **2006,** *22*, 209-222.

68. Eckert, G. P.; Hooff, G. P.; Strandjord, D. M.; Igbavboa, U.; Volmer, D. A.; Muller, W. E.; Wood, W. G., Regulation of the brain isoprenoids farnesyl- and geranylgeranylpyrophosphate is altered in male Alzheimer patients. *Neurobiol. Dis.* **2009,** 35, 251-257.

69. Fiacco, T. A.; Agulhon, C.; McCarthy, K. D., Sorting out astrocyte physiology from pharmacology. *Annu. Rev. Pharmacol. Toxicol.* **2009,** *49*, 151-174.

70. Zhang, F. L.; Casey, P. J., Protein prenylation: molecular mechanisms and functional consequences. *Annu. Rev. Biochem.* **1996,** *65*, 241-269.

71. Pereira-Leal J.B.; Hume, A. N. S., M.C., Prenylation of Rab GTPases: Molecular mechanisms and involvement in genetic disease. *FEBS Lett.* **2001,** *498*, 197-200.

72. Weerapana, E.; Speers, A. E.; Cravatt, B. F., Tandem orthogonal proteolysis-activity-based protein profiling (TOP-ABPP)--a general method for mapping sites of probe modification in proteomes. *Nat. Protoc.* **2007,** *2*, 1414-1425.

73. Speers, A. E.; Cravatt, B. F., A tandem orthogonal proteolysis strategy for high-content chemical proteomics. *J. Am. Chem. Soc.* **2005,** *127*, 10018-10019.

74. Yang, Y.; Chaerkady, R.; Beer, M. A.; Mendell, J. T.; Pandey, A., Identification of miR-21 targets in breast cancer cells using a quantitative proteomic approach. *Proteomics* **2009,** *9*, 1374-1384.

75. Tenorio-Laranga, J.; Valero, M. L.; Maennistoe, P. T.; del Pino, M. S.; Garcia-Horsman, J. A., Combination of snap freezing, differential pH two-dimensional reverse-phase high-performance liquid chromatography, and iTRAQ technology for the peptidomic analysis of the effect of prolyl oligopeptidase inhibition in the rat brain. *Anal. Biochem.* **2009,** *393*, 80-87.

76. White, F. M., On the iTRAQ of kinase inhibitors. *Nat. Biotechnol.* **2007,** *25*, 994-996.

77. Peters, E. C. and Gray, N. S., Chemical proteomics identifies unanticipated targets of clinical kinase inhibitors. *ACS Chem. Biol.* **2007,** *2*, 661-664.

78. Bantscheff, M.; Eberhard, D.; Abraham, Y.; Bastuck, S.; Boesche, M.; Hobson, S.; Mathieson, T.; Perrin, J.; Raida, M.; Rau, C.; Reader, V.; Sweetman, G.; Bauer, A.; Bouwmeester, T.; Hopf, C.; Kruse, U.; Neubauer, G.; Ramsden, N.; Rick, J.; Kuster, B.; Drewes, G., Quantitative chemical proteomics reveals mechanisms of action of clinical ABL kinase inhibitors. *Nat. Biotechnol.* **2007,** *25*, 1035-1044.

79. Weerapana, E.; Cravatt, B. F., A quantitative mass spectrometry platform for activity-based protein profiling. *Abstract of Papers, 238th ACS National Meeting, Washington, DC, United States, August 16-20, 2009* **2009**, ORGN-240.

Bibliography

Liang, P.-H.; Ko, T.-P.; Wang, A. H. J., Structure, mechanism and function of prenyltransferases. *Eur. J. Biochem.* **2002,** *269*, 3339-3354.

Poulter, C. D.; Rilling, H. C., Prenyl transferases and isomerase. *Biosynth. Isoprenoid Compd.* **1981,** *1*, 161-224.

Robyt, J. F., *Essentials of Carbohydrate Chemistry*. **1998**; p 400.

Sato, M.; Sato, K.; Nishikawa, S.-I.; Hirata, A.; Kato, J.-I.; Nakano, A., The yeast RER2 gene, identified by endoplasmic reticulum protein localization mutations, encodes cis-prenyltransferase, a key enzyme in dolichol synthesis. *Mol. Cell. Biol.* **1999,** *19*, 471-483.

Cornish, K., Biochemistry of natural rubber, a vital raw material, emphasizing biosynthetic rate, molecular weight and compartmentalization, in evolutionarily divergent plant species (1963 to 2000). *Nat. Prod. Rep.* **2001,** *18*, 182-189.

Zhang, F. L.; Casey, P. J., Protein prenylation: molecular mechanisms and functional consequences. *Annu. Rev. Biochem.* **1996,** *65*, 241-269.

Gelb, M. H.; Brunsveld, L.; Hrycyna, C. A.; Michaelis, S.; Tamanoi, F.; Van Voorhis, W. C.; Waldmann, H., Therapeutic intervention based on protein prenylation and associated modifications. *Nat. Chem. Biol.* **2006,** *2*, 518-528.

Sebti, S. M., Protein farnesylation: Implications for normal physiology, malignant transformation, and cancer therapy. *Cancer Cell* **2005,** *7*, 297-300.

Lowy, D. R.; Willumsen, B. M., Function and regulation of ras. *Annu. Rev. Biochem.* **1993,** *62*, 851-891.

Hirsch, A. K. H.; Diederich, F., The non-mevalonate pathway to isoprenoid biosynthesis: a potential source of new drug targets. *Chimia* **2008,** *62*, 226-230.

Lange, B. M.; Rujan, T.; Martin, W.; Croteau, R., Isoprenoid biosynthesis: the evolution of two ancient and distinct pathways across genomes. *Proc. Natl. Acad. Sci. U. S. A.* **2000,** *97*, 13172-13177.

Koyama, T., Molecular analysis of prenyl chain elongating enzymes. *Biosci., Biotechnol., Biochem.* **1999,** *63*, 1671-1676.

Koyama, T.; Ogura, K., Isopentenyl diphosphate isomerase and prenyltransferases. *Compr. Nat. Prod. Chem.* **1999,** *2*, 69-96.

Ogura, K.; Koyama, T., Enzymic aspects of isoprenoid chain elongation. *Chem. Rev.* **1998,** *98*, 1263-1276.
Zhang, Y. W.; Koyama, T.; Marecak, D. M.; Prestwich, G. D.; Maki, Y.; Ogura, K., Two subunits of heptaprenyl diphosphate synthase of *Bacillus subtilis* form a catalytically active complex. *Biochemistry* **1998,** *37*, 13411-13420.

Ohnuma, S.; Koyama, T.; Ogura, K., Purification of solanesyl-diphosphate synthase from *Micrococcus luteus*. A new class of prenyltransferase. *J. Biol. Chem.* **1991,** *266*, 23706-23713.

Takahashi, S.; Koyama, T., Structure and function of cis-prenyl chain elongating enzymes. *Chem. Rec.* **2006,** *6*, 194-205.

Kharel, Y.; Koyama, T., Molecular analysis of cis-prenyl chain elongating enzymes. *Nat. Prod. Rep.* **2003,** *20*, 111-118.

Fujihashi, M.; Zhang, Y.-W.; Higuchi, Y.; Li, X.-Y.; Koyama, T.; Miki, K., Crystal structure of cis-prenyl chain elongating enzyme, undecaprenyl diphosphate synthase. *Proc. Natl. Acad. Sci. U. S. A.* **2001,** *98*, 4337-4342.

Reid, T. S.; Terry, K. L.; Casey, P. J.; Beese, L. S., Crystallographic analysis of CaaX prenyltransferases complexed with substrates defines rules of protein substrate selectivity. *J. Mol. Biol.* **2004,** *343*, 417-433.

Maurer-Stroh, S.; Koranda, M.; Benetka, W.; Schneider, G.; Sirota, F. L.; Eisenhaber, F., Towards complete sets of farnesylated and geranylgeranylated proteins. *PLoS Comput. Biol.* **2007,** *3*, e66.

Tamanoi, F.; Kato-Stankiewicz, J.; Jiang, C.; Machado, I.; Thapar, N., Farnesylated proteins and cell cycle progression. *J. Cell. Biochem. Suppl.* **2001,** *37*, 64-70.
23. Armstrong, S. A.; Hannah, V. C.; Goldstein, J. L.; Brown, M. S., CAAX geranylgeranyl transferase transfers farnesyl as efficiently as geranylgeranyl to RhoB. *J. Biol. Chem.* **1995,** *270*, 7864-7868.

Dolence, J. M.; Cassidy, P. B.; Mathis, J. R.; Poulter, C. D., Yeast protein farnesyltransferase: steady-state kinetic studies of substrate binding. *Biochemistry* **1995,** *34*, 16687-16694.

Furfine, E. S.; Leban, J. J.; Landavazo, A.; Moomaw, J. F.; Casey, P. J., Protein farnesyltransferase: kinetics of farnesyl pyrophosphate binding and product release. *Biochemistry* **1995,** *34*, 6857-6862.

Rozema, D. B.; Poulter, C. D., Yeast protein farnesyltransferase. pKas of peptide substrates bound as zinc thiolates. *Biochemistry* **1999,** *38*, 13138-13146.

Sousa, S. F.; Fernandes, P. A.; Ramos, M. J., Unraveling the mechanism of the farnesyltransferase enzyme. *J. Biol. Inorg. Chem.* **2005,** *10*, 3-10.
Dolence, J. M.; Poulter, C. D., A mechanism for posttranslational modifications of proteins by yeast protein farnesyltransferase. *Proc. Natl. Acad. Sci. U. S. A.* **1995,** *92*, 5008-5011.

Lenevich, S.; Hosokawa, A.; Cramer, C. J.; Distefano, M. D., Transition state analysis of model and enzymatic prenylation reactions. *J. Am. Chem. Soc.* **2007,** *129*, 5796-5797.

Pais, J. E.; Bowers, K. E.; Fierke, C. A., Measurement of the α-secondary kinetic isotope effect for the reaction catalyzed by mammalian protein farnesyltransferase. *J. Am. Chem. Soc.* **2006,** *128*, 15086-15087.

Turek, T. C.; Gaon, I.; Distefano, M. D.; Strickland, C. L., Synthesis of farnesyl diphosphate analogues containing ether-linked photoactive benzophenones and their application in studies of protein prenyltransferases. *J. Org. Chem.* **2001,** *66*, 3253-3264.

Kale, T. A.; Hsieh, S. A.; Rose, M. W.; Distefano, M. D., Use of synthetic isoprenoid analogues for understanding protein prenyltransferase mechanism and structure. *Curr. Top. Med. Chem.* **2003,** *3*, 1043-1074.

Scholte, A. A.; Eubanks, L. M.; Poulter, C. D.; Vederas, J. C., Synthesis and biological activity of isopentenyl diphosphate analogues. *Bioorg. Med. Chem.* **2004,** *12*, 763-770.

Labadie, G. R.; Viswanathan, R.; Poulter, C. D., Farnesyl diphosphate analogues with omega-bioorthogonal azide and alkyne functional groups for protein farnesyl transferase-catalyzed ligation reactions. *J. Org. Chem.* **2007,** *72*, 9291-9297.

Duckworth, B. P.; Zhang, Z.; Hosokawa, A.; Distefano, M. D., Selective labeling of proteins by using protein farnesyltransferase. *Chembiochem* **2007,** *8*, 98-105.

Hosokawa, A.; Wollack, J.W.; Zhang, Z.; Chen, L.; Barany, G.; Distefano, M.D., Evaluation of an alkyne-containing analogue of farnesyldiphosphate as a dual substrate for protein-prenyltransferases. *Int. J. Pep. Res. Ther.* **2007,** *13*, 345-354.

Chen, A. P.; Chen, Y. H.; Liu, H. P.; Li, Y. C.; Chen, C. T.; Liang, P. H., Synthesis and application of a fluorescent substrate analogue to study ligand interactions for undecaprenyl pyrophosphate synthase. *J. Am. Chem. Soc.* **2002,** *124*, 15217-15224.

DeGraw, A. J.; Zhao, Z.; Strickland, C. L.; Taban, A. H.; Hsieh, J.; Jefferies, M.; Xie, W.; Shintani, D. K.; McMahan, C. M.; Cornish, K.; Distefano, M. D., A photoactive isoprenoid diphosphate analogue containing a stable phosphonate linkage: synthesis and biochemical studies with prenyltransferases. *J. Org. Chem.* **2007,** *72*, 4587-4595.

Henry, O.; Lopez-Gallego, F.; Agger, S. A.; Schmidt-Dannert, C.; Sen, S.; Shintani, D.; Cornish, K.; Distefano, M. D., A versatile photoactivatable probe designed to label the

diphosphate binding site of farnesyl diphosphate utilizing enzymes. *Bioorg. Med. Chem.* **2009,** *17*, 4797-4805.

Backhaus, R. A., Rubber formation in plants - a mini-review. *Isr. J. Bot.* **1985,** *34*, 283-293.

Bonner, J., Effects of temperature on rubber accumulation by the guayule plant. *Bot. Gaz.* **1943,** *105*, 233-243.

Madhavan, S.; Greenblatt, G. A.; Foster, M. A.; Benedict, C. R., Stimulation of isopentenyl pyrophosphate incorporation into polyisoprene in extracts from guayule plants (Parthenium argentatum Gray) by low temperature and 2-(3,4-dichlorophenoxy)triethylamine. *Plant Physiol.* **1989,** *89*, 506-511.

Whitworth, J. W. W., E.E., *Guayule natural rubber: a technical publication with emphasis on recent findings*. Office of Arid Land Studies, The University of Arizona Tucson, Arizona, **1991**; p 445.

Veatch, M. E.; Ray, D. T.; Mau, C. J. D.; Cornish, K., Growth, rubber, and resin evaluation of two-year-old transgenic guayule. *Ind. Crops Prod.* **2005,** *22*, 65-74.

Cornish, K. C., J.; Chapman, M.H., *Membrane-bound cis-prenyltransferase activity: regulation and substrate specificity*. Wiley-VCH-Verlag: **1998**; p 316-323.

Tanaka, Y., Structural characterization of natural polyisoprenes: solve the mystery of natural rubber based on structural study. *Rubber Chem. Technol.* **2001,** *74*, 355-375.

Walsh, C., *Enzymatic Reaction Mechanisms*. **1979**; p 978.

Archer, B. L.; Audley, B. G., Biosynthesis of rubber. *Adv. Enzymol. Relat. Subj. Biochem.* **1967,** *29*, 221-257.

Light, D. R.; Dennis, M. S., Purification of a prenyltransferase that elongates cis-polyisoprene rubber from the latex of *Hevea brasiliensis*. *J. Biol. Chem.* **1989,** *264*, 18589-18597.

Archer, B. L. A., B.G., New aspects of rubber biosynthesis. *Bot. J. Linn. Soc.* **1987,** *94*, 181-196.

Tanaka, Y., Structure and biosynthesis mechanism of natural polyisoprene. *Prog. Polym. Sci.* **1989,** *14*, 339-371.

Tanaka, Y.; Aik-Hwee, E.; Ohya, N.; Nishiyama, N.; Tangpakdee, J.; Kawahara, S.; Wititsuwannakul, R., Initiation of rubber biosynthesis in *Hevea brasiliensis*: characterization of initiating species by structural analysis. *Phytochemistry* **1996,** *41*, 1501-1505.

Cornish, K., Similarities and differences in rubber biochemistry among plant species. *Phytochemistry* **2001,** *57*, 1123-1134.

Cornish, K., Biochemistry of natural rubber, a vital raw material, emphasizing biosynthetic rate, molecular weight and compartmentalization, in evolutionarily divergent plant species (1963 to 2000). *Nat. Prod. Rep.* **2001,** *18*, 182-189.

Cornish, K. S., D.J.; Grosjean, O-K.; Goodman, N., Fundamental similarities in rubber particle architecture and function in three evolutionarily divergent plant species. *J. Nat. Rubb. Res.* **1993,** *8*, 275-285.

Webb, Y.; Zhou, X.; Ngo, L.; Cornish, V.; Stahl, J.; Erdjument-Bromage, H.; Tempst, P.; Rifkind, R. A.; Marks, P. A.; Breslow, R.; Richon, V. M., Photoaffinity labeling and mass spectrometry identify ribosomal protein S3 as a potential target for hybrid polar cytodifferentiation agents. *J. Biol. Chem.* **1999,** *274*, 14280-14287.

Zhang, C. X.; Chang, P. V.; Lippard, S. J., Identification of nuclear proteins that interact with platinum-modified DNA by photoaffinity labeling. *J. Am. Chem. Soc.* **2004,** *126*, 6536-6537.

Gaon, I.; Turek, T. C.; Weller, V. A.; Edelstein, R. L.; Singh, S. K.; Distefano, M. D., Photoactive analogs of farnesyl pyrophosphate containing benzoylbenzoate esters: synthesis and application to photoaffinity labeling of yeast protein farnesyltransferase. *J. Org. Chem.* **1996,** *61*, 7738-7745.

Turek, T. C.; Gaon, I.; Gamache, D.; Distefano, M. D., Synthesis and evaluation of benzophenone-based photoaffinity labeling analogs of prenyl pyrophosphates containing stable amide linkages. *Bioorg. Med. Chem. Lett.* **1997,** *7*, 2125-2130.

Turek-Etienne, T. C.; Strickland, C. L.; Distefano, M. D., Biochemical and structural studies with prenyl diphosphate analogues provide insights into isoprenoid recognition by protein farnesyl transferase. *Biochemistry* **2003,** *42*, 3716-3724.

Gaon, I.; Turek, T. C.; Distefano, M. D., Farnesyl and geranylgeranyl pyrophosphate analogs incorporating benzoylbenzyl ethers: synthesis and inhibition of yeast protein farnesyltransferase. *Tet. Lett.* **1996,** *37*, 8833-8836.

Omer, C. A.; Kral, A. M.; Diehl, R. E.; Prendergast, G. C.; Powers, S.; Allen, C. M.; Gibbs, J. B.; Kohl, N. E., Characterization of recombinant human farnesyl-protein transferase: cloning, expression, farnesyl diphosphate binding, and functional homology with yeast prenyl-protein transferases. *Biochemistry* **1993,** *32*, 5167-5176.

Turek, T. C.; Gaon, I.; Distefano, M. D.; Strickland, C. L., Synthesis of farnesyl diphosphate analogues containing ether-linked photoactive benzophenones and their application in studies of protein prenyltransferases. *J. Org. Chem.* **2001,** *66*, 3253-3264.

Yokoyama, K.; McGeady, P.; Gelb, M. H., Mammalian protein geranylgeranyltransferase-I: substrate specificity, kinetic mechanism, metal requirements, and affinity labeling. *Biochemistry* **1995,** *34*, 1344-1354.

Dorman, G.; Prestwich, G. D., Benzophenone photophores in biochemistry. *Biochemistry* **1994,** *33*, 5661-5673.

Marecak, D. M.; Horiuchi, Y.; Arai, H.; Shimonaga, M.; Maki, Y.; Koyama, T.; Ogura, K.; Prestwich, G. D., Benzoylphenoxy analogs of isoprenoid diphosphates as photoactivatable substrates for bacterial prenyltransferases. *Bioorg. Med. Chem. Lett.* **1997,** *7*, 1973-1978.

Zhang, Y. W.; Koyama, T.; Marecak, D. M.; Prestwich, G. D.; Maki, Y.; Ogura, K., Two subunits of heptaprenyl diphosphate synthase of *Bacillus subtilis* form a catalytically active complex. *Biochemistry* **1998,** *37*, 13411-13420.

Blau, N. F. W., T.S.; Buess, C.M., Potential Inhibitors of cholesterol biosynthesis. Phosphonates derived from geraniol and congeners. *J. Chem. Eng. Data* **1970,** *15*, 206-208.

Popjak, G.; Hadley, C., Inhibition of liver prenyltransferase by citronellyl and geranyl phosphonate and phosphonylphosphate. *J. Lipid Res.* **1985,** *26*, 1151-1159.

Zgani, I.; Menut, C.; Seman, M.; Gallois, V.; Laffont, V.; Liautard, J.; Liautard, J.-P.; Criton, M.; Montero, J.-L., Synthesis of prenyl pyrophosphonates as new potent phosphoantigens inducing selective activation of human Vg9Vd2 T lymphocytes. *J. Med. Chem.* **2004,** *47*, 4600-4612.

Bartlett, D. L.; King, C. H. R.; Poulter, C. D., An affinity column for the purification of prenyltransferases. *Anal. Biochem.* **1985,** *149*, 507-515.

Sagami, H.; Morita, Y.; Ogura, K., Purification and properties of geranylgeranyl-diphosphate synthase from bovine brain. *J. Biol. Chem.* **1994,** *269*, 20561-20566.

Strickland, C. L.; Weber, P. C.; Windsor, W. T.; Wu, Z.; Le, H. V.; Albanese, M. M.; Alvarez, C. S.; Cesarz, D.; del Rosario, J.; Deskus, J.; Mallams, A. K.; Njoroge, F. G.; Piwinski, J. J.; Remiszewski, S.; Rossman, R. R.; Taveras, A. G.; Vibulbhan, B.; Doll, R. J.; Girijavallabhan, V. M.; Ganguly, A. K., Tricyclic farnesyl protein transferase inhibitors: crystallographic and calorimetric studies of structure-activity relationships. *J. Med. Chem.* **1999,** *42*, 2125-2135.

Strickland, C. L.; Windsor, W. T.; Syto, R.; Wang, L.; Bond, R.; Wu, Z.; Schwartz, J.; Le, H. V.; Beese, L. S.; Weber, P. C., Crystal structure of farnesyl protein transferase complexed with a CaaX peptide and farnesyl diphosphate analogue. *Biochemistry* **1998,** *37*, 16601-16611.

Bartlett, D. L.; King, C. H.; Poulter, C. D., Purification of farnesylpyrophosphate synthetase by affinity chromatography. *Methods Enzymol.* **1985,** *110*, 171-184.

Turek, T. C.; Gaon, I.; Distefano, M. D., Synthesis and rapid purification of 32P-labeled photoactive analogs of farnesyl pyrophosphate. *J. Labelled Comp. Radiopharm.* **1997,** *39*, 139-146.

Yeang, H. Y.; Cheong, K. F.; Sunderasan, E.; Hamzah, S.; Chew, N. P.; Hamid, S.; Hamilton, R. G.; Cardosa, M. J., The 14.6 kd rubber elongation factor (Hev b 1) and 24 kd (Hev b 3) rubber particle proteins are recognized by IgE from patients with spina bifida and latex allergy. *J. Allergy Clin. Immun.* **1996,** *98*, 628-639.

Dennis, M. S.; Light, D. R., Rubber elongation factor from *Hevea brasiliensis*. Identification, characterization, and role in rubber biosynthesis. *J. Biol. Chem.* **1989,** *264*, 18608-18617.

Durauer, A.; Csaszar, E.; Mechtler, K.; Jungbauer, A.; Schmid, E., Characterisation of the rubber elongation factor from ammoniated latex by electrophoresis and mass spectrometry. *J. Chrom. A* **2000,** *890*, 145-158.

Dennis, M. S.; Henzel, W. J.; Bell, J.; Kohr, W.; Light, D. R., Amino acid sequence of rubber elongation factor protein associated with rubber particles in Hevea latex. *J. Biol. Chem.* **1989,** *264*, 18618-18626.

Mayer, M. P.; Prestwich, G. D.; Dolence, J. M.; Bond, P. D.; Wu, H. Y.; Poulter, C. D., Protein farnesyltransferase: production in Escherichia coli and immunoaffinity purification of the heterodimer from *Saccharomyces cerevisiae*. *Gene* **1993,** *132*, 41-47.

Stirtan, W. G.; Poulter, C. D., Yeast protein geranylgeranyltransferase type-I: overproduction, purification, and characterization. *Arch. Biochem. Biophys.* **1995,** *321*, 182-190.

Zhang, F. L.; Diehl, R. E.; Kohl, N. E.; Gibbs, J. B.; Giros, B.; Casey, P. J.; Omer, C. A., cDNA cloning and expression of rat and human protein geranylgeranyltransferase type-I. *J. Biol. Chem.* **1994,** *269*, 3175-3180.

Ohkanda, J.; Knowles, D. B.; Blaskovich, M. A.; Sebti, S. M.; Hamilton, A. D., Inhibitors of protein farnesyltransferase as novel anticancer agents. *Curr. Top. Med. Chem.* **2002,** *2*, 303-323.

Crul, M.; de Klerk, G. J.; Beijnen, J. H.; Schellens, J. H., Ras biochemistry and farnesyl transferase inhibitors: a literature survey. *Anti-cancer drugs* **2001,** *12*, 163-84.

Jaffe, A. B.; Hall, A., Rho GTPases in transformation and metastasis. *Adv. Cancer Res.* **2002,** *84*, 57-80.

Sebti, S. M.; Hamilton, A. D., Inhibition of Rho GTPases using protein geranylgeranyltransferase I inhibitors. *Methods Enzymol.* **2000,** *325*, 381-388.

Bell, I. M., Inhibitors of farnesyltransferase: A rational approach to cancer chemotherapy? *J. Med. Chem.* **2004,** *47*, 1869-1878.

Whyte, D. B.; Kirschmeier, P.; Hockenberry, T. N.; Nunez-Oliva, I.; James, L.; Catino, J. J.; Bishop, W. R.; Pai, J. K., K- and N-Ras are geranylgeranylated in cells treated with farnesyl protein transferase inhibitors. *J. Biol. Chem.* **1997,** *272*, 14459-14464.

Rowell, C. A.; Kowalczyk, J. J.; Lewis, M. D.; Garcia, A. M., Direct demonstration of geranylgeranylation and farnesylation of Ki-Ras in vivo. *J. Biol. Chem.* **1997,** *272*, 14093-14097.

Lerner, E. C.; Zhang, T. T.; Knowles, D. B.; Qian, Y.; Hamilton, A. D.; Sebti, S. M., Inhibition of the prenylation of K-Ras, but not H- or N-Ras, is highly resistant to CAAX peptidomimetics and requires both a farnesyltransferase and a geranylgeranyltransferase I inhibitor in human tumor cell lines. *Oncogene* **1997,** *15*, 1283-1288.

Sousa, S. F.; Fernandes, P. A.; Ramos, M. J., Farnesyltransferase inhibitors: a detailed chemical view on an elusive biological problem. *Curr. Med. Chem.* **2008,** *15*, 1478-1492.

Rowinsky, E. K., Lately, it occurs to me what a long, strange trip it's been for the farnesyltransferase inhibitors. *J. Clin. Oncol.* **2006,** *24*, 2981-2984.

Young, D. D.; Deiters, A., Photochemical control of biological processes. *Org. Biomol. Chem.* **2007,** *5*, 999-1005.

Ellis-Davies, G. C., Caged compounds: photorelease technology for control of cellular chemistry and physiology. *Nat. Methods* **2007,** *4*, 619-628.

Mayer, G.; Heckel, A., Biologically active molecules with a "light switch". *Angew. Chem. Int. Ed.* **2006,** *45*, 4900-4921.

Pelliccioli, A. P.; Wirz, J., Photoremovable protecting groups: reaction mechanisms and applications. *Photochem. Photobiol. Sci.* **2002,** *1*, 441-458.

Curley, K.; Lawrence, D. S., Caged regulators of signaling pathways. *Pharmacol. Ther.* **1999,** *82*, 347-354.

Adams, S. R.; Tsien, R. Y., Controlling cell chemistry with caged compounds. *Annu. Rev. Physiol.* **1993,** *55*, 755-784.

Parker, L. L.; Kurutz, J. W.; Kent, S. B.; Kron, S. J., Control of the yeast cell cycle with a photocleavable alpha-factor analogue. *Angew. Chem. Int. Ed.* **2006,** *45*, 6322-6325.

Rathert, P.; Rasko, T.; Roth, M.; Slaska-Kiss, K.; Pingoud, A.; Kiss, A.; Jeltsch, A. Reversible inactivation of the CG specific SssI DNA (cytosine-C5)-methyltransferase with a photocleavable protecting group. *Chembiochem* **2007,** *8*, 202-207.

Schlichting, I.; Rapp, G.; John, J.; Wittinghofer, A.; Pai, E. F.; Goody, R. S., Biochemical and crystallographic characterization of a complex of c-Ha-ras p21 and caged GTP with flash photolysis. *Proc. Natl. Acad. Sci. U. S. A.* **1989,** *86*, 7687-7690.

DeGraw, A. J.; Hast, M. A.; Xu, J.; Mullen, D.; Beese, L. S.; Barany, G.; Distefano, M. D., Caged protein prenyltransferase substrates: tools for understanding protein prenylation. *Chem. Biol. Drug. Des.* **2008,** *72*, 171-181.

Cambridge, S. B.; Geissler, D.; Keller, S.; Curten, B., A caged doxycycline analogue for photoactivated gene expression. *Angew. Chem. Int. Ed.* **2006,** 45, 2229-2231.

Link, K. H.; Cruz, F. G.; Ye, H. F.; O'Reilly K, E.; Dowdell, S.; Koh, J. T., Photo-caged agonists of the nuclear receptors RARgamma and TRbeta provide unique time-dependent gene expression profiles for light-activated gene patterning. *Bioorg. Med. Chem.* **2004,** *12*, 5949-5959.

Pompliano, D. L.; Gomez, R. P.; Anthony, N. J., Intramolecular fluorescence enhancement: a continuous assay of Ras farnesyl:protein transferase. *J. Am. Chem. Soc.* **1992,** 114, 7945-7946.

He, Z.; Stienen, G. J.; Barends, J. P.; Ferenczi, M. A., Rate of phosphate release after photoliberation of adenosine 5'-triphosphate in slow and fast skeletal muscle fibers. *Biophys. J.* **1998,** *75*, 2389-2401.

Hartung, K.; Froehlich, J. P.; Fendler, K., Time-resolved charge translocation by the Ca-ATPase from sarcoplasmic reticulum after an ATP concentration jump. *Biophys. J.* **1997,** *72*, 2503-2514.

Gropp, T.; Cornelius, F.; Fendler, K., K+-dependence of electrogenic transport by the NaK-ATPase. *Biochim. Biophys. Acta.* **1998,** *1368*, 184-200.

Allen, D. G.; Lannergren, J.; Westerblad, H., The use of caged adenine nucleotides and caged phosphate in intact skeletal muscle fibres of the mouse. *Acta. Physiol. Scand.* **1999,** *166*, 341-347.

Corrie, J. E. T.; Trentham, D. R., Synthetic, Mechanistic and Photochemical Studies of Phosphate Esters of Substituted Benzoins. *J. Chem. Soc. Perkin Trans.* **1992**, 2409-2417.

Zhu, Y.; Pavlos, C. M.; Toscano, J. P.; Dore, T. M., 8-Bromo-7-hydroxyquinoline as a photoremovable protecting group for physiological use: mechanism and scope. *J. Am. Chem. Soc.* **2006,** *128*, 4267-4276.

Fedoryak, O. D.; Dore, T. M., Brominated hydroxyquinoline as a photolabile protecting group with sensitivity to multiphoton excitation. *Org. Lett.* **2002,** *4*, 3419-3422.

Furuta, T.; Takeuchi, H.; Isozaki, M.; Takahashi, Y.; Kanehara, M.; Sugimoto, M.; Watanabe, T.; Noguchi, K.; Dore, T. M.; Kurahashi, T.; Iwamura, M.; Tsien, R. Y., Bhc-cNMPs as either water-soluble or membrane-permeant photoreleasable cyclic nucleotides for both one- and two-photon excitation. *Chembiochem* **2004,** *5*, 1119-1128.

Das, S.; Schapira, M.; Tomic-Canic, M.; Goyanka, R.; Cardozo, T.; Samuels, H. H., Farnesyl pyrophosphate is a novel transcriptional activator for a subset of nuclear hormone receptors. *Mol. Endocrinol.* **2007,** *21*, 2676-2686.

Lowy, D. R.; Willumsen, B. M., Function and regulation of ras. *Annu. Rev. Biochem.* **1993,** *62*, 851-891.

Xue, C. B. B., J.M.; Naider, F., Efficient regioselective isoprenylation of peptides in acidic aqueous solution using zinc acetate as a catalyst. *Tet. Lett.* **1992,** *33*, 1435-1438.

Khan, S. G.; Mukhtar, H.; Agarwal, R., A rapid and convenient filter-binding assay for ras p21 processing enzyme farnesyltransferase. *J. Biochem. Biophys. Methods* **1995,** *30*, 133-144.

Graham, S. L.; deSolms, S. J.; Giuliani, E. A.; Kohl, N. E.; Mosser, S. D.; Oliff, A. I.; Pompliano, D. L.; Rands, E.; Breslin, M. J.; Deana, A. A.; et al., Pseudopeptide inhibitors of Ras farnesyl-protein transferase. *J. Med. Chem.* **1994,** *37*, 725-732.

Hatchard, C. G.; Parker, C. A., A new sensitive chemical actinometer. II. Potassium ferrioxalate as a standard chemical actinometer. *Proc. Roy. Soc.* **1956,** *A235*, 518-536.

Mayer, M. P.; Prestwich, G. D.; Dolence, J. M.; Bond, P. D.; Wu, H. Y.; Poulter, C. D., Protein farnesyltransferase: production in *Escherichia coli* and immunoaffinity purification of the heterodimer from *Saccharomyces cerevisiae*. *Gene* **1993,** *132*, 41-47.

Cassidy, P. B.; Dolence, J. M.; Poulter, C. D., Continuous fluorescence assay for protein prenyltransferases. *Methods Enzymol.* **1995,** *250*, 30-43.

Fu, H. W.; Moomaw, J. F.; Moomaw, C. R.; Casey, P. J., Identification of a cysteine residue essential for activity of protein farnesyltransferase. Cys299 is exposed only upon removal of zinc from the enzyme. *J. Biol. Chem.* **1996,** *271*, 28541-28548.

Han, Y.; Albericio, F.; Barany, G., Occurrence and minimization of cysteine racemization during stepwise solid-phase peptide synthesis. *J. Org. Chem.* **1997,** *62*, 4307-4312.

King, D. S.; Fields, C. G.; Fields, G. B., A cleavage method which minimizes side reactions following Fmoc solid phase peptide synthesis. *Int. J. Pept. Protein. Res.* **1990,** *36*, 255-266.

Grewer, C.; Jager, J.; Carpenter, B. K.; Hess, G. P., A new photolabile precursor of glycine with improved properties: A tool for chemical kinetic investigations of the glycine receptor. *Biochemistry* **2000,** *39*, 2063-2070.

Chen, W. J.; Moomaw, J. F.; Overton, L.; Kost, T. A.; Casey, P. J., High level expression of mammalian protein farnesyltransferase in a baculovirus system. The purified protein contains zinc. *J. Biol. Chem.* **1993,** *268*, 9675-9680.

Long, S. B.; Casey, P. J.; Beese, L. S., The basis for K-Ras4B binding specificity to protein farnesyltransferase revealed by 2Å resolution ternary complex structures. *Structure* **2000,** *8*, 209-222.

Reid, T. S.; Terry, K. L.; Casey, P. J.; Beese, L. S., Crystallographic analysis of CaaX prenyltransferases complexed with substrates defines rules of protein substrate selectivity. *J. Mol. Biol.* **2004,** *343*, 417-433.

Otwinowski, Z.; Minor, W., Processing of x-ray diffraction data collected in oscillation mode. *Methods Enzymol.* **1997,** *276*, 307-326.

McCoy, A. J.; Grosse-Kunstleve, R. W.; Adams, P. D.; Winn, M. D.; Storoni, L. C.; Read, R. J., Phaser crystallographic software. *J. Appl. Crystallogr.* **2007,** *40*, 658-674.

Emsley, P.; Cowtan, K., Coot: model-building tools for molecular graphics. *Acta. Crystallogr. D Biol. Crystallogr.* **2004,** *60*, 2126-2132.

Murshudov, G. N.; Vagin, A. A.; Dodson, E. J., Refinement of macromolecular structures by the maximum-likelihood method. *Acta. Crystallogr. D Biol. Crystallogr.* **1997,** *53*, 240-255.

Sebti, S. M.; Hamilton, A. D., Inhibition of Rho GTPases using protein geranylgeranyltransferase I inhibitors. *Methods Enzymol.* **2000,** *325*, 381-388.

Sebti, S. M.; Hamilton, A. D., Farnesyltransferase and geranylgeranyltransferase I inhibitors and cancer therapy: lessons from mechanism and bench-to-bedside translational studies. *Oncogene* **2000,** *19*, 6584-6593.

Crul, M.; de Klerk, G. J.; Beijnen, J. H.; Schellens, J. H., Ras biochemistry and farnesyl transferase inhibitors: a literature survey. *Anti-cancer drugs* **2001,** *12*, 163-184.

End, D. W. M., L.; Angibaud, P., Farnesyl protein transferase inhibitors: medicinal chemistry, molecular mechanisms, and progress in the Clinic. *Top. Med. Chem.* **2007,** *1*, 133-168.

Du, W.; Lebowitz, P. F.; Prendergast, G. C., Cell growth inhibition by farnesyltransferase inhibitors is mediated by gain of geranylgeranylated RhoB. *Mol. Cell. Biol.* **1999,** *19*, 1831-40.

Du, W.; Prendergast, G. C., Geranylgeranylated RhoB mediates suppression of human tumor cell growth by farnesyltransferase inhibitors. *Cancer Res.* **1999,** *59*, 5492-5496.

Lebowitz, P. F.; Casey, P. J.; Prendergast, G. C.; Thissen, J. A., Farnesyltransferase inhibitors alter the prenylation and growth-stimulating function of RhoB. *J. Biol. Chem.* **1997,** *272*, 15591-15594.

van Golen, K. L.; Bao, L.; DiVito, M. M.; Wu, Z.; Prendergast, G. C.; Merajver, S. D., Reversion of RhoC GTPase-induced inflammatory breast cancer phenotype by treatment with a farnesyl transferase inhibitor. *Mol. Cancer Ther.* **2002,** *1*, 575-583.

Castro, A. F.; Rebhun, J. F.; Clark, G. J.; Quilliam, L. A., Rheb binds tuberous sclerosis complex 2 (TSC2) and promotes S6 kinase activation in a rapamycin- and farnesylation-dependent manner. *J. Biol. Chem.* **2003,** *278,* 32493-32496.

Jiang, K.; Coppola, D.; Crespo, N. C.; Nicosia, S. V.; Hamilton, A. D.; Sebti, S. M.; Cheng, J. Q., The phosphoinositide 3-OH kinase/AKT2 pathway as a critical target for farnesyltransferase inhibitor-induced apoptosis. *Mol. Cell. Biol.* **2000,** 20, 139-148.

Law, B. K.; Norgaard, P.; Moses, H. L., Farnesyltransferase inhibitor induces rapid growth arrest and blocks p70s6k activation by multiple stimuli. *J. Biol. Chem.* **2000,** *275*, 10796-10801.

Liu, A.; Prendergast, G. C., Geranylgeranylated RhoB is sufficient to mediate tissue-specific suppression of Akt kinase activity by farnesyltransferase inhibitors. *FEBS Lett.* **2000,** *481*, 205-208.

Tamanoi, F.; Kato-Stankiewicz, J.; Jiang, C.; Machado, I.; Thapar, N., Farnesylated proteins and cell cycle progression. *J. Cell. Biochem. Suppl.* **2001,** *37*, 64-70.

Ashar, H. R.; James, L.; Gray, K.; Carr, D.; Black, S.; Armstrong, L.; Bishop, W. R.; Kirschmeier, P., Farnesyl transferase inhibitors block the farnesylation of CENP-E and CENP-F and alter the association of CENP-E with the microtubules. *J. Biol. Chem.* **2000,** *275*, 30451-30457.

Crespo, N. C.; Ohkanda, J.; Yen, T. J.; Hamilton, A. D.; Sebti, S. M., The farnesyltransferase inhibitor, FTI-2153, blocks bipolar spindle formation and chromosome alignment and causes prometaphase accumulation during mitosis of human lung cancer cells. *J. Biol. Chem.* **2001,** *276*, 16161-16167.

Adnane, J.; Bizouarn, F. A.; Qian, Y.; Hamilton, A. D.; Sebti, S. M., p21(WAF1/CIP1) is upregulated by the geranylgeranyltransferase I inhibitor GGTI-298 through a transforming growth factor beta- and Sp1-responsive element: involvement of the small GTPase rhoA. *Mol. Cell. Biol.* **1998,** *18*, 6962-6970.

Vogt, A.; Sun, J.; Qian, Y.; Hamilton, A. D.; Sebti, S. M., The geranylgeranyltransferase-I inhibitor GGTI-298 arrests human tumor cells in G0/G1 and induces p21(WAF1/CIP1/SDI1) in a p53-independent manner. *J. Biol. Chem.* **1997,** *272*, 27224-27229.

Prendergast, G. C., Actin' up: RhoB in cancer and apoptosis. *Nat. Rev. Cancer* **2001,** *1*, 162-168.

Sebti, S. M.; Der, C. J., Opinion: Searching for the elusive targets of farnesyltransferase inhibitors. *Nat. Rev. Cancer* **2003,** *3*, 945-951.

Lackner, M. R.; Kindt, R. M.; Carroll, P. M.; Brown, K.; Cancilla, M. R.; Chen, C.; de Silva, H.; Franke, Y.; Guan, B.; Heuer, T.; Hung, T.; Keegan, K.; Lee, J. M.; Manne, V.; O'Brien, C.; Parry, D.; Perez-Villar, J. J.; Reddy, R. K.; Xiao, H.; Zhan, H.; Cockett, M.; Plowman, G.; Fitzgerald, K.; Costa, M.; Ross-Macdonald, P., Chemical genetics identifies Rab geranylgeranyl transferase as an apoptotic target of farnesyl transferase inhibitors. *Cancer Cell* **2005,** *7*, 325-336.

Sebti, S. M., Protein farnesylation: implications for normal physiology, malignant transformation, and cancer therapy. *Cancer Cell* **2005,** *7*, 297-300.

Maurer-Stroh, S.; Koranda, M.; Benetka, W.; Schneider, G.; Sirota, F. L.; Eisenhaber, F., Towards complete sets of farnesylated and geranylgeranylated proteins. *PLoS Comput. Biol.* **2007,** *3*, e66.

Kislinger, T.; Emili, A., Multidimensional protein identification technology: current status and future prospects. *Expert Rev. Proteomics* **2005,** *2*, 27-39.

Reinders, J.; Lewandrowski, U.; Moebius, J.; Wagner, Y.; Sickmann, A., Challenges in mass spectrometry-based proteomics. *Proteomics* **2004,** *4*, 3686-3703.

Tate, E. W., Recent advances in chemical proteomics: exploring the post-translational proteome. *J. Biol. Chem.* **2008,** *1*, 17-26.

Sletten, E. M. and Bertozzi, C.R., Bioorthogonal chemistry: fishing for selectivity in a sea of functionality. *Angew. Chem. Int. Ed.* **2009,** *48*, 6974-6998.

Mahal, L. K. Y., K.J.; Bertozzi, C.R., Engineering chemical reactivity on cell surfaces through oligosaccharide biosynthesis. *Science* **1997,** *276*, 1125-1128.

Hang, H. C., Bertozzi, C. R., Ketone Isosteres of 2-N-Acetamidosugars as substrates for metabolic cell surface engineering. *J. Am. Chem. Soc.* **2001,** *123*, 1242-1243.

Saxon, E. a. B., C.R., Cell surface engineering by a modified Staudinger reaction. *Science* **2000,** *287*, 2007-2010.

Saxon, E. L., S. J.; Hang, H. C.; Yu, C.; Lee, S. C.; Bertozzi, C. R., Investigating cellular metabolism of synthetic azidosugars using the Staudinger ligation. *J. Am. Chem. Soc.* **2002,** *124*, 14893-14902.

Prescher, J. A. D., D. H.; Bertozzi, C. R., Chemical remodelling of cell surfaces in living animals. *Nature* **2004,** *430*, 873-877.

Lin, F., Hoyt, H. M.; van Halbeek, H.; Bergman, R. G.; Bertozzi, C. R., Mechanistic investigation of the Staudinger ligation. *J. Am. Chem. Soc.* **2005,** *127*, 2686-2695.

Huisgen, R., Kinetics and mechanism of 1,3-dipolar cycloaddition. *Angew. Chem. Int. Ed.* **1963,** *2*, 633-645.

Tornoe, C. W.; Christensen, C.; Meldal, M., Peptidotriazoles on solid phase: [1,2,3]-triazoles by regiospecific copper(I)-catalyzed 1,3-dipolar cycloadditions of terminal alkynes to azides. *J. Org. Chem.* **2002,** *67*, 3057-3064.

Rostovtsev, V. V.; Green, L. G.; Fokin, V. V.; Sharpless, K. B., A stepwise huisgen cycloaddition process: copper(I)-catalyzed regioselective "ligation" of azides and terminal alkynes. *Angew. Chem. Int. Ed.* **2002,** *41*, 2596-2599.

Chan, T. R.; Hilgraf, R.; Sharpless, K. B.; Fokin, V. V., Polytriazoles as copper(I)-stabilizing ligands in catalysis. *Org. Lett.* **2004,** *6*, 2853-2855.

Kolb, H. C.; Finn, M. G.; Sharpless, K. B., Click chemistry: diverse chemical function from a few good reactions. *Angew. Chem. Int. Ed.* **2001,** *40*, 2004-2021.

Fokin, V. V., Click imaging of biochemical processes in living systems. *ACS Chem. Biol.* **2007,** *2*, 775-778.

Dieterich, D. C.; Lee, J. J.; Link, A. J.; Graumann, J.; Tirrell, D. A.; Schuman, E. M., Labeling, detection and identification of newly synthesized proteomes with bioorthogonal non-canonical amino-acid tagging. *Nat. Protoc.* **2007,** *2*, 532-540.

Breinbauer, R.; Kohn, M., Azide-alkyne coupling: a powerful reaction for bioconjugate chemistry. *Chembiochem* **2003,** *4*, 1147-1149.

Agard, N. J.; Prescher, J. A.; Bertozzi, C. R., A strain-promoted [3 + 2] azide-alkyne cycloaddition for covalent modification of biomolecules in living systems. *J. Am. Chem. Soc.* **2004,** *126*, 15046-15047.

Baskin, J. M.; Prescher, J. A.; Laughlin, S. T.; Agard, N. J.; Chang, P. V.; Miller, I. A.; Lo, A.; Codelli, J. A.; Bertozzi, C. R., Copper-free click chemistry for dynamic in vivo imaging. *Proc. Natl. Acad. Sci. U. S. A.* **2007,** *104*, 16793-16797.

Codelli, J. A.; Baskin, J. M.; Agard, N. J.; Bertozzi, C. R., Second-generation difluorinated cyclooctynes for copper-free click chemistry. *J. Am. Chem. Soc.* **2008,** *130*, 11486-11493.

Ning, X.; Guo, J.; Wolfert, M. A.; Boons, G. J., Visualizing metabolically labeled glycoconjugates of living cells by copper-free and fast huisgen cycloadditions. *Angew. Chem. Int. Ed.* **2008,** *47*, 2253-2255.

Bertozzi, C. R.; Kiessling, L. L., Chemical glycobiology. *Science* **2001,** *291*, 2357-2364.

Gama, C. I.; Hsieh-Wilson, L. C., Chemical approaches to deciphering the glycosaminoglycan code. *Curr. Opin. Chem. Biol.* **2005,** *9*, 609-619.

Laughlin, S. T.; Bertozzi, C. R., Metabolic labeling of glycans with azido sugars and subsequent glycan-profiling and visualization via Staudinger ligation. *Nat. Protoc.* **2007,** *2*, 2930-44.

Luchansky, S. J.; Argade, S.; Hayes, B. K.; Bertozzi, C. R., Metabolic functionalization of recombinant glycoproteins. *Biochemistry* **2004,** *43*, 12358-12366.

Sprung, R.; Nandi, A.; Chen, Y.; Kim, S. C.; Barma, D.; Falck, J. R.; Zhao, Y., Tagging-via-substrate strategy for probing O-GlcNAc modified proteins. *J. Proteome Res.* **2005,** *4*, 950-957.

Warthaka, M.; Karwowska-Desaulniers, P.; Pflum, M. K., Phosphopeptide modification and enrichment by oxidation-reduction condensation. *ACS Chem. Biol.* **2006,** *1*, 697-701.

Zhou, H.; Watts, J. D.; Aebersold, R., A systematic approach to the analysis of protein phosphorylation. *Nat. Biotechnol.* **2001,** *19*, 375-378.

Charron, G.; Zhang, M. M.; Yount, J. S.; Wilson, J.; Raghavan, A. S.; Shamir, E.; Hang, H. C., Robust fluorescent detection of protein fatty-acylation with chemical reporters. *J. Am. Chem. Soc.* **2009,** 131, 4967-4975.

Hang, H. C.; Geutjes, E. J.; Grotenbreg, G.; Pollington, A. M.; Bijlmakers, M. J.; Ploegh, H. L., Chemical probes for the rapid detection of Fatty-acylated proteins in Mammalian cells. *J. Am. Chem. Soc.* **2007,** *129*, 2744-2745.

Heal, W. P.; Wickramasinghe, S. R.; Bowyer, P. W.; Holder, A. A.; Smith, D. F.; Leatherbarrow, R. J.; Tate, E. W., Site-specific N-terminal labeling of proteins in vitro and in vivo using N-myristoyl transferase and bioorthogonal ligation chemistry. *Chem. Commun.* **2008**, *4*, 480-482.

Kostiuk, M. A.; Corvi, M. M.; Keller, B. O.; Plummer, G.; Prescher, J. A.; Hangauer, M. J.; Bertozzi, C. R.; Rajaiah, G.; Falck, J. R.; Berthiaume, L. G., Identification of palmitoylated mitochondrial proteins using a bio-orthogonal azido-palmitate analogue. *Faseb J.* **2008,** *22*, 721-732.

Martin, B. R.; Cravatt, B. F., Large-scale profiling of protein palmitoylation in mammalian cells. *Nat Methods* **2009,** *6*, 135-138.

Roth, A. F.; Wan, J.; Green, W. N.; Yates, J. R.; Davis, N. G., Proteomic identification of palmitoylated proteins. *Methods* **2006,** *40*, 135-142.

Chan, L. N.; Hart, C.; Guo, L.; Nyberg, T.; Davies, B. S.; Fong, L. G.; Young, S. G.; Agnew, B. J.; Tamanoi, F., A novel approach to tag and identify geranylgeranylated proteins. *Electrophoresis* **2009,** *30*, 3598-3606.

Kho, Y.; Kim, S. C.; Jiang, C.; Barma, D.; Kwon, S. W.; Cheng, J.; Jaunbergs, J.; Weinbaum, C.; Tamanoi, F.; Falck, J.; Zhao, Y., A tagging-via-substrate technology for detection and proteomics of farnesylated proteins. *Proc. Natl. Acad. Sci. U. S. A.* **2004,** *101*, 12479-12484.

Nguyen, U. T.; Guo, Z.; Delon, C.; Wu, Y.; Deraeve, C.; Franzel, B.; Bon, R. S.; Blankenfeldt, W.; Goody, R. S.; Waldmann, H.; Wolters, D.; Alexandrov, K., Analysis of the eukaryotic prenylome by isoprenoid affinity tagging. *Nat. Chem. Biol.* **2009,** *5*, 227-235.

Labadie, G. R.; Viswanathan, R.; Poulter, C. D., Farnesyl diphosphate analogues with omega-bioorthogonal azide and alkyne functional groups for protein farnesyl transferase-catalyzed ligation reactions. *J. Org. Chem.* **2007,** *72*, 9291-9297.

Xu, J.; Degraw, A. J.; Duckworth, B. P.; Lenevich, S.; Tann, C. M.; Jenson, E. C.; Gruber, S. J.; Barany, G.; Distefano, M. D., Synthesis and reactivity of 6,7-dihydrogeranylazides: reagents for primary azide incorporation into peptides and subsequent staudinger ligation. *Chem. Biol. Drug Des.* **2006,** *68*, 85-96.

Duckworth, B. P.; Xu, J.; Taton, T. A.; Guo, A.; Distefano, M. D., Site-specific, covalent attachment of proteins to a solid surface. *Bioconjugate Chem.* **2006,** *17*, 967-974.

Duckworth, B. P.; Zhang, Z.; Hosokawa, A.; Distefano, M. D., Selective labeling of proteins by using protein farnesyltransferase. *Chembiochem* **2007,** *8*, 98-105.

Hosokawa, A. W., J.W.; Zhang, Z.; Chen, L.; Barany, G.; Distefano, M.D., Evaluation of an alkyne-containing analogue of farnesyldiphosphate as a dual substrate for protein-prenyltransferases. *Int. J. Pep. Res. Ther.* **2007,** *13*, 345-354.

Speers, A. E.; Cravatt, B. F., Profiling enzyme activities in vivo using click chemistry methods. *Chem. Biol.* **2004,** *11*, 535-546.

Cole, S. L. V., R., Isoprenoids and Alzheimer's disease: A complex relationship. *Neurobiol. Dis.* **2006,** *22*, 209-222.

Eckert, G. P.; Hooff, G. P.; Strandjord, D. M.; Igbavboa, U.; Volmer, D. A.; Muller, W. E.; Wood, W. G., Regulation of the brain isoprenoids farnesyl- and geranylgeranylpyrophosphate is altered in male Alzheimer patients. *Neurobiol. Dis.* **2009,** 35, 251-257.

Fiacco, T. A.; Agulhon, C.; McCarthy, K. D., Sorting out astrocyte physiology from pharmacology. *Annu. Rev. Pharmacol. Toxicol.* **2009,** *49*, 151-174.

Pereira-Leal J.B.; Hume, A. N. S., M.C., Prenylation of Rab GTPases: Molecular mechanisms and involvement in genetic disease. *FEBS Lett.* **2001,** *498*, 197-200.

Weerapana, E.; Speers, A. E.; Cravatt, B. F., Tandem orthogonal proteolysis-activity-based protein profiling (TOP-ABPP)--a general method for mapping sites of probe modification in proteomes. *Nat. Protoc.* **2007,** *2*, 1414-1425.

Speers, A. E.; Cravatt, B. F., A tandem orthogonal proteolysis strategy for high-content chemical proteomics. *J. Am. Chem. Soc.* **2005,** *127*, 10018-10019.

Yang, Y.; Chaerkady, R.; Beer, M. A.; Mendell, J. T.; Pandey, A., Identification of miR-21 targets in breast cancer cells using a quantitative proteomic approach. *Proteomics* **2009,** *9*, 1374-1384.

Tenorio-Laranga, J.; Valero, M. L.; Maennistoe, P. T.; del Pino, M. S.; Garcia-Horsman, J. A., Combination of snap freezing, differential pH two-dimensional reverse-phase high-performance liquid chromatography, and iTRAQ technology for the peptidomic analysis of the effect of prolyl oligopeptidase inhibition in the rat brain. *Anal. Biochem.* **2009,** *393*, 80-87.

White, F. M., On the iTRAQ of kinase inhibitors. *Nat. Biotechnol.* **2007,** *25*, 994-996.

Peters, E. C. and Gray, N. S., Chemical proteomics identifies unanticipated targets of clinical kinase inhibitors. *ACS Chem. Biol.* **2007,** *2*, 661-664.

Bantscheff, M.; Eberhard, D.; Abraham, Y.; Bastuck, S.; Boesche, M.; Hobson, S.; Mathieson, T.; Perrin, J.; Raida, M.; Rau, C.; Reader, V.; Sweetman, G.; Bauer, A.; Bouwmeester, T.; Hopf, C.; Kruse, U.; Neubauer, G.; Ramsden, N.; Rick, J.; Kuster, B.; Drewes, G., Quantitative chemical proteomics reveals mechanisms of action of clinical ABL kinase inhibitors. *Nat. Biotechnol.* **2007,** *25*, 1035-1044.

Weerapana, E.; Cravatt, B. F., A quantitative mass spectrometry platform for activity-based protein profiling. *Abstract of Papers, 238th ACS National Meeting, Washington, DC, United States, August 16-20, 2009* **2009**, ORGN-240.

Appendix A. Application of a difluorinated-cyclooctyne (DIFO) in the modification of azide-isoprenoid labeled proteins

A.1 Introduction

A number of chemoselective ligation reactions exist for the coupling of two functional groups together in the presence of other biological functionalities.[1] The copper-catalyzed 1,3-dipolar cycloaddition of azides and alkynes (otherwise known as the click reaction) is often the reaction of choice given its intrinsic selectivity.[2] For some applications though, such as the labeling of biomolecules in copper-sensitive environments, the click reaction cannot be applied.[1] To circumvent this problem, alkyne molecules activated by ring-strain instead of copper-coordination have been created.[3-6] These probes are often referred to as "copper-free click reagents".

A.2 Research Objectives

The Distefano lab has previously demonstrated the use of copper-catalyzed click chemistry to site-specifically attach proteins to surfaces[7] and create DNA-based nanostructures[8], and is currently utilizing it in chemical proteomics experiments to study protein prenylation (see Chapter 4). The goal of this work was to explore the use of the difluorinated-cyclooctyne (DIFO, Figure A.1) copper-free click chemistry reagent in the modification of azide-isoprenoid labeled proteins.

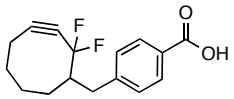

DIFO

Figure A.1 The copper-free click chemistry reagent under examination in these studies

A.3 Results and Discussion

A.3.1 Modification of RFP-N_3 and attachment to a solid surface

A red fluorescent protein (RFP), mCherry[9], was altered to contain the C-terminal protein farnesylation sequence CVIA.[10] RFP-CVIA (**1**) was then enzymatically labeled with the dihydro-azide farnesyldiphoshpate analogue (**2**) by protein farnesyltransferase (PFTase) to create a model protein for the study of attaching azide-isoprenoid modified proteins to solid surfaces using DIFO (Scheme A.1).

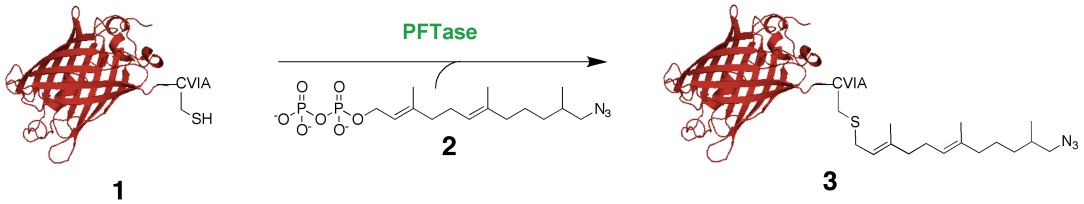

Scheme A.1 Azide-isoprenoid modification of the RFP protein

Pure RFP-N_3 was incubated with biotinylated-DIFO (**4**) overnight at 4°C, then exposed to streptavidin-agarose resin (**6**) for immobilization (Scheme A.2).

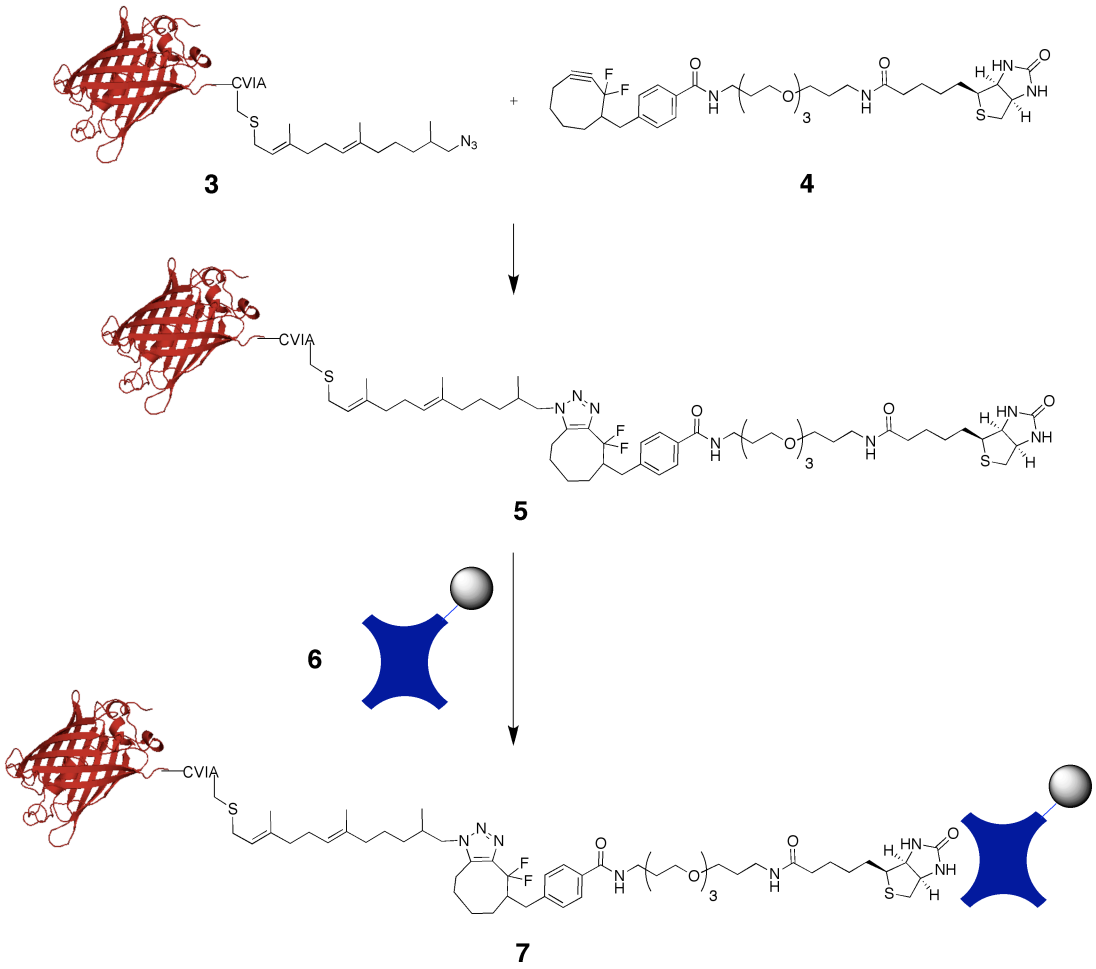

Scheme A.2 Attachment of RFP-N_3 to a solid support

Upon washing of the resin with PBS and PBS containing 0.2% SDS to remove non-covalently bound protein, fluorescence was still observed on the beads (Figure A.2, tube 1). Control reactions where either alkyne or azide was missing (tubes 2 and 3) did not show fluorescence verifying that the observed fluorescence was due to the click reaction proceeding and binding between the immobilized streptavidin and biotinylated RFP-N_3. Non-specific binding of RFP to the resin was not observed (tube 4).

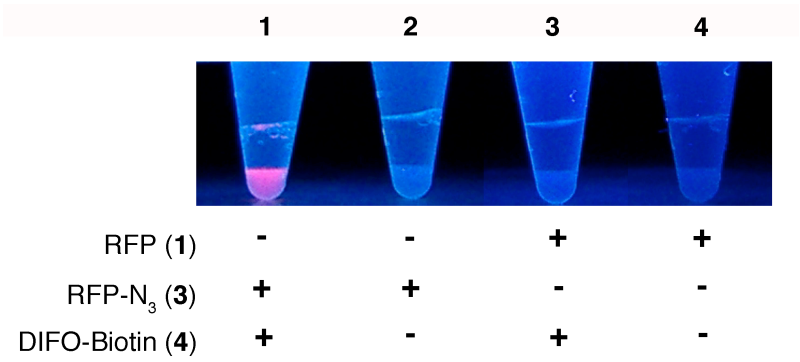

Figure A.2 Selective attachment of a protein to a solid support using DIFO

RFP-N_3 was next spiked in to crude HeLa cell lysate at varying mass percents in order to evaluate the ability of the copper-free click reaction to occur on proteins in crude mixtures, even at minimal concentrations. Protein samples were exposed to DIFO2-Biotin and the biotinylated proteins were pulled down with agarose-immobilized streptavidin. Upon washing of the resin, it was placed on a glass side and exposed to UV light to look for the presence of fluorescence. As can be seen in Figure A.3, RFP-N_3 could be clicked with DIFO2-Biotin and pulled down selectively from a complex mixture of proteins, even when RFP-N_3 was only 0.5% (by weight) of the total protein in the sample.

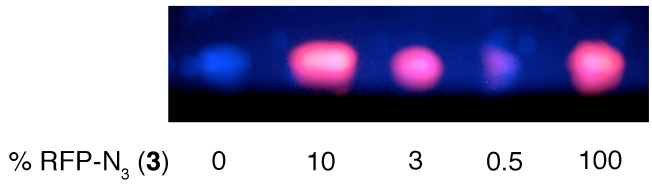

Figure A.3 Immobilization of RFP-N_3 in the presence of crude cell lysate

A.3.2 Evaluating the intra-cellular attachment of an azide-isoprenoid onto endogenously prenylated proteins

Previous studies have shown that prenylated proteins can be tagged with an azide-moiety through metabolic incorporation of an azide-isoprenoid (**8**, Figure A.4).[11, 12] Verification of this labeling was performed by copper-catalyzed click reaction with an alkyne-biotin[12] or alkyne-fluorophore.[11] We applied DIFO-Biotin towards the analysis of the *in vivo* incorporation of azide-isoprenoid analogue **9**.

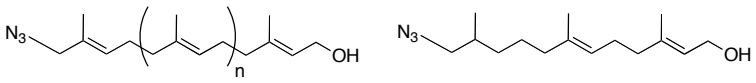

8 n = 1 or 2 **9**

Figure A.4 Azide-modified isoprenoids

COS cells were treated with **9** and lovastatin to inhibit the biosynthesis of FPP and GGPP to ensure that **9** would be utilized as a substrate. Other COS cells were left untreated or treated with lovastatin only as controls. Upon 24 h treatment, cells were lysed and reacted DIFO-Biotin. Because the H-, N-, and K-Ras proteins are known to be processed by protein prenylation, and this change can be detected by a shift is SDS-PAGE mobility[12], the cell lysates were subjected to western blotting against Ras. If Ras had been modified with **9**, subsequent reaction with DIFO-Biotin would result in an even larger shift. A western blot against biotin was also performed on the lysates to visualize labeling with DIFO directly.

In COS cells that were not exposed to treatment with an isoprenoid analogue, there is an approximate 2:1 ratio of processed to unprocessed Ras (Figure A.5, Lane 3). Upon treatment with lovastatin, this ratio decreases to 1:1, suggesting that endogenous isoprenoids are still present and can be used to modify Ras (Figure A.5, Lane 2). Despite this, incorporation of isoprenoid analogue **9** still appears to be occurring based on the Ras protein being detected at higher molecular weight than the unprocessed Ras (Figure A.5, Lane 1). A protein of higher molecular weight than unprocessed Ras would result upon reaction with DIFO-Biotin.

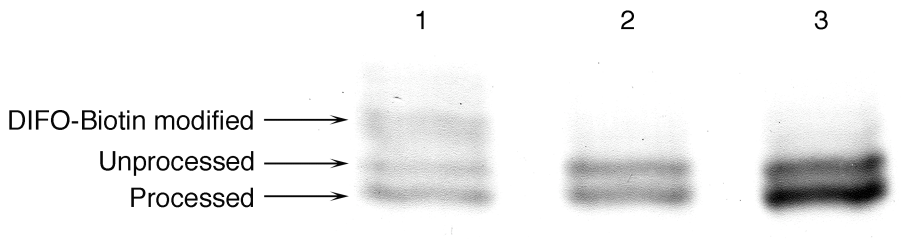

Figure A.5 Western blot analysis of the *in vivo* incorporation of isoprenoid-azide onto Ras proteins and subsequent modification by DIFO-Biotin. Lane 1 = Cells treated with lovastatin and C15-dh-N_3-OH (**9**). Lane 2 = Cells treated with lovastatin only. Lane 3 = Cells that were not subjected to treatment.

Shown in Figure A.6 are the proteins that appear to be labeled with DIFO-Biotin. Nearly every protein in the sample appears to be labeled, regardless of the presence of isoprenoid analogue. A western blot against biotin on the same cell lysates prior to reaction with DIFO-Biotin did not give the same results (data not shown) suggesting that the amount of background signal observed is due to non-specific binding of DIFO to proteins and not a problem with the western blot conditions. This may be explained by the belief that DIFO can undergo decomposition through a radical intermediate upon

heating.[13] Because the DIFO-Biotin is in excess during the click reactions and the remaining unreacted alkyne is not quenched or removed, heating of the samples prior to SDS-PAGE analysis led to non-specific labeling of proteins in the sample. For future studies, excess DIFO-Biotin must be either quenched with another azide such as benzyl azide or azidoethanol, or the protein must be precipitated out and re-dissolved for analysis.

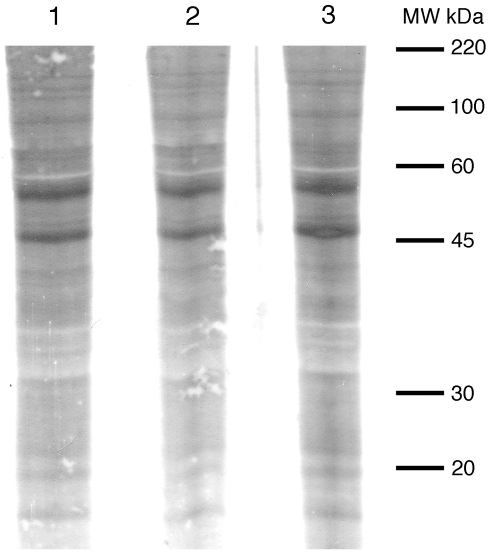

Figure A.6 Western blot analysis of protein modified by DIFO-Biotin. Lane 1 = Cells treated with lovastatin and C15-dh-N_3-OH. Lane 2 = Cells treated with lovastatin only. Lane 3 = Cells that were not subjected to treatment.

A.3.3 Enrichment of prenylated proteins for identification by mass spectrometry

Despite the previously observed background labeling observed in cell lystes reacted with DIFO-Biotin, we decided to apply it towards the enrichment of prenylated proteins for

identification by mass spectrometry. COS cells were treated with an azide-isoprenoid analogue (Figure A.7), lysed, and then reacted with DIFO-Biotin. Prior to enrichment of the labeled proteins with immobilized streptavidin, excess DIFO-Biotin was removed by protein precipitation. Tryptic digestion of the proteins on resin and liquid chromatography with tandem mass spectrometry (LC-MSMS) was then performed on the peptides, while the Protein Pilot software (Applied Biosystems) was used to ascertain the protein identities. A depiction of the experimental procedure is shown in Figure 4.9.

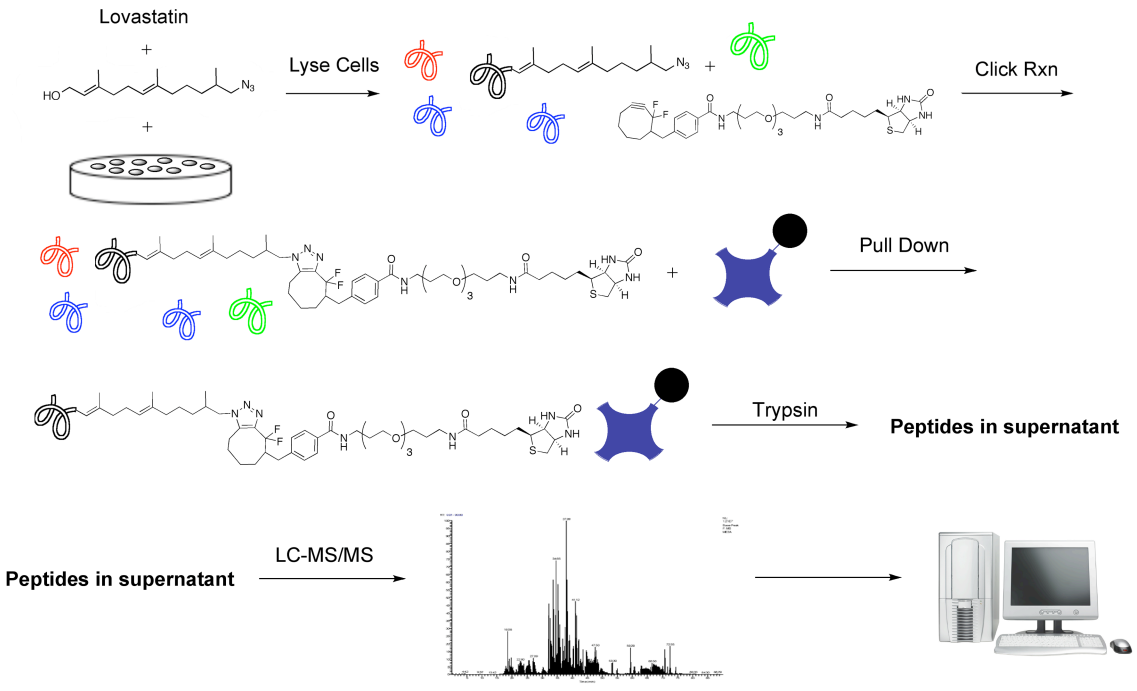

Figure A.7 Procedure for identifying azide-isoprenoid modified proteins using DIFO-Biotin

A total of 19 proteins were identified using the Protein Pilot software at greater than 99% confidence (Table A.1). Unfortunately, none of these proteins contain the C-

terminal consensus sequence that is known to dictate prenylation. Because of the significant amount of background labeling previously observed with DIFO-Biotin, the proteins identified are most likely a reflection of their natural abundance with the COS cell. It is interesting to note that the Annexin A2 protein was identified, which contains the unprecedented CAAXX. This protein was also identified using an alkyne-modified isoprenoid analogue to enrich for protein prenylated *in vivo* in COS cells (see Chapter 4). Currently we are synthesizing the C-terminal peptide of this protein, LYLCGGDD, to test it as a substrate of the prenyltransferase enzymes PFTase and PGGTase-I *in vitro*.

Table A.1 Proteins identified by chemical prenylomics with DIFO

Protein Name	Accession #	% Coverage
Vimentin	gi|62414289	26.8
histone cluster 1, H2bl	gi|12025526	53.6
PREDICTED: similar to histone H4	gi|119930610	60.4
PREDICTED: similar to plectin 1 isoform 3	gi|109087706	5.7
beta-tubulin	gi|74136187	11
prohibitin 2	gi|61556754	12
PREDICTED: annexin A2	gi|114657295	19.1
PREDICTED: similar to Actin, cytoplasmic 2	gi|109507063	17.3
PREDICTED: similar to Histone H1.4	gi|126309070	22.3
PREDICTED: similar to Leucine rich repeat containing 28	gi|149730823	12.4
PREDICTED: similar to Heat shock protein HSP 90-alpha	gi|73989600	10.6
PREDICTED: similar to voltage-dependent anion channel 2	gi|88955151	12
ATP synthase	gi|54792127	12.3
eukaryotic translation elongation factor 1 alpha 2	gi|82697357	13.8
heat shock 70kDa protein 8	gi|76253709	11.1
PREDICTED: similar to 60S ribosomal protein L7a	gi|109111376	14.5
PREDICTED: similar to importin beta subunit isoform 2	gi|76644624	4.5
brain abundant, membrane attached signal protein 1	gi|27807507	8.8
PREDICTED: similar to H2afj protein	gi|83030222	43.4

A.4 Conclusions

DIFO-fluorophores have been shown to be great tools for the labeling and visualization of azide-modified cell surface glycans, even in living organisms.[3, 4] Applying DIFO-biotin towards the attachment of proteins to solid surfaces or in chemical proteomics experiments has not been well documented as of yet. Here we show that applying DIFO-biotin towards these techniques, while useful, must be approached with careful forethought. When the sample is being introduced to heat, such as when running a Western Blot, excess DIFO-biotin must be quenched with an azide. When using DIFO-biotin for protein enrichment, it is necessary to remove the excess reagent prior to pull-down with immobilized-streptavidin resin. Protein precipitation methods where acid is used to prevent non-specific binding of small molecules (such as the case with CalBiochems's ProteoExtract protein precipitation kit) seem to induce non-specific labeling, which suggests that DIFO is acid sensitive. Further study is needed to confirm this. Based on these studies, it is recommended that quenching of DIFO always be performed prior to any sample manipulation.

A.5 Experimental

A.5.1 Enzymatic modification of RFP with isoprenoid-azide

Prenylation reaction (45 mL) contained Tris-HCl (50 mm, pH 7.5), $MgCl_2$ (10 mM), $ZnCl_2$ (10 mM), DTT (5.0 mm), **1** (2.4 μM), **2** (5 μM), and yeast PFTase (9 μg, 2.2 nM). **1** and DTT were combined first and left to sit at rt for 30 min. The remaining reagents were added and the reaction was incubated at 37 °C for 2 h. Reaction was concentrated to

1.5 mL in a Amicon Ultracentrifuge Tube (10k MWCO) and applied to a PBS pre-equilibrated NAP-5 column (Waters). The eluted RFP-N_3 (**3**) was collected and the concentration was determined by absorbance at 570 nm (ε_{570} = 72,000 $M^{-1}cm^{-1}$).[9]

A.5.2 Attachment of RFP-N_3 to a solid surface

To 0.1 mg/mL RFP-CVIA (**1**) or RFP-N_3 (**3**) in PBS was added a solution of **4** (DIFO-Biotin, 1 mM in 95:5 PBS/DMF) to a final concentration of 10 μM. Reactions were left to tumble overnight at 4 °C. A 50% slurry (50 μL) of agarose-immobilized streptavidin (Pierce, binding capacity of 15-28 μg biotin/mL of settled resin) in 0.02% aqueous sodium azide was pipetted into a Handee Spin Column (Pierce). PBS (250 μL) was added and column was centrifuged at 1250 × *g* for 60 s. The click reaction (200 μL) was added to suspend the resin and then column was shook at 150 rpm for 1 h at rt. After discarding the supernatant, the resin was washed with 250 μL PBS, 250 μL TBS + 0.2% SDS, and 250 μL PBS. Resin was suspended in 100 μL PBS, allowed to settle, and then exposed to UV light to look for fluorescence.

A.5.3 Attachment of RFP-N_3 to a solid surface in the presence of crude cell lystate

The same procedure as previously described for pure RFP-N_3 was utilized with the following modification: RFP-N_3 was added to crude HeLa cell lysate at 0.5, 3, and 10% w/w of the total protein. A total of 200 μg of protein was used in each reaction (1 mg/mL).

A.5.4 General procedure for COS cell growth and lysis

Cells (40-50% confluence) were grown in DMEM supplemented with 10% FBS, 25 μM lovastatin, and 40 μM **9**. The cells were allowed to reach 80-90% confluence (~ 24 h) then washed with PBS. Cells were then suspended in PBS, placed in 1.5 mL microcentrifuge tube, and pelleted by centrifugation at 2,000 × *g*, 4 °C, for 5 min. After discarding the supernatant, a PBS solution containing 0.1% SDS, 0.2% Triton X-100, protease inhibitor cocktail (Sigma Aldrich), Benzonase (Sigma Aldrich) and 2.4 μM PMSF was added to the cell pellet. After vigorous vortexing, cell lysate was harvested by sonicating 4 times for 10 sec each with 20 sec intervals between sonications. The concentration of protein in the lysate was determined using BioRad's DC protein assay.

A.5.5 Reaction of isoprenoid-azide modified protein with DIFO-Biotin for Western blot analysis

To COS cell lysate from one 100 mm plate was added a solution of **4** (DIFO-Biotin, 1 mM in 95:5 PBS/DMF) to a final concentration of 10 μM. Reactions were left to tumble at 4 °C for 5 h. Unreacted DIFO-Biotin was removed by protein precipitation with Calbiochem's ProteoExtract protein precipitation kit. Protein pellets (200-400 μg of total protein) were suspended 1X SDS-PAGE loading buffer for Western Blot analysis. Protein concentrations in loading buffer were determined using BioRad's RC-DC protein assay.

A.5.6 Western blot evaluation of Ras protein modification by DIFO-Biotin

20 μg of COS cell lysate was separated on a 12% acrylamide SDS-PAGE gel. Proteins were then transferred to PVDF membrane and soaked in blocking buffer (BB) at rt for 2 h (BB contains Tris-buffered saline containing 0.1% Tween-20 (TBST) and 5% non-fat dry milk). After washing the membrane 3X for 15 min with TBST, it was soaked in TBST containing anti-Ras antibodies (Millipore) at a 1:2,000 dilution overnight at 4 °C. The membrane was washed again 3X 15 min with TBST and then exposed to the colorimetric substrates BCIP and NBT (Invitrogen) per manufacturers instructions to visualize H-, N-, and K-Ras.

A.5.7 Western blot evaluation of DIFO-Biotin modified proteins

5.0 μg of COS cell lysate was separated on a 12% acrylamide SDS-PAGE gel. Proteins were then transferred to PVDF membrane and then blocked overnight at 4 °C in Tris-buffered saline containing 0.1% Tween-20 (TBST) and 5% Casein (Blocking buffer, BB). After washing the membrane 3X for 15 min with TBST, it was incubated with streptavidin-alkaline phosphatase conjugate in BB (1:100,000 dilution) for 1 h at rt. The membrane was washed again 3X 15 min with TBST and then exposed to the colorimetric substrates BCIP and NBT (Invitrogen) per manufacturers instructions to visualize the biotinylated proteins.

A.5.8 Enrichment of prenylated proteins from COS cells with DIFO-Biotin

To the COS cell lysate (1-2 mg/mL of protein, ~ 2 mg total protein) was added 30 μM DIFO-Biotin (20 mM in DMF). The reaction was left to mix at 4 °C overnight. Excess DIFO-Biotin was removed by protein precipitation with Calbiochem's ProteoExtract protein precipitation kit. Protein pellets (1-2 mg of total protein) were suspended in PBS containing 1.2% SDS, sonicated until solubilized, and then diluted 6X with PBS. Neutravidin-agarose beads (Thermo Scientific) were added and the samples were rotated for 2 h at rt, then washed 3X with 10 mL of PBS containing 0.2% SDS, 3X with 10 mL of PBS, and 1X with 10 mL of 50 mM NH_4HCO_3. Resin was then incubated with 0.04% SDS in 50 mM NH_4HCO_3, reduced with 1 mM TCEP for 1 h at 60 °C, and alkylated with 4 mM MMTS for 10 min at rt. Next, the solution was adjusted to contain 1 mM $CaCl_2$ and the samples were digested with sequence grade trypsin (Applied Biosystems) overnight at 37 °C. Supernatants were collected the following day, acidified with 10% formic acid, and vacufuged to dryness. The resulting pellet was dissolved in nanopure H_2O containing 0.1% formic acid and solid phase extraction with an MCX cartridge (Waters) was used to desalt the peptides. First, peptides were bound to the column, then washed with 5% MeOH in H_2O containing 0.1% formic acid and 100% MeOH. The peptides were then eluted with 1.4 % NH_4OH in MeOH and vacufuged to dryness.

A.5.9 LC-MS/MS analysis of prenylated proteins enriched from COS cells with DIFO-Biotin

Dried MCX eluent was reconstituted with reversed-phase load buffer (98:2 water/acetonitrile, 0.1% formic acid) and injected onto an Agilent 1100 series capillary HPLC system online with a 4000 Q-Trap MS/MS system (Applied Biosystems/MDS Sciex, Concord, ON, Canada). Peptides were loaded onto a LC Packings (Dionex Company) μ-precolumn™ cartridge (PepMap C18 5 μm, 0.3 mm internal diameter x 5 mm length) for desalting prior to loading onto a 0.075 x 100 mm fused silica column (IntegraFrit CAPILLARY, New Objective, Woburn, MA), packed in house with C18 packing material (5 mm particle size, 200 Å pore size; Michrom BioResources, Auburn, CA)[14]. The peptides were eluted with a linear gradient from 3% to 75% B over 15 min and 75% to 90% B over 5 min where solvent B was 2:95 water/acetonitrile, 0.1% formic acid and solvent A was the same as load buffer above or with a longer gradient from 2% to 35% B over 60 min and 35% to 80% B over 15 min. MS/MS spectra were collected in information-dependent acquisition (IDA) mode which included continuous cycles of one enhanced MS (EMS) scan from *m/z* 400 to 2400 (0.5 s), one enhanced resolution (ER) scan (0.5 s) to determine charge state and four product ion scans from *m/z* 50 to 2,000 (2 s each). Analyst™ software selected precursor *m/z* values (top 4 most intense ions) from a peak list automatically generated from the EMS scan during acquisition. ProteinPilot™ 3.0 software (Applied Biosystems) with the Paragon Algorithm[15] was used for the protein identification. Tandem mass spectrometry data were searched against the NCBI reference sequence mammalian protein database v20080307 (318899 proteins) plus common contaminants (179 proteins). The search parameters were ≥95% confidence for protein identification threshold, trypsin as enzyme, methylmethanethiosulfonate-labeled cysteines as fixed modification and thorough ID as search method. Greater than 150 variable

modifications, such as oxidation of methionine and deamidation of asparagines, were included in the selection of the biological modifications parameter. MS/MS spectra were also searched against the above database using Mascot® software.

A.6 References

1. Sletten, E. M. and Bertozzi, C.R., Bioorthogonal chemistry: fishing for selectivity in a sea of functionality. *Angew. Chem. Int. Ed.* **2009,** *48*, 6974-6998.

2. Breinbauer, R.; Kohn, M., Azide-alkyne coupling: a powerful reaction for bioconjugate chemistry. *Chembiochem* **2003,** *4*, 1147-1149.

3. Agard, N. J.; Prescher, J. A.; Bertozzi, C. R., A strain-promoted [3 + 2] azide-alkyne cycloaddition for covalent modification of biomolecules in living systems. *J. Am. Chem. Soc.* **2004,** *126*, 15046-15047.

4. Baskin, J. M.; Prescher, J. A.; Laughlin, S. T.; Agard, N. J.; Chang, P. V.; Miller, I. A.; Lo, A.; Codelli, J. A.; Bertozzi, C. R., Copper-free click chemistry for dynamic in vivo imaging. *Proc. Natl. Acad. Sci. U. S. A.* **2007,** *104*, 16793-16797.

5. Codelli, J. A.; Baskin, J. M.; Agard, N. J.; Bertozzi, C. R., Second-generation difluorinated cyclooctynes for copper-free click chemistry. *J. Am. Chem. Soc.* **2008,** *130*, 11486-11493.

6. Ning, X.; Guo, J.; Wolfert, M. A.; Boons, G. J., Visualizing metabolically labeled glycoconjugates of living cells by copper-free and fast huisgen cycloadditions. *Angew. Chem. Int. Ed.* **2008,** *47*, 2253-2255.

7. Duckworth, B. P.; Xu, J.; Taton, T. A.; Guo, A.; Distefano, M. D., Site-specific, covalent attachment of proteins to a solid surface. *Bioconjug. Chem.* **2006,** *17*, 967-974.

8. Duckworth, B. P.; Chen, Y.; Wollack, J. W.; Sham, Y.; Mueller, J. D.; Taton, T. A.; Distefano, M. D., A universal method for the preparation of covalent protein-DNA conjugates for use in creating protein nanostructures. *Angew. Chem. Int. Ed.* **2007,** *46*, 8819-8822.

9. Shaner, N. C.; Campbell, R.E.; Steinbach, P.A.; Giepmans, B.N.G.; Palmer, A.E.; Tsien, R.Y., Improved monomeric red, orange, and yellow fluorescent proteins derived from *Discosoma sp*. red fluorescent protein. *Nat. Biotech.* **2004,** *22*, 1567-1572.

10. Chung, J. A.; Wollack, J.W.; Hovlid, M.L.; Okesli, A.; Chen, Y.; Mueller, J.D.; Distefano, M.D.; Taton, T.A., Purification of prenylated proteins by affinity chromatography on cyclodextrin-modified agarose. *Anal. Biochem.* **2009,** *386*, 1-8.

11. Chan, L. N.; Hart, C.; Guo, L.; Nyberg, T.; Davies, B. S.; Fong, L. G.; Young, S. G.; Agnew, B. J.; Tamanoi, F., A novel approach to tag and identify geranylgeranylated proteins. *Electrophoresis* **2009,** *30*, 3598-3606.

12. Kho, Y.; Kim, S. C.; Jiang, C.; Barma, D.; Kwon, S. W.; Cheng, J.; Jaunbergs, J.; Weinbaum, C.; Tamanoi, F.; Falck, J.; Zhao, Y., A tagging-via-substrate technology for detection and proteomics of farnesylated proteins. *Proc. Natl. Acad. Sci. U. S. A.* **2004,** *101*, 12479-12484.

13. Baskin, J. M. personal communication. 2008.

14. Moseley, M. A.; Deterding, L. J.; Tomer, K. B.; Jorgenson, J. W., Nanoscale packed-capillary liquid chromatography coupled with mass spectrometry using a coaxial continuous-flow fast atom bombardment interface. *Anal. Chem.* **1991,** *63*, 1467-1473.

15. Shilov, I. V.; Seymour, S. L.; Patel, A. A.; Loboda, A.; Tang, W. H.; Keating, S. P.; Hunter, C. L.; Nuwaysir, L. M.; Schaeffer, D. A., The paragon algorithm, a next generation search engine that uses sequence temperature values and feature probabilities to identify peptides from tandem mass spectra. *Mol. Cell. Proteomics* **2007,** *6*, 1638-1655.

Appendix B. Prediction and evaluation of protein farnesyltransferase inhibition by commercial drugs

B.1 Introduction

Bringing a novel chemical entity to market cost 868 million USD in 2006[1], with most costs accumulating during clinical testing when drug candidates fail due to unforeseen pathway interactions. While these interactions are often harmful, causing adverse effects, they may also be beneficial, leading to useful properties. Accurate prediction of off-target drug activity prior to clinical testing may benefit patient safety and also lead to new therapeutic indications, as has been promoted by Wermuth, among others.[2-5]

The Similarity Ensemble Approach (SEA) uses chemical similarity among ligands organized by their targets to calculate similarities among those targets and to predict drug off-target activity.[6-8] From the perspective of molecular pharmacology and bioinformatics, the approach is counter-intuitive, as it relies on ligand chemical information exclusively, using no target structure or sequence information whatsoever. Instead, SEA and related cheminformatics approaches[9-15] return to an older, classical pharmacology view, where biological targets were characterized by the ligands that bind to them. To that older view, SEA adds modern methods for measuring chemical similarity for sets of ligands, and applies the BLAST[16] sequence-similarity algorithms to control for the similarity among ligands and ligand sets that one would expect at random (an innovation of this method).[7, 17] The technique has been used to discover several drugs

activities as unanticipated targets. The opioid receptor antagonists methadone and loperamide were predicted and subsequently found to be ligands of the muscarinic and neurokinin NK2 receptors, respectively.[7] More recently, the antihistamines dimetholazine and mebhydrolin base were predicted and found to have activities against α_1 adrenergic, 5-HT_{1A} and D_4 receptors, and 5-HT_{5A}, respectively; the anticholinergic diphemanil methylsulfate was predicted and found to have δ-opioid activity; the transport inhibitor fluoxetine was predicted and found to bind to the β_1-adrenergic receptor; and the α_1 blocker indoramin was predicted and found to have dopamine D_4 activity, among others.[6-8]

Many of these predictions have been among drugs that bind aminergic G-protein coupled receptors (GPCRs)[6-8], and whereas there have been cases of predictions crossing receptor classification boundaries (e.g., ion channel blockers acting on GPCRs and transporters[8]), a criticism to which the approach may be liable is that it has been focused on targets for which polypharmacology is not without precedent. We thought it interesting to investigate whether off-target activity may be predicted for drugs that target enzymes, especially for those drugs predicted to be active against an enzyme that has little or no similarity to the canonical target for that drug. As a target enzyme we focused on protein farnesyltransferase (PFTase), using SEA to compare 746 commercial drugs against ligand sets built from the 1,640 known non-peptide PFTase ligands reported in ligand-receptor annotation databases (see Methods).

The post-translational attachment of lipid moieties to proteins is critical for membrane anchorage of signal transduction proteins.[18] PFTase catalyzes the attachment of the C_{15} isoprenoid to a cysteine residue of proteins containing a C-terminal CAAX consensus

sequence, where C is the cysteine to be prenylated, A is an aliphatic amino acid, and X is commonly Ser or Met.[19] Upon attachment of the isoprene unit, an endoprotease cleaves off the –AAX residues. Using S-adenosylmethionine as a methyl-group donor, a methyltransferase then caps the –COOH of the prenylated protein. It is the increase in hydrophobicity, as well as the lack of charge at the C-terminus, that allows for membrane localization.[20] Proteins that are farnesylated include the nuclear lamins and members of the Ras superfamily of small guanosine triphosphatases.[20]

The finding that mutant Ras proteins must be prenylated to exert their oncogenic effects[21, 22] led to the development of a number of inhibitors of protein prenylation, specifically through the inhibition of PFTase. Compounds were either rationally designed, based on peptide- or isoprenoid-substrate characteristics, or were discovered through screening of in-house chemical libraries. To date, five compounds have been brought to clinical trials as inhibitors of PFTase.[23] Results of these trials have been modest at best, with very few compounds showing anti-tumor activity.[23-25] Two drug candidates, Lonafarnib (Schearing-Plough) and Tipifarnib (Janssen Pharmaceutica) are the only compounds to make it to late-stage clinical trials[26] and are currently being explored as single agents or adjunct therapies for breast cancer[27] and leukemia.[28, 29]

While farnesyltransferase inhibitors (FTIs) have yet to live up to their promise as anti-cancer agents, they are showing applicability towards the treatment of other diseases. Hutchinson-Gilford Progeria syndrome results from a mutation in the LMNA gene, which causes an unusable form of the protein Lamin A. Because the precursor to Lamin A is farnesylated, it was proposed that FTIs may be capable of ameliorating the disease phenotypes in those suffering from progeria.[30] Studies published in 2006 found that

treatment of progeria mice with the FTI Lonafarnib could dramatically prevent the development of disease characteristics.[31, 32] These results prompted the launch of a phase II clinical trial examining the use of Lonafarnib in progeria patients.[33] FTIs are also capable of blocking farnesylation in the protozoan parasites *Trypanosoma cruzi*, *Trypanosoma brucei*, and *Plasmodium falciparum*.[34] The cessation of farnesylation in these parasites by inhibiting PFTase appears to be particularly toxic, indicating the potential of FTIs for the treatment of Chagas disease[35] (caused by *T. cruzi*), African sleeping sickness[36] (caused by *T. brucei*) and malaria[37, 38] (caused by *P. falciparum*).

B.2 Research Objectives

The clinical relevance of FTIs towards a number of diseases necessitates the development of more potent and selective inhibitors. A starting point for identifying new PFTase inhibitors is exploring those drugs already in use for other diseases. The goal of this work was to apply SEA towards the prediction of commercially available drugs that are capable on inhibiting protein farnesyltransferase. Compounds predicted to bind to PFTase were tested first in an *in vitro* continuous fluorescence assay. Those found to be inhibitors were then tested in a cell based assay to monitor the prenylation of a known PFTase target, H-Ras.

B.3 Results

B.3.1 Applying SEA to Protein Farnesyltransferase

To predict which compounds may have off-target activity against PFTase, we first asked what affinity ranges are relevant. Many known inhibitors have 10-20 μM affinity for this enzyme. To be comprehensive, we considered three thresholds of FTI affinity, each at increasingly greater stringency. In the first instance, we considered all those 1,692 FTIs known to have 100 μM or better affinity, reasoning that this would allow for the greatest breadth of predictions. We then narrowed our focus to include only those 1,423 FTIs with 10 μM or better affinity, and finally excluded all but the 1,188 FTIs with affinity ≤ 1 μM. We considered each threshold independently, and later extracted each commercial drug's best SEA match with the set of known PFTase ligands at any of the three thresholds. For example, Loratadine matched most strongly against the FTIs known to have ≤ 10 μM for their target, with a SEA expectation value (E-value) of 1.07×10^{-81} (Table B.1). On the other hand, Ubenimex was most similar to the ≤ 100 μM FTIs, with an E-value of 1.53×10^{-16} for them (Table B.1), compared to weaker E-values of 4.97×10^{-13} and 7.23×10^{-9} for its similarity against the ≤ 10 μM and ≤ 1 μM FTIs, respectively (Table B.2). An E-value, much like a p-value, denotes the likelihood of a particular event. In this case, the E-value represents the degree of chemical similarity for a commercial drug against the set of ligands for protein farnesyltransferase as compared to the similarity that would have been found by random chance alone. When applied across all 746 commercial drugs, this analysis found 13 of them (comprising 1.9% of the total drugs screened) to have measurable similarity to at least one of the three FTI sets (Table B.1).

Several of the predictions have relatively modest SEA values (Table B.1). Formally, SEA E-values have the same meaning as the more familiar BLAST E-values, quantifying the expectation that an observed similarity would occur by chance. The underlying

expectation of randomness is, of course, different for the mostly synthetic annotated ligands analyzed by SEA and naturally evolved sequences, and a pragmatic E-value cut-off for making a prediction is not yet clear. In earlier work we have often looked for E-values better (lower) than 10^{-10}, but this is an arbitrary and conservative cutoff, and novel, potent off-target effects have been predicted based on SEA values as low as 10^{-4} for Vadilex's activity against serotonin transporter and for activity of RO-25-6981 against the κ opiod receptor, 5×10^{-6} for dimethyltryptamine's activity against the $5HT_{5A}$ receptor, and 10^{-7} for Paroxetine's activity against the ß1 adrenergic receptor.[8] Currently, the choice of E-value cutoff for testing predictions will vary depending on pragmatic considerations, including the intrepidness of the experimental team. In principle, and E-value below 1 is significant.

Of the thirteen commercial drugs predicted to have off-target PFTase binding by SEA, eight already had literature precedent or were difficult to source (see Methods). We tested the remaining five by *in vitro* analysis, and advanced two to analysis in a mammalian cell line engineered for monitoring the prenylation of H-Ras.[39]

Table B.1. Top SEA predictions of off-target PFTase binding for commercial drugs

	Drug	Best SEA E-value	Best FTI Match
1	Loratadine	1.07×10^{-81}	10 μM
2	Rupatadine	1.10×10^{-49}	10 μM
3	Desloratadine	1.22×10^{-30}	10 μM
4	Ubenimex	1.53×10^{-16}	100 μM
5	Azatadine	2.68×10^{-11}	100 μM
6	Phenylalanine S	1.70×10^{-4}	100 μM
7	Miconazole	2.00×10^{-4}	100 μM
8	Diazepam[69]	5.52×10^{-4}	1 μM
9	Temazepam[69]	1.21×10^{-3}	1 μM
10	Thymopentin	2.10×10^{-3}	100 μM
11	Cortisone acetate[70]	6.57×10^{-3}	100 μM
12	Prednisone[70]	3.81×10^{-2}	100 μM

Drugs in red have PFTase activity already reported in the literature. Drugs in blue were either peptides or unavailable.

Table B.2 SEA predictions for potential PFTase ligands at various thresholds of similarity to known ligands and their subsequent analysis as PFTase inhibitors.

	Drug	FTIs by affinity threshold (SEA E-values)			IC_{50} (μM)
		1 μM	10 μM	100 μM	
1	Loratadine 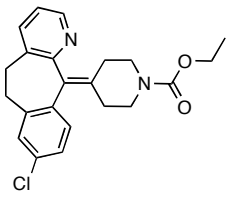	7.87×10^{-53}	**1.07×10^{-81}**	**1.53×10^{-81}**	13.3 ± 1.8
2	Rupatadine 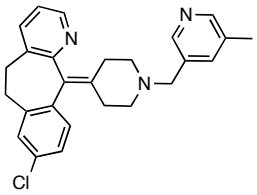	5.90×10^{-41}	**1.10×10^{-49}**	**8.15×10^{-49}**	76 ± 18
3	Desloratadine 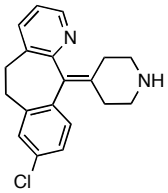	3.45×10^{-27}	**1.22×10^{-30}**	**1.83×10^{-30}**	> 100
4	Ubenimex 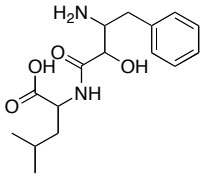	7.23×10^{-9}	4.97×10^{-13}	**1.53×10^{-16}**	> 200
5	Miconazole 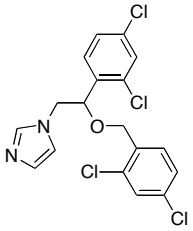	$8.26\times10^{+2}$	**2.86×10^{-3}**	**2.00×10^{-4}**	18.9 ± 3.6

6	Econazole 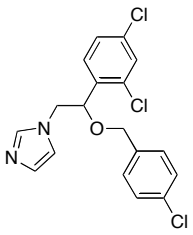	N/A	N/A	N/A	23.3 ± 2.0

SEA E-values are shown denoting the statistical significance of each drug's similarity to known protein farnesyltransferase inhibitors (FTIs). The more the E-value approaches zero, the more significant the similarity; the strongest prediction for each drug is in bold. Each drug was compared against three different sets of known FTIs. For instance, for the "1 μM FTIs" set, we only considered those FTIs known to have 1 μM affinity or greater for PFTase. For the "10 μM FTIs" set, we considered all FTIs known to have 10 μM or greater affinity for PFTase, etc. Where a drug's PFTase predictions by SEA are very close (within approximately a single order of magnitude), both E-values are bolded.

B.3.2 In vitro analysis of PFTase inhibition

A continuous-fluorescence assay, based on the time-dependent increase in dansyl group fluorescence that occurs as the CAAX-peptide *N*-dansyl-GCVLS is prenylated,[40, 41] was employed to measure PFTase activity in the presence of the predicted inhibitors. This assay was used to calculate IC_{50} values; for confirmation, the extent of inhibition at the IC_{50} concentration was confirmed for each compound in a separate HPLC-based assay.[42] The five commercial drugs tested comprised of three histamine H_1 receptor antagonists (Loratadine, Desloratadine, and Rupatadine), an antineoplastic (Ubenimex), and an azole antifungal (Miconazole) (Table B.1). In our enzymatic assay, two of the antihistamines

and the azole antifungal were effective inhibitors of PFTase in the low-to-mid micromolar range (Table B.2). For all but Ubenimex, the 100 μM and 10 μM FTI sets resulted in the strongest SEA predictions, with little difference in prediction strength between the two affinity classes (Table B.2). This was consistent with their calculated PFTase IC_{50} values, which we found to be between 20-80 μM—with the exception of Desloratadine and Ubenimex, which did not inhibit PFTase up to 100 μM and 200 μM, respectively.

After conducting this work, we discovered that analogues of Loratadine have been investigated for PFTase inhibition via a high-throughput screening approach;[43] Miconazole, to the best of our knowledge, is a novel PFTase inhibitor class. We thus asked whether other azole antifungals, not predicted by SEA but established members of that class, also had unreported activity with PFTase, controlling for the non-specific small-molecule aggregation in which some azoles are known to participate.[44] To this end, we tested the non-aggregators Econazole, Fluconazole, and Ketoconazole, and the aggregator Clotrimazole in our continuous fluorescence assay.[45] In accordance with previous work on preventing non-specific enzyme inhibition by small molecule aggregation[45], Triton X-100 was included in all assay solutions to prevent aggregate formation. A non-azole, small molecule aggregator, Tetraiodophenolphthalein (TIPT), previously shown to non-specifically inhibit enzymes via this mechanism,[44] was also tested for PFTase inhibition as an internal control. Only Econazole showed appreciable inhibition of PFTase with an IC_{50} value similar to that measured for Miconazole. The other azole antifungals, including the known aggregator Clotrimazole, showed little to no inhibition at concentrations as high as 100 μM. TPIT was not an inhibitor of PFTase,

confirming that the assay conditions did not allow for *in vitro* small-molecule aggregation.

B.3.3 Analysis of Loratadine and Miconazole using a cell based in vitro assay.

For a FTI to have clinical relevance, it must block the targets of protein farnesylation from functioning properly. A mammalian cell line engineered to express a chimera of the green fluorescent protein (GFP) and H-Ras[46] was employed to assess the ability of Loratadine and Miconazole to block the membrane localization of Ras through inhibition of farnesylation. GFP-H-Ras that has been processed by PFTase and the subsequent enzymes in the protein prenylation pathway will be localized at the cell's Golgi and plasma membrane. If prenylation has been inhibited, GFP-H-Ras will be present in the cellular cytosol.

Cells were treated for 24 h with varying concentrations of Loratadine and Miconazole in DMSO ranging from 1X to 5X the experimentally observed enzymatic IC_{50} value or DMSO vehicle alone. At 25 μM Loratadine (2.5X the IC_{50}), appreciable inhibition of GFP-H-Ras processing was observed as evidenced by the diffuse cytosolic fluorescence not present when treated with DMSO alone (Figure B.1).

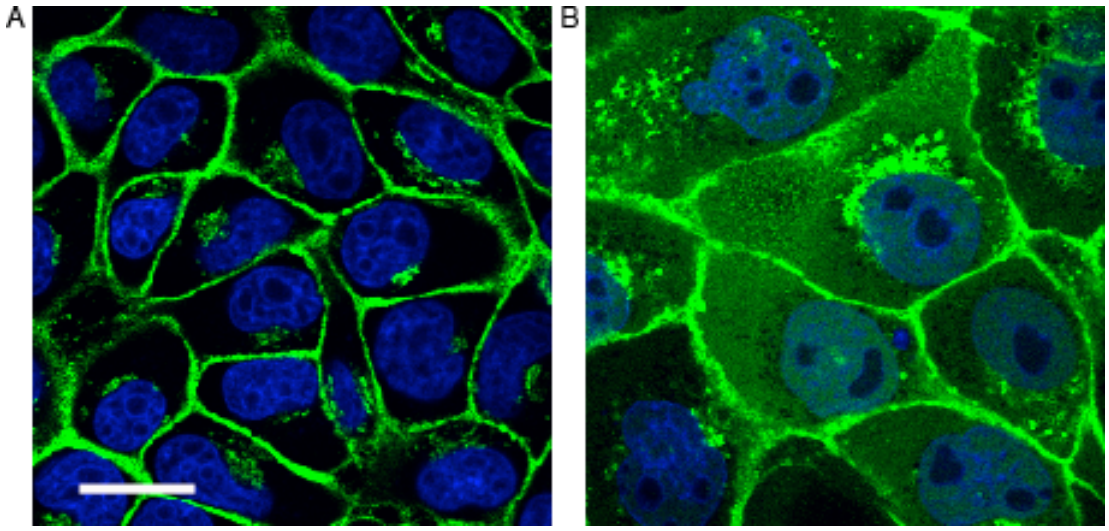

Figure B.1 Intra-cellular inhibition of H-Ras processing by Loratadine (**1**). Scale bar represents 10 μm. GFP-H-Ras is shown in green. The cell nucleus is shown in blue. A: Cells grown in FBS supplemented DMEM containing 0.5% DMSO for 24 h. B: Cells grown in FBS supplemented DMEM containing 0.5% DMSO and 25 μM Loratadine for 24 h.

Localization of fluorescence at the Golgi and plasma membrane is also evident, meaning either total inhibition of the GFP-H-Ras was not achieved, or GFP-H-Ras synthesized and processed prior to treatment had not been degraded yet. Treating cells with higher concentrations of Loratadine was toxic and led to death, while lower concentrations did not manifest observable inhibition of prenylation. Treatment of cells with Miconazole at concentrations at or above the IC_{50} value also lead to toxicity and cell death. Therefore, treating with 10 μM Miconazole (0.5X the IC_{50}) for 48 h was tested. A number of cells died in this case and were subsequently washed from the plate during nuclear staining procedure (see Methods) but those cells remaining alive and still adhered to the plate had significant inhibition of GFP-H-Ras processing (Figure B.2).

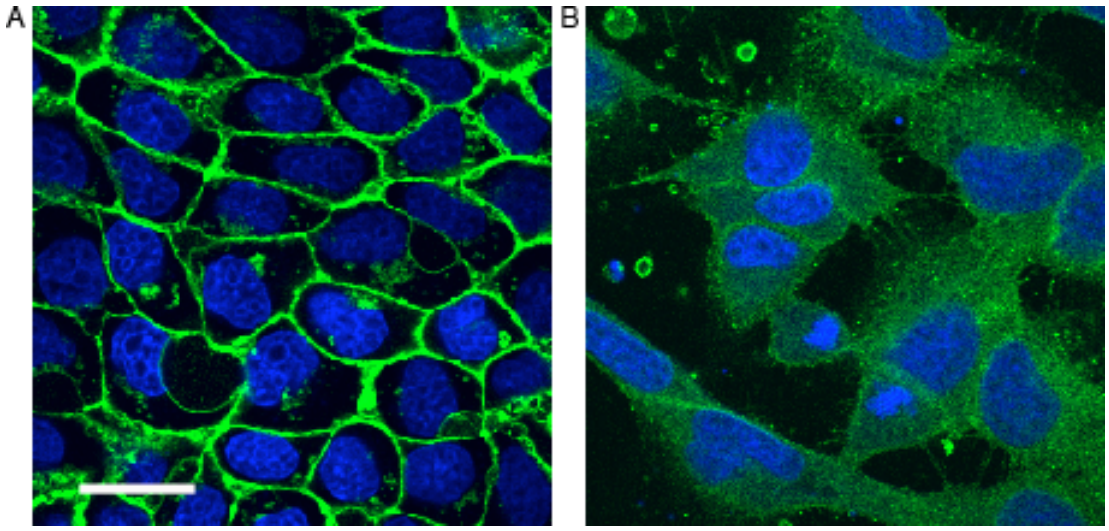

Figure B.2. Intra-cellular inhibition of H-Ras processing by Miconazole (**5**). Scale bar represents 10 μm. GFP-H-Ras is shown in green. The cell nucleus is shown in blue. A: Cells grown in FBS supplemented DMEM containing 0.5% DMSO for 48 h. B: Cells grown in FBS supplemented DMEM containing 0.5% DMSO and 10 μM Miconazole for 48 h.

B.4 Discussion

Whereas the previous drug polypharmacology predicted by SEA focused on drugs that target aminergic GPCRs,[6-8] Loratadine and Miconazole were predicted to bind PFTase in violation of these traditional target-class boundaries. The antihistamine Loratadine represents one of the first uses of this approach to demonstrate that a commercial drug thought to be specific for a GPCR also binds an enzyme, while the activity of the anti-fungal P450 Miconazole represents the approach's first enzyme-enzyme cross-talk prediction among commercial drugs. While the IC_{50} values obtained for these compounds against PFTase are modest at best, they do offer starting points for inhibitor design optimization.

Loratadine is a second-generation antihistamine that binds the H_1 receptor—a cross-membrane target that shares no evolutionary history, functional role, or structural similarity with the enzyme PFTase. We found Loratadine to have an exceptionally strong E-value of 1.07×10^{-81} for PFTase ligands in the 10 μM – 100 μM range (Table 2), and SEA also predicted strong scores for two of its analogs, Rupatadine and Desloratadine (1.10×10^{-49} and 1.22×10^{-30}, respectively, Table 2). These off-target predictions were confirmed for Loratadine and Rupatadine, at 13 μM and 76 μM IC_{50}s, whereas Desloratadine, the primary metabolite of both Loratadine and Rupatadine, showed no appreciable inhibition up to 100 μM. For Loratadine, the ability to block the processing of H-Ras *in vivo* was also confirmed in our GFP-H-Ras chimera mammalian cell line. Loratadine has been reported to be active only at the histamine H1 receptor[47], while Rupatadine is active at both the histamine H_1 and platelet-activating factor receptors.[48] Both, as well as Desloratadine, have shown good safety profiles over prolonged treatment.[47, 49, 50] Anti-muscarinic receptor activity, often associated with the earlier generation of H_1 receptor antagonists, is not commonly observed with these drugs.[51, 52]

Whether or not the off-target inhibition of PFTase by Loratadine has any clinical relevance has yet to be determined. At therapeutic doses, the active metabolite of Loratadine (Desloratadine) reaches plasma concentrations of approximately 300 nM (based on information available in DRUGDEX®).[53] In our study, Desloratadine was not an inhibitor of PFTase. While it appears that Loratadine will not have any clinical significance in terms of PFTase inhibition, synergistic effects with other drugs known to affect protein prenylation levels, such as the commonly prescribed statin drugs that inhibit HMG-CoA reductase[54, 55], may reveal themselves. An extensive literature search

revealed no evidence towards clinical off-label use of Loratadine for the indications related to PFTase. Recently, a high-throughput screening of commercial drugs for toxicity towards the parasite *T. cruzi* revealed Loratadine to have an IC_{50} value 23 μM.[56] Inhibition of *T. cruzi* PFTase could be the cause of this observed toxicity and warrants further investigation. The presence of such off-target drug activity across GPCR and enzyme class boundaries even among well-studied commercial drugs suggests opportunities for both drug development and potential side-effect management. Whether or not the compounds developed as FTIs have any activity against the histamine H_1 receptor have yet to be investigated or reported.

Miconazole and Econazole are topical imidazole antifungals that increase cell membrane permeability in fungi, resulting in leakage of cellular contents. Both of these anti-fungals inhibit 14-α demethylase, a cytochrome P-450 enzyme necessary to convert lanosterol to ergosterol, which is an essential component of cell membranes.[53] Using SEA, we found that Miconazole had weak yet significant similarity to the set of 100 μM PFTase inhibitors, with an E-value of 2.00×10^{-4} (Table 1). Upon validating Miconazole's 19 μM IC_{50} for PFTase, we also tested Econazole, which has a highly similar chemical structure, and found it to have an IC_{50} of 23 μM against this target (Table 2). Analyses of Miconazole's ability to block prenylation *in vivo* revealed it to be toxic at concentrations high enough to result in observable inhibition. The inhibition of ergosterol biosynthesis contributes to Miconazole's anti-fungal mechanism of action and also, it is thought, to Miconazole's activity against the parasite *T. cruzi*.[57] It is intriguing to consider that interactions with PFTase may complement the drugs' anti-fungal and anti-parasitic activity. Nonetheless, the enzymes PFTase and 14-α demethylase share no

evolutionary history or structural similarity, and this cross-talk may suggest new directions for anti-fungal development.

There is no evidence in the literature pertaining towards the use of Miconazole for indications related to PFTase. Based on the information available in the DRUGDEX® system[53], the peak concentration of Miconazole reached in the body upon subcutaneous delivery (the common dosage form) is approximately 25 nM. This is well below our experimental IC_{50} value suggesting that topical administration of Miconazole does not have any clinical significance in terms of PFTase inhibition. It is interesting to note that Miconazole has been tested by the NCI/NIH Developmental Therapeutics Program as an anti-cancer agent. According to the NCI/DTP Open Chemical Repository (NSC 170986), intraperitoneal delivery of Miconazole was shown to promote survival in mouse models of leukemia and melanoma.[58] While FTIs are not currently be explored in the treatment of melanoma, they are candidate leukemia chemotherapeutics.[28, 29] Compounds developed as inhibitors of PFTase have not been reported to bind 14-α demethylase.

B.5 Conclusions

From a target-based perspective, the activities of Loratadine and Miconazole against PFTase are perplexing–neither the H_1 histamine GPCR nor the fungal P450 have detectable sequence or structural similarity to protein farnesyltransferase. From an older, classical pharmacology perspective, the cross-reactivities are perhaps less surprising, as many drugs share common provenances as chemical series. What recent cheminformatics-based approaches[5, 10-15] bring to this older view is a systematic analysis

of all drug space–allowed by the creation of target-ligand annotation databases like WOMBAT[59] and ChEMBL StARlite[60]–and quantitative models that separate similarity expected at random from similarity that is quantifiably significant among ligand sets. A contribution of this work is to suggest that the similarities observed among targets, based on their ligands, may cross receptor-enzyme and enzyme-enzyme boundaries, and thus techniques that exploit a ligand-based view of pharmacology may have a wide application. [60]

B.6 Experimental

B.6.1 General materials and methods

All tested compounds were purchased from LKT Laboratories (St. Paul, MN) at >98% purity as determined by HPLC. All other reagents were purchased from Sigma Aldrich. *N*-Dansyl-GCVLS was prepared as described in Gaon et. al.[61] The PFTase utilized was obtained and purified as described in DeGraw et. al.[62] Fluorescence measurements were made on a Beckman Coulter DTX 880 plate reader fitted with a 340 nm excitation filter and 535 nm emission filter. Hoescht nuclear dye was obtained from Invitrogen.

B.6.2 Sources of known protein farnesyltransferase ligands

We used several subsets of the known FTIs as our reference sets. To do so, we built the set of known ligands corresponding to each major drug target in the literature

extracted from the World of Molecular BioAcTivity (WOMBAT) 2006.2 database, as in previous work.[6] After removal of duplicates, molecules that we could not process, and ligands with affinities worse than 100 μM for their protein targets, this database comprised 169,046 molecules annotated into 1,469 target-function sets (e.g., the PFTase *inhibitors* and the PFTase *binders* of unknown function comprised two distinct sets). We then extracted the 1,723 molecules from this collection that were annotated as PFTase inhibitors (1,648 molecules) or PFTase binders (75 molecules), and filtered out all molecules containing two sequential peptide bonds along a standard peptide backbone, using a SMARTS filter in Scitegic PipelinePilot. We further subdivided these PFTase binders (collectively termed "FTIs" or "FTI sets" in main text) by their affinities for PFTase, into 100 μM, 10 μM, and 1 μM FTI sets, containing 1,692 molecules, 1,423 molecules, and 1,188 molecules, respectively. The remaining 1,467 target-function sets from WOMBAT were not considered in this analysis.

PFTase ligands used in the WOMBAT training sets included few marketed drugs. One exception, cortisone acetate, has an IC_{50} of 14 μM for PFTase.[63] Secondly, the amino-bisphosphonates ibandronic acid, pamidronic acid, risedronic acid, and alendronic acid were included in the 1 μM PFTase ligand set due to their annotations in WOMBAT, although subsequent investigation revealed that direct binding of these bisphosphonates to PFTase has not been demonstrated, to our knowledge. The remaining marketed drugs shown in Table 1 were not included in the training sets, as they were not reported as PFTase ligands in WOMBAT.

B.6.3 Choice of ligand set thresholds

While we included a PFTase ligand set at 100 μM for completeness and to increase the chance of finding novel PFTase ligands, we note that SEA predictions for ligand sets at 10 μM compared to those at 100 μM did not substantially differ. Ubenimex was the only exception (Table 2), and in this case, the SEA prediction yielded no detectable binding at < 100 μM. Ligand set thresholds of 1 μM and 10 μM may be sufficient for future analysis directed at PFTase.

B.6.4 Collection of commercial drugs

We extracted all molecules annotated as marketed drugs in the WOMBAT 2006.2 database, and processed them as above (excepting peptide and 100 μM affinity filtering). This yielded 746 commercial drugs, each of which we screened individually against the FTI sets using SEA.

B.6.5 Similarity measures

We used 1024-bit folded Scitegic ECFP_4 topological fingerprints as previously described.[6] Although we later also tested 2048-bit Daylight[6, 7] fingerprints, these resulted in a narrower and weaker subset of the PFTase predictions found via ECFP_4, and are not reported here. As before, we used the Tanimoto coefficient to calculate pair-wise similarity between fingerprints.[6, 7]

B.6.7 Similarity Ensemble Approach (SEA)

SEA is based on the premise that chemically similar molecules will bind similar targets[64, 65] and thus have similar biological profiles[66]. A raw score is calculated for ligand set similarity by summing the Tanimoto similarities[67-69] between all ligand sets of interest. This score in itself is not an accurate assessment of similarity because it is dependent on the number of ligands in each set and it does not take into account random similarities. Set-size dependence is corrected for by SEA using a statistically determined threshold. Pairs of molecules that score below it are discarded and do not contribute to the overall set similarity. The raw score gets converted to a z-score, free of set-size bias, using the mean and standard deviation of raw scores modeled from sets of random molecules. The final similarity score is expressed as an expectation value (E-value) based on the probability of observing a given z-score using random data. Small E-values reflect relationships between ligand-sets that are stronger than would be expected by random chance alone. SEA effectively links ligand sets and their corresponding protein targets together in minimal spanning trees, resulting in biological related proteins being clustered together.

B.6.8 Predictions of off-target PFTase binding using SEA

We ran SEA as previously described.[7] The query collection consisted of the 746 commercial drugs, each drug as its own "set" of one molecule. The reference collection comprised the three overlapping sets of PFTase ligands ("FTIs"), binned into each set at

(a) 1 μM, (b) 10 μM, or (c) 100 μM affinity thresholds. A FTI set with a weaker affinity threshold, such as 100 μM, comprised an all-inclusive superset of those sets at stronger affinity threshold (both the 1 μM and 10 μM sets, in this example). After each drug was compared independently against each of the three FTI sets by SEA, their E-values were compared (e.g., see Table B.2), and all commercial drugs with measurable best-match E-values across sets were reported (Table B.1).

B.6.9 Choice of drugs for testing

We excluded Diazepam and Temazepam because diazepam's weak PFTase activity is already reported[70], and the steroids because Cortisone's and Prednisone's PFTase activities are likewise known.[63] We chose not to persue Azatadine, due to sourcing issues and did not test Thymopentin or Phenylalanine-S because they are peptides. We excluded both the known peptide FTIs and the predicted peptide drugs because SEA's statistical models were built using small-molecule drug chemical similarity descriptors. As peptides contain oft-repeated chemical patterns in their backbones—and thus strong opportunities for *uninformative* similarity—they may have the potential to skew small-molecule similarity models if included. We nonetheless tested one peptide prediction, Ubenimex, because it appeared highly similar to a known FTI.

B.6.10 PFTase in vitro assay

The continuous fluorescence assay developed by Pompliano and coworkers[41] was adapted to a 96-well plate format. Assay solutions in individual wells contained 50 mM Tris-HCl, pH 7.5, 10 mM $MgCl_2$, 10 μM $ZnCl_2$, 5.0 mM DTT, 0.02% (w/v) *n*-octylglucopyranoside, 2.0 μM *N*-dansyl-GCVLS, FPP (10 μM), and inhibitor at varying concentrations (from 0 to 200 μM). All inhibitors were dissolved in DMSO due to limited solubility. For analysis of the H1 receptor agonists, a total of 5% (v/v) DMSO was in each sample. For analysis of the azole antifungals, a total of 20% (v/v) DMSO was in each sample as well as 0.04% (v/v) Triton X-100 to prevent aggregate formation. Each sample was analyzed in triplicate. PFTase was prepared by diluting purified enzyme with buffer (52mM Tris-HCl, pH 7.0, 5.8 mM DTT, 12 mM $MgCl_2$, 12 μM $ZnCl_2$) containing 1 mg/mL bovine serum albumin. Samples were equilibrated at 30°C and the reaction was initiated by the addition of dilute PFTase. Fluorescence intensity was monitored via a time-based scan for 60 min or longer depending on when fluorescence enhancement ceased. The enzymatic rate of each reaction was determined by converting the rate of increase in fluorescence intensity units (FIU/s) to μM/s with eq 1,

$$v_i = \frac{RP}{F_{\max}} \tag{1}$$

where v_i is the enzymatic rate in μM/s. R is the measured rate in FIU/s and P is the concentration of *N*-Dansyl-GCVLS used in the assay. F_{MAX} is the fluorescence intensity of the fully prenylated peptide.

B.6.11 Cell based analysis of H-Ras processing

MDCK cells engineered to over-express a GFP-H-Ras chimera were used to visualize Ras processing *in vivo*. For all experiments, 2.6 x 10^4 cells/cm^2 were seeded in culture dishes. The cells were grown in DMEM media supplemented with 10% fetal bovine serum at 37°C with 5.0% CO_2 and grown to approximately 50% confluency (generally 24 h). The cells were then washed twice with serum-free DMEM and fresh serum-free DMEM was added. The desired inhibitor (Loratadine or Miconazole) in DMSO was added at varying concentrations (1 μM to 200 μM drug, 0.5 % to 1.0 % (v/v) DMSO) and incubated for 24 h at 37°C and 5.0% CO_2. Hoechst 34580 nuclear stain was added to a final concentration of 1 μg/mL during the final 20 min of incubation. The cells were then washed twice with PBS and placed back in DMEM. Imaging was performed on an Olympus FluoView 1000 confocal microscope with a 60X objective. The Hoechst 34580 nuclear stain was imaged with 405 nm excitation and 461 nm emission. The GFP-H-Ras chimera was imaged with 488 nm excitation and 519 nm emission.

B.7 References

1. Adams, C. P.; Brantner, V. V., Estimating the cost of new drug development: is it really 802 million dollars? *Health Aff. (Millwood)* **2006,** *25*, 420-428.

2. Hopkins, A. L., Network pharmacology: the next paradigm in drug discovery. *Nat. Chem. Biol.* **2008,** *4*, 682-690.

3. Oprea, T. I.; Tropsha, A.; Faulon, J. L.; Rintoul, M. D., Systems chemical biology. *Nat. Chem. Biol.* **2007,** *3*, 447-450.

4. Scheiber, J.; Jenkins, J. L., Chemogenomic analysis of safety profiling data. *Methods Mol. Biol.* **2009,** *575*, 207-223.

5. Wermuth, C. G., Selective optimization of side activities: the SOSA approach. *Drug Discov. Today* **2006,** *11*, 160-164.

6. Hert, J.; Keiser, M. J.; Irwin, J. J.; Oprea, T. I.; Shoichet, B. K., Quantifying the relationships among drug classes. *J. Chem. Inf. Model* **2008,** *48*, 755-765.

7. Keiser, M. J.; Roth, B. L.; Armbruster, B. N.; Ernsberger, P.; Irwin, J. J.; Shoichet, B. K., Relating protein pharmacology by ligand chemistry. *Nat. Biotechnol.* **2007,** *25*, 197-206.

8. Keiser, M. J.; Vincent, S.; Irwin, J. J.; Laggner, C.; Abbas, A. I.; Hufeisen, S. J.; Jensen, N. H.; Kuijer, M. B.; Matos, R. C.; Tran, T. B.; Whaley, R.; Glennon, R. A.; Hert, J.; Thomas, K. L. H.; Edwards, D. D.; Shoichet, B. K.; Roth, B. L., Predicting new molecular targets for known drugs. *Nature* **2009,** *462*, 175-181.

9. Bajorath, J., Computational analysis of ligand relationships within target families. *Curr. Opin. Chem. Biol.* **2008,** *12*, 352-358.

10. Campillos, M.; Kuhn, M.; Gavin, A. C.; Jensen, L. J.; Bork, P., Drug target identification using side-effect similarity. *Science* **2008,** *321*, 263-266.

11. Lounkine, E.; Stumpfe, D.; Bajorath, J., Molecular formal concept analysis for compound selectivity profiling in biologically annotated databases. *J. Chem. Inf. Model* **2009,** *49*, 1359-1368.

12. Muchmore, S. W.; Debe, D. A.; Metz, J. T.; Brown, S. P.; Martin, Y. C.; Hajduk, P. J., Application of belief theory to similarity data fusion for use in analog searching and lead hopping. *J. Chem. Inf. Model* **2008,** *48*, 941-948.

13. Scheiber, J.; Jenkins, J. L.; Sukuru, S. C.; Bender, A.; Mikhailov, D.; Milik, M.; Azzaoui, K.; Whitebread, S.; Hamon, J.; Urban, L.; Glick, M.; Davies, J. W., Mapping adverse drug reactions in chemical space. *J. Med. Chem.* **2009,** *52*, 3103-3107.

14. Vieth, M.; Erickson, J.; Wang, J.; Webster, Y.; Mader, M.; Higgs, R.; Watson, I., Kinase inhibitor data modeling and de novo inhibitor design with fragment approaches. *J. Med. Chem.* **2009,** *52*, 6456-6666.

15. Young, D. W.; Bender, A.; Hoyt, J.; McWhinnie, E.; Chirn, G. W.; Tao, C. Y.; Tallarico, J. A.; Labow, M.; Jenkins, J. L.; Mitchison, T. J.; Feng, Y., Integrating high-content screening and ligand-target prediction to identify mechanism of action. *Nat. Chem. Biol.* **2008,** *4*, 59-68.

16. Altschul, S. F.; Gish, W.; Miller, W.; Myers, E. W.; Lipman, D. J., Basic local alignment search tool. *J. Mol. Biol.* **1990,** *215*, 403-410.

17. Keiser, M. J.; Hert, J., Off-target networks derived from ligand set similarity. *Methods Mol. Biol.* **2009,** *575*, 195-205.

18. Walsh, C. T.; Garneau-Tsodikova, S.; Gatto, G. J., Jr., Protein posttranslational modifications: The chemistry of proteome diversifications. *Angew. Chem. Int. Ed.* **2005,** *44*, 7342-7372.

19. Reid, T. S.; Terry, K. L.; Casey, P. J.; Beese, L. S., Crystallographic analysis of CaaX prenyltransferases complexed with substrates defines rules of protein substrate selectivity. *J. Mol. Biol.* **2004,** *343*, 417-433.

20. Zhang, F. L.; Casey, P. J., Protein prenylation: molecular mechanisms and functional consequences. *Annu. Rev. Biochem.* **1996,** *65*, 241-269.

21. Lowy, D. R.; Willumsen, B. M., Function and regulation of ras. *Annu. Rev. Biochem.* **1993,** *62*, 851-891.

22. Kato, K.; Cox, A. D.; Hisaka, M. M.; Graham, S. M.; Buss, J. E.; Der, C. J., Isoprenoid addition to Ras protein is the critical modification for its membrane association and transforming activity. *Proc. Natl. Acad. Sci. U. S. A.* **1992,** *89*, 6403-6407.

23. Bell, I. M., Inhibitors of Farnesyltransferase: A Rational Approach to Cancer Chemotherapy? *J. Med. Chem.* **2004,** *47*, 1869-1878.

24. Zhu, K.; Hamilton, A. D.; Sebti, S. M., Farnesyltransferase inhibitors as anticancer agents: current status. *Curr. Opin. Investig. Drugs* **2003,** *4*, 1428-1435.

25. Brunner, T. B.; Hahn, S. M.; Gupta, A. K.; Muschel, R. J.; McKenna, W. G.; Bernhard, E. J., Farnesyltransferase inhibitors: an overview of the results of preclinical and clinical investigations. *Cancer Res.* **2003,** *63*, 5656-5668.

26. Doll, R. J.; Kirschmeier, P.; Bishop, W. R., Farnesyltransferase inhibitors as anticancer agents: critical crossroads. *Curr. Opin. Drug. Discov. Devel.* **2004,** *7*, 478-486.

27. Sparano, J. A.; Moulder, S.; Kazi, A.; Coppola, D.; Negassa, A.; Vahdat, L.; Li, T.; Pellegrino, C.; Fineberg, S.; Munster, P.; Malafa, M.; Lee, D.; Hoschander, S.; Hopkins, U.; Hershman, D.; Wright, J. J.; Kleer, C.; Merajver, S.; Sebti, S. M., Phase II trial of tipifarnib plus neoadjuvant doxorubicin-cyclophosphamide in patients with clinical stage IIB-IIIC breast cancer. *Clin. Cancer. Res.* **2009,** *15*, 2942-2948.

28. Karp, J. E.; Flatten, K.; Feldman, E. J.; Greer, J. M.; Loegering, D. A.; Ricklis, R. M.; Morris, L. E.; Ritchie, E.; Smith, B. D.; Ironside, V.; Talbott, T.; Roboz, G.; Le, S. B.; Meng, X. W.; Schneider, P. A.; Dai, N. T.; Adjei, A. A.; Gore, S. D.; Levis, M. J.;

Wright, J. J.; Garrett-Mayer, E.; Kaufmann, S. H., Active oral regimen for elderly adults with newly diagnosed acute myelogenous leukemia: a preclinical and phase 1 trial of the farnesyltransferase inhibitor tipifarnib (R115777, Zarnestra) combined with etoposide. *Blood* **2009,** *113*, 4841-4852.

29. Feldman, A. L.; Law, M.; Remstein, E. D.; Macon, W. R.; Erickson, L. A.; Grogg, K. L.; Kurtin, P. J.; Dogan, A., Recurrent translocations involving the IRF4 oncogene locus in peripheral T-cell lymphomas. *Leukemia* **2009,** *23*, 574-580.

30. Meta, M.; Yang, S. H.; Bergo, M. O.; Fong, L. G.; Young, S. G., Protein farnesyltransferase inhibitors and progeria. *Trends. Mol. Med.* **2006,** *12*, 480-487.

31. Yang, S. H.; Meta, M.; Qiao, X.; Frost, D.; Bauch, J.; Coffinier, C.; Majumdar, S.; Bergo, M. O.; Young, S. G.; Fong, L. G., A farnesyltransferase inhibitor improves disease phenotypes in mice with a Hutchinson-Gilford progeria syndrome mutation. *J. Clin. Invest.* **2006,** *116*, 2115-2121.

32. Fong, L. G.; Frost, D.; Meta, M.; Qiao, X.; Yang, S. H.; Coffinier, C.; Young, S. G., A protein farnesyltransferase inhibitor ameliorates disease in a mouse model of progeria. *Science* **2006,** *311*, 1621-1623.

33. Gordon, L. B.; Harling-Berg, C. J.; Rothman, F. G., Highlights of the 2007 Progeria Research Foundation scientific workshop: progress in translational science. *J. Gerontol. A Biol. Sci. Med. Sci.* **2008,** *63*, 777-787.

34. Eastman, R. T.; Buckner, F. S.; Yokoyama, K.; Gelb, M. H.; Van Voorhis, W. C., Thematic review series: lipid posttranslational modifications. Fighting parasitic disease by blocking protein farnesylation. *J. Lipid. Res.* **2006,** *47*, 233-240.

35. Kraus, J. M.; Verlinde, C. L.; Karimi, M.; Lepesheva, G. I.; Gelb, M. H.; Buckner, F. S., Rational modification of a candidate cancer drug for use against Chagas disease. *J. Med. Chem.* **2009,** *52*, 1639-1647.

36. Ohkanda, J.; Buckner, F. S.; Lockman, J. W.; Yokoyama, K.; Carrico, D.; Eastman, R.; de Luca-Fradley, K.; Davies, W.; Croft, S. L.; Van Voorhis, W. C.; Gelb, M. H.; Sebti, S. M.; Hamilton, A. D., Design and synthesis of peptidomimetic protein farnesyltransferase inhibitors as anti-Trypanosoma brucei agents. *J. Med. Chem.* **2004,** *47*, 432-445.

37. Carrico, D.; Ohkanda, J.; Kendrick, H.; Yokoyama, K.; Blaskovich, M. A.; Bucher, C. J.; Buckner, F. S.; Van Voorhis, W. C.; Chakrabarti, D.; Croft, S. L.; Gelb, M. H.; Sebti, S. M.; Hamilton, A. D., In vitro and in vivo antimalarial activity of peptidomimetic protein farnesyltransferase inhibitors with improved membrane permeability. *Bioorg. Med. Chem.* **2004,** *12*, 6517-6526.

38. Ohkanda, J.; Lockman, J. W.; Yokoyama, K.; Gelb, M. H.; Croft, S. L.; Kendrick, H.; Harrell, M. I.; Feagin, J. E.; Blaskovich, M. A.; Sebti, S. M.; Hamilton, A. D., Peptidomimetic inhibitors of protein farnesyltransferase show potent antimalarial activity. *Bioorg. Med. Chem. Lett.* **2001,** *11*, 761-764.

39. Keller, P. J.; Fiordalisi, J. J.; Berzat, A. C.; Cox, A. D., Visual monitoring of post-translational lipid modifications using EGFP-GTPase probes in live cells. *Methods* **2005,** *37*, 131-137.

40. Cassidy, P. B.; Dolence, J. M.; Poulter, C. D., Continuous fluorescence assay for protein prenyltransferases. *Methods Enzymol.* **1995,** *250*, 30-43.

41. Pompliano, D. L.; Gomez, R. P.; Anthony, N. J., Intramolecular fluorescence enhancement: a continuous assay of Ras farnesyl:protein transferase. *J. Am. Chem. Soc.* **1992,** *114*, 7945-7946.

42. Wollack, J. S., J.; Petzold, C.; Mougous, J.; Distefano, M. D., A minimalist substrate for enzymatic peptide and protein conjugation. *ChemBiochem* **2009,** *10*, 2934-2943

43. Njoroge, F. G.; Doll, R. J.; Vibulbhan, B.; Alvarez, C. S.; Bishop, W. R.; Petrin, J.; Kirschmeier, P.; Carruthers, N. I.; Wong, J. K.; Albanese, M. M.; Piwinski, J. J.; Catino, J.; Girijavallabhan, V.; Ganguly, A. K., Discovery of novel nonpeptide tricyclic inhibitors of Ras farnesyl protein transferase. *Bioorg. Med. Chem.* **1997,** *5*, 101-113.

44. Coan, K. E.; Shoichet, B. K., Stoichiometry and physical chemistry of promiscuous aggregate-based inhibitors. *J. Am. Chem. Soc.* **2008,** *130*, 9606-9612.

45. Feng, B. Y.; Simeonov, A.; Jadhav, A.; Babaoglu, K.; Inglese, J.; Shoichet, B. K.; Austin, C. P., A high-throughput screen for aggregation-based inhibition in a large compound library. *J. Med. Chem.* **2007,** *50*, 2385-2390.

46. Choy, E.; Chiu, V. K.; Silletti, J.; Feoktistov, M.; Morimoto, T.; Michaelson, D.; Ivanov, I. E.; Philips, M. R., Endomembrane trafficking of ras: the CAAX motif targets proteins to the ER and Golgi. *Cell* **1999,** *98*, 69-80.

47. Morgan, M. M.; Khan, D. A.; Nathan, R. A., Treatment for allergic rhinitis and chronic idiopathic urticaria: focus on oral antihistamines. *Ann. Pharmacother.* **2005,** *39*, 2056-2064.

48. Picado, C., Rupatadine: pharmacological profile and its use in the treatment of allergic disorders. *Expert Opin. Pharmacother.* **2006,** *7*, 1989-2001.

49. Bachert, C., A review of the efficacy of desloratadine, fexofenadine, and levocetirizine in the treatment of nasal congestion in patients with allergic rhinitis. *Clin. Ther*. **2009,** *31*, 921-944.

50. Mullol, J.; Bousquet, J.; Bachert, C.; Canonica, W. G.; Gimenez-Arnau, A.; Kowalski, M. L.; Marti-Guadano, E.; Maurer, M.; Picado, C.; Scadding, G.; Van Cauwenberge, P., Rupatadine in allergic rhinitis and chronic urticaria. *Allergy* **2008,** *63*, 5-28.

51. Liu, H.; Farley, J. M., Effects of first and second generation antihistamines on muscarinic induced mucus gland cell ion transport. *BMC Pharmacol*. **2005,** *5*, 8.

52. Howell, G., 3rd; West, L.; Jenkins, C.; Lineberry, B.; Yokum, D.; Rockhold, R., In vivo antimuscarinic actions of the third generation antihistaminergic agent, desloratadine. *BMC Pharmacol*. **2005,** *5*, 13.

53. DRUGDEX *MICROMEDEX*, Thomson Reuters: Greenwood Village, Colorado, 2008.

54. Ogunwobi, O. O.; Beales, I. L., Statins inhibit proliferation and induce apoptosis in Barrett's esophageal adenocarcinoma cells. *Am. J. Gastroenterol*. **2008,** *103*, 825-837.

55. Farwell, W. R.; Scranton, R. E.; Lawler, E. V.; Lew, R. A.; Brophy, M. T.; Fiore, L. D.; Gaziano, J. M., The association between statins and cancer incidence in a veterans population. *J. Natl. Cancer Inst*. **2008,** *100*, 134-9.

56. Engel, J. C., *unpublished* **2009**.

57. Docampo, R.; Moreno, S. N. J.; Turrens, J. F.; Katzin, A. M.; Gonzalez-Cappa, S. M.; Stoppani, A. O. M., Biochemical and ultrastructural alterations produced by

miconazole and econazole in Trypanosoma cruzi. *Mol. Biochem. Parasitol.* **1981,** *3*, 169-180.

58. National Cancer Institute. The NCI/DTP Open Chemical Repository, http://dtp.cancer.gov. NSC agent numbers 170986 and 169434**.** In 2009

59. M. Olah; R. Rad; L. Ostopovici; A. Bora; N. Hadaruga; D. Hadaruga; R. Moldovan; A. Fulias; M. Mracec; Oprea, T. I., WOMBAT and WOMBAT-PK: Bioactivity databases for lead and drug discovery. In *Chemical Biology: From Small Molecules to Systems Biology and Drug Design*, SL Schreiber, T. K., G. Wess, Ed. Wiley-VCH: 2007; pp 760-786.

60. EMBL-EBI, ChEMBL StARlite, http://www.ebi.ac.uk/chembl/. In 2009.

61. Gaon, I.; Turek, T. C.; Weller, V. A.; Edelstein, R. L.; Singh, S. K.; Distefano, M. D., Photoactive analogs of farnesyl pyrophosphate containing benzoylbenzoate esters: synthesis and application to photoaffinity labeling of yeast protein farnesyltransferase. *J. Org. Chem.* **1996,** *61*, 7738-7745.

62. DeGraw, A. J.; Hast, M. A.; Xu, J.; Mullen, D.; Beese, L. S.; Barany, G.; Distefano, M. D., Caged protein prenyltransferase substrates: tools for understanding protein prenylation. *Chem. Biol. Drug. Des.* **2008,** *72*, 171-181.

63. Lingham, R. B.; Silverman, K. C.; Jayasuriya, H.; Kim, B. M.; Amo, S. E.; Wilson, F. R.; Rew, D. J.; Schaber, M. D.; Bergstrom, J. D.; Koblan, K. S.; Graham, S. L.; Kohl, N. E.; Gibbs, J. B.; Singh, S. B., Clavaric acid and steroidal analogues as Ras- and FPP-directed inhibitors of human farnesyl-protein transferase. *J. Med. Chem.* **1998,** *41*, 4492-4501.

64. Frye, S. V., Structure-activity relationship homology (SARAH); a conceptual framework for drug discovery in the genomic era. *Chem. Biol.* **1999,** *6*, R3-R7.

65. Jacoby, E.; Schuffenhauer, A.; Floersheim, P., Chemogenomics knowledge-based strategies in drug discovery. *Drug News Perspect.* **2003,** *16*, 93-102.

66. Maggiora, G. M.; Johnson, M. A., Introduction to similarity in chemistry. *Concepts Appl. Mol. Sim.* **1990**, 1-13.

67. Altschul, S. F.; Gish, W.; Miller, W.; Myers, E. W.; Lipman, D. J., Basic local alignment search tool. *J. Mol. Biol.* **1990,** *215*, 403-410.

68. Karlin, S.; Altschul, S. F., Methods for assessing the statistical significance of molecular sequence features by using general scoring schemes. *Proc. Natl. Acad. Sci. U. S. A.* **1990,** *87*, 2264-2268.

69. Pearson, W. R., Empirical statistical estimates for sequence similarity searches. *J. Mol. Biol.* **1998,** *276*, 71-84.

70. Roskoski, R., Jr.; Ritchie, P. A., Time-dependent inhibition of protein farnesyltransferase by a benzodiazepine peptide mimetic. *Biochemistry* **2001,** *40*, 9329-9335.

Appendix C. Bibliography of Appendices

Sletten, E. M. and Bertozzi, C.R., Bioorthogonal chemistry: fishing for selectivity in a sea of functionality. *Angew. Chem. Int. Ed.* **2009,** *48*, 6974-6998.

Breinbauer, R.; Kohn, M., Azide-alkyne coupling: a powerful reaction for bioconjugate chemistry. *Chembiochem* **2003,** *4*, 1147-1149.

Agard, N. J.; Prescher, J. A.; Bertozzi, C. R., A strain-promoted [3 + 2] azide-alkyne cycloaddition for covalent modification of biomolecules in living systems. *J. Am. Chem. Soc.* **2004,** *126*, 15046-15047.

Baskin, J. M.; Prescher, J. A.; Laughlin, S. T.; Agard, N. J.; Chang, P. V.; Miller, I. A.; Lo, A.; Codelli, J. A.; Bertozzi, C. R., Copper-free click chemistry for dynamic in vivo imaging. *Proc. Natl. Acad. Sci. U. S. A.* **2007,** *104*, 16793-16797.

Codelli, J. A.; Baskin, J. M.; Agard, N. J.; Bertozzi, C. R., Second-generation difluorinated cyclooctynes for copper-free click chemistry. *J. Am. Chem. Soc.* **2008,** *130*, 11486-11493.

Ning, X.; Guo, J.; Wolfert, M. A.; Boons, G. J., Visualizing metabolically labeled glycoconjugates of living cells by copper-free and fast huisgen cycloadditions. *Angew. Chem. Int. Ed.* **2008,** *47*, 2253-2255.

Duckworth, B. P.; Xu, J.; Taton, T. A.; Guo, A.; Distefano, M. D., Site-specific, covalent attachment of proteins to a solid surface. *Bioconjug. Chem.* **2006,** *17*, 967-974.

Duckworth, B. P.; Chen, Y.; Wollack, J. W.; Sham, Y.; Mueller, J. D.; Taton, T. A.; Distefano, M. D., A universal method for the preparation of covalent protein-DNA conjugates for use in creating protein nanostructures. *Angew. Chem. Int. Ed.* **2007,** *46*, 8819-8822.

Shaner, N. C.; Campbell, R.E.; Steinbach, P.A.; Giepmans, B.N.G.; Palmer, A.E.; Tsien, R.Y., Improved monomeric red, orange, and yellow fluorescent proteins derived from *Discosoma sp*. red fluorescent protein. *Nat. Biotech.* **2004,** *22*, 1567-1572.

Chung, J. A.; Wollack, J.W.; Hovlid, M.L.; Okesli, A.; Chen, Y.; Mueller, J.D.; Distefano, M.D.; Taton, T.A., Purification of prenylated proteins by affinity chromatography on cyclodextrin-modified agarose. *Anal. Biochem.* **2009,** *386*, 1-8.

Chan, L. N.; Hart, C.; Guo, L.; Nyberg, T.; Davies, B. S.; Fong, L. G.; Young, S. G.; Agnew, B. J.; Tamanoi, F., A novel approach to tag and identify geranylgeranylated proteins. *Electrophoresis* **2009,** *30*, 3598-3606.

Kho, Y.; Kim, S. C.; Jiang, C.; Barma, D.; Kwon, S. W.; Cheng, J.; Jaunbergs, J.; Weinbaum, C.; Tamanoi, F.; Falck, J.; Zhao, Y., A tagging-via-substrate technology for

detection and proteomics of farnesylated proteins. *Proc. Natl. Acad. Sci. U. S. A.* **2004,** *101*, 12479-12484.

Baskin, J. M. personal communication. 2008.

Moseley, M. A.; Deterding, L. J.; Tomer, K. B.; Jorgenson, J. W., Nanoscale packed-capillary liquid chromatography coupled with mass spectrometry using a coaxial continuous-flow fast atom bombardment interface. *Anal. Chem.* **1991,** *63*, 1467-1473.

Shilov, I. V.; Seymour, S. L.; Patel, A. A.; Loboda, A.; Tang, W. H.; Keating, S. P.; Hunter, C. L.; Nuwaysir, L. M.; Schaeffer, D. A., The paragon algorithm, a next generation search engine that uses sequence temperature values and feature probabilities to identify peptides from tandem mass spectra. *Mol. Cell. Proteomics* **2007,** *6*, 1638-1655.

Adams, C. P.; Brantner, V. V., Estimating the cost of new drug development: is it really 802 million dollars? *Health Aff. (Millwood)* **2006,** *25*, 420-428.

Hopkins, A. L., Network pharmacology: the next paradigm in drug discovery. *Nat. Chem. Biol.* **2008,** *4*, 682-690.

Oprea, T. I.; Tropsha, A.; Faulon, J. L.; Rintoul, M. D., Systems chemical biology. *Nat. Chem. Biol.* **2007,** *3*, 447-450.

Scheiber, J.; Jenkins, J. L., Chemogenomic analysis of safety profiling data. *Methods Mol. Biol.* **2009,** *575*, 207-223.

Wermuth, C. G., Selective optimization of side activities: the SOSA approach. *Drug Discov. Today* **2006,** *11*, 160-164.

Hert, J.; Keiser, M. J.; Irwin, J. J.; Oprea, T. I.; Shoichet, B. K., Quantifying the relationships among drug classes. *J. Chem. Inf. Model* **2008,** *48*, 755-765.

Keiser, M. J.; Roth, B. L.; Armbruster, B. N.; Ernsberger, P.; Irwin, J. J.; Shoichet, B. K., Relating protein pharmacology by ligand chemistry. *Nat. Biotechnol.* **2007,** *25*, 197-206.

Keiser, M. J.; Vincent, S.; Irwin, J. J.; Laggner, C.; Abbas, A. I.; Hufeisen, S. J.; Jensen, N. H.; Kuijer, M. B.; Matos, R. C.; Tran, T. B.; Whaley, R.; Glennon, R. A.; Hert, J.; Thomas, K. L. H.; Edwards, D. D.; Shoichet, B. K.; Roth, B. L., Predicting new molecular targets for known drugs. *Nature* **2009,** *462*, 175-181.

Bajorath, J., Computational analysis of ligand relationships within target families. *Curr. Opin. Chem. Biol.* **2008,** *12*, 352-358.

Campillos, M.; Kuhn, M.; Gavin, A. C.; Jensen, L. J.; Bork, P., Drug target identification using side-effect similarity. *Science* **2008,** *321*, 263-266.

Lounkine, E.; Stumpfe, D.; Bajorath, J., Molecular formal concept analysis for compound selectivity profiling in biologically annotated databases. *J. Chem. Inf. Model* **2009,** *49*, 1359-1368.

Muchmore, S. W.; Debe, D. A.; Metz, J. T.; Brown, S. P.; Martin, Y. C.; Hajduk, P. J., Application of belief theory to similarity data fusion for use in analog searching and lead hopping. *J. Chem. Inf. Model* **2008,** *48*, 941-948.

Scheiber, J.; Jenkins, J. L.; Sukuru, S. C.; Bender, A.; Mikhailov, D.; Milik, M.; Azzaoui, K.; Whitebread, S.; Hamon, J.; Urban, L.; Glick, M.; Davies, J. W., Mapping adverse drug reactions in chemical space. *J. Med. Chem.* **2009,** *52*, 3103-3107.

Vieth, M.; Erickson, J.; Wang, J.; Webster, Y.; Mader, M.; Higgs, R.; Watson, I., Kinase inhibitor data modeling and de novo inhibitor design with fragment approaches. *J. Med. Chem.* **2009,** *52*, 6456-6666.

Young, D. W.; Bender, A.; Hoyt, J.; McWhinnie, E.; Chirn, G. W.; Tao, C. Y.; Tallarico, J. A.; Labow, M.; Jenkins, J. L.; Mitchison, T. J.; Feng, Y., Integrating high-content screening and ligand-target prediction to identify mechanism of action. *Nat. Chem. Biol.* **2008,** *4*, 59-68.

Altschul, S. F.; Gish, W.; Miller, W.; Myers, E. W.; Lipman, D. J., Basic local alignment search tool. *J. Mol. Biol.* **1990,** *215*, 403-410.

Keiser, M. J.; Hert, J., Off-target networks derived from ligand set similarity. *Methods Mol. Biol.* **2009,** *575*, 195-205.

Walsh, C. T.; Garneau-Tsodikova, S.; Gatto, G. J., Jr., Protein posttranslational modifications: The chemistry of proteome diversifications. *Angew. Chem. Int. Ed.* **2005,** *44*, 7342-7372.

Reid, T. S.; Terry, K. L.; Casey, P. J.; Beese, L. S., Crystallographic analysis of CaaX prenyltransferases complexed with substrates defines rules of protein substrate selectivity. *J. Mol. Biol.* **2004,** *343*, 417-433.

Zhang, F. L.; Casey, P. J., Protein prenylation: molecular mechanisms and functional consequences. *Annu. Rev. Biochem.* **1996,** *65*, 241-269.

Lowy, D. R.; Willumsen, B. M., Function and regulation of ras. *Annu. Rev. Biochem.* **1993,** *62*, 851-891.

Kato, K.; Cox, A. D.; Hisaka, M. M.; Graham, S. M.; Buss, J. E.; Der, C. J., Isoprenoid addition to Ras protein is the critical modification for its membrane association and transforming activity. *Proc. Natl. Acad. Sci. U. S. A.* **1992,** *89*, 6403-6407.

Bell, I. M., Inhibitors of Farnesyltransferase: A Rational Approach to Cancer Chemotherapy? *J. Med. Chem.* **2004,** *47*, 1869-1878.

Zhu, K.; Hamilton, A. D.; Sebti, S. M., Farnesyltransferase inhibitors as anticancer agents: current status. *Curr. Opin. Investig. Drugs* **2003,** *4*, 1428-1435.

Brunner, T. B.; Hahn, S. M.; Gupta, A. K.; Muschel, R. J.; McKenna, W. G.; Bernhard, E. J., Farnesyltransferase inhibitors: an overview of the results of preclinical and clinical investigations. *Cancer Res.* **2003,** *63*, 5656-5668.

Doll, R. J.; Kirschmeier, P.; Bishop, W. R., Farnesyltransferase inhibitors as anticancer agents: critical crossroads. *Curr. Opin. Drug. Discov. Devel.* **2004,** *7*, 478-486.

Sparano, J. A.; Moulder, S.; Kazi, A.; Coppola, D.; Negassa, A.; Vahdat, L.; Li, T.; Pellegrino, C.; Fineberg, S.; Munster, P.; Malafa, M.; Lee, D.; Hoschander, S.; Hopkins, U.; Hershman, D.; Wright, J. J.; Kleer, C.; Merajver, S.; Sebti, S. M., Phase II trial of tipifarnib plus neoadjuvant doxorubicin-cyclophosphamide in patients with clinical stage IIB-IIIC breast cancer. *Clin. Cancer. Res.* **2009,** *15*, 2942-2948.

Karp, J. E.; Flatten, K.; Feldman, E. J.; Greer, J. M.; Loegering, D. A.; Ricklis, R. M.; Morris, L. E.; Ritchie, E.; Smith, B. D.; Ironside, V.; Talbott, T.; Roboz, G.; Le, S. B.; Meng, X. W.; Schneider, P. A.; Dai, N. T.; Adjei, A. A.; Gore, S. D.; Levis, M. J.; Wright, J. J.; Garrett-Mayer, E.; Kaufmann, S. H., Active oral regimen for elderly adults with newly diagnosed acute myelogenous leukemia: a preclinical and phase 1 trial of the farnesyltransferase inhibitor tipifarnib (R115777, Zarnestra) combined with etoposide. *Blood* **2009,** *113*, 4841-4852.

Feldman, A. L.; Law, M.; Remstein, E. D.; Macon, W. R.; Erickson, L. A.; Grogg, K. L.; Kurtin, P. J.; Dogan, A., Recurrent translocations involving the IRF4 oncogene locus in peripheral T-cell lymphomas. *Leukemia* **2009,** *23*, 574-580.

Meta, M.; Yang, S. H.; Bergo, M. O.; Fong, L. G.; Young, S. G., Protein farnesyltransferase inhibitors and progeria. *Trends. Mol. Med.* **2006,** *12*, 480-487.

Yang, S. H.; Meta, M.; Qiao, X.; Frost, D.; Bauch, J.; Coffinier, C.; Majumdar, S.; Bergo, M. O.; Young, S. G.; Fong, L. G., A farnesyltransferase inhibitor improves disease phenotypes in mice with a Hutchinson-Gilford progeria syndrome mutation. *J. Clin. Invest.* **2006,** *116*, 2115-2121.

Fong, L. G.; Frost, D.; Meta, M.; Qiao, X.; Yang, S. H.; Coffinier, C.; Young, S. G., A protein farnesyltransferase inhibitor ameliorates disease in a mouse model of progeria. *Science* **2006,** *311*, 1621-1623.

Gordon, L. B.; Harling-Berg, C. J.; Rothman, F. G., Highlights of the 2007 Progeria Research Foundation scientific workshop: progress in translational science. *J. Gerontol. A Biol. Sci. Med. Sci.* **2008,** *63*, 777-787.

Eastman, R. T.; Buckner, F. S.; Yokoyama, K.; Gelb, M. H.; Van Voorhis, W. C., Thematic review series: lipid posttranslational modifications. Fighting parasitic disease by blocking protein farnesylation. *J. Lipid. Res.* **2006,** *47*, 233-240.

Kraus, J. M.; Verlinde, C. L.; Karimi, M.; Lepesheva, G. I.; Gelb, M. H.; Buckner, F. S., Rational modification of a candidate cancer drug for use against Chagas disease. *J. Med. Chem.* **2009,** *52*, 1639-1647.

Ohkanda, J.; Buckner, F. S.; Lockman, J. W.; Yokoyama, K.; Carrico, D.; Eastman, R.; de Luca-Fradley, K.; Davies, W.; Croft, S. L.; Van Voorhis, W. C.; Gelb, M. H.; Sebti, S. M.; Hamilton, A. D., Design and synthesis of peptidomimetic protein farnesyltransferase inhibitors as anti-Trypanosoma brucei agents. *J. Med. Chem.* **2004,** *47*, 432-445.

Carrico, D.; Ohkanda, J.; Kendrick, H.; Yokoyama, K.; Blaskovich, M. A.; Bucher, C. J.; Buckner, F. S.; Van Voorhis, W. C.; Chakrabarti, D.; Croft, S. L.; Gelb, M. H.; Sebti, S. M.; Hamilton, A. D., In vitro and in vivo antimalarial activity of peptidomimetic protein farnesyltransferase inhibitors with improved membrane permeability. *Bioorg. Med. Chem.* **2004,** *12*, 6517-6526.

Ohkanda, J.; Lockman, J. W.; Yokoyama, K.; Gelb, M. H.; Croft, S. L.; Kendrick, H.; Harrell, M. I.; Feagin, J. E.; Blaskovich, M. A.; Sebti, S. M.; Hamilton, A. D., Peptidomimetic inhibitors of protein farnesyltransferase show potent antimalarial activity. *Bioorg. Med. Chem. Lett.* **2001,** *11*, 761-764.

Keller, P. J.; Fiordalisi, J. J.; Berzat, A. C.; Cox, A. D., Visual monitoring of post-translational lipid modifications using EGFP-GTPase probes in live cells. *Methods* **2005,** *37*, 131-137.

Cassidy, P. B.; Dolence, J. M.; Poulter, C. D., Continuous fluorescence assay for protein prenyltransferases. *Methods Enzymol.* **1995,** *250*, 30-43.

Pompliano, D. L.; Gomez, R. P.; Anthony, N. J., Intramolecular fluorescence enhancement: a continuous assay of Ras farnesyl:protein transferase. *J. Am. Chem. Soc.* **1992,** *114*, 7945-7946.

Wollack, J. S., J.; Petzold, C.; Mougous, J.; Distefano, M. D., A minimalist substrate for enzymatic peptide and protein conjugation. *ChemBiochem* **2009,** *10*, 2934-2943

Njoroge, F. G.; Doll, R. J.; Vibulbhan, B.; Alvarez, C. S.; Bishop, W. R.; Petrin, J.; Kirschmeier, P.; Carruthers, N. I.; Wong, J. K.; Albanese, M. M.; Piwinski, J. J.; Catino, J.; Girijavallabhan, V.; Ganguly, A. K., Discovery of novel nonpeptide tricyclic inhibitors of Ras farnesyl protein transferase. *Bioorg. Med. Chem.* **1997,** *5*, 101-113.

Coan, K. E.; Shoichet, B. K., Stoichiometry and physical chemistry of promiscuous aggregate-based inhibitors. *J. Am. Chem. Soc.* **2008,** *130*, 9606-9612.

Feng, B. Y.; Simeonov, A.; Jadhav, A.; Babaoglu, K.; Inglese, J.; Shoichet, B. K.; Austin, C. P., A high-throughput screen for aggregation-based inhibition in a large compound library. *J. Med. Chem.* **2007,** *50*, 2385-2390.

Choy, E.; Chiu, V. K.; Silletti, J.; Feoktistov, M.; Morimoto, T.; Michaelson, D.; Ivanov, I. E.; Philips, M. R., Endomembrane trafficking of ras: the CAAX motif targets proteins to the ER and Golgi. *Cell* **1999,** *98*, 69-80.

Morgan, M. M.; Khan, D. A.; Nathan, R. A., Treatment for allergic rhinitis and chronic idiopathic urticaria: focus on oral antihistamines. *Ann. Pharmacother.* **2005,** *39*, 2056-2064.

Picado, C., Rupatadine: pharmacological profile and its use in the treatment of allergic disorders. *Expert Opin. Pharmacother.* **2006,** *7*, 1989-2001.

Bachert, C., A review of the efficacy of desloratadine, fexofenadine, and levocetirizine in the treatment of nasal congestion in patients with allergic rhinitis. *Clin. Ther.* **2009,** *31*, 921-944.

Mullol, J.; Bousquet, J.; Bachert, C.; Canonica, W. G.; Gimenez-Arnau, A.; Kowalski, M. L.; Marti-Guadano, E.; Maurer, M.; Picado, C.; Scadding, G.; Van Cauwenberge, P., Rupatadine in allergic rhinitis and chronic urticaria. *Allergy* **2008,** *63*, 5-28.

Liu, H.; Farley, J. M., Effects of first and second generation antihistamines on muscarinic induced mucus gland cell ion transport. *BMC Pharmacol.* **2005,** *5*, 8.

Howell, G., 3rd; West, L.; Jenkins, C.; Lineberry, B.; Yokum, D.; Rockhold, R., In vivo antimuscarinic actions of the third generation antihistaminergic agent, desloratadine. *BMC Pharmacol.* **2005,** *5*, 13.

DRUGDEX *MICROMEDEX*, Thomson Reuters: Greenwood Village, Colorado, 2008.

Ogunwobi, O. O.; Beales, I. L., Statins inhibit proliferation and induce apoptosis in Barrett's esophageal adenocarcinoma cells. *Am. J. Gastroenterol.* **2008,** *103*, 825-837.

Farwell, W. R.; Scranton, R. E.; Lawler, E. V.; Lew, R. A.; Brophy, M. T.; Fiore, L. D.; Gaziano, J. M., The association between statins and cancer incidence in a veterans population. *J. Natl. Cancer Inst.* **2008,** *100*, 134-9.

Engel, J. C., *unpublished* **2009**.

Docampo, R.; Moreno, S. N. J.; Turrens, J. F.; Katzin, A. M.; Gonzalez-Cappa, S. M.; Stoppani, A. O. M., Biochemical and ultrastructural alterations produced by miconazole and econazole in Trypanosoma cruzi. *Mol. Biochem. Parasitol.* **1981,** *3*, 169-180.

National Cancer Institute. The NCI/DTP Open Chemical Repository, http://dtp.cancer.gov. NSC agent numbers 170986 and 169434**.** In 2009
M. Olah; R. Rad; L. Ostopovici; A. Bora; N. Hadaruga; D. Hadaruga; R. Moldovan; A. Fulias; M. Mracec; Oprea, T. I., WOMBAT and WOMBAT-PK: Bioactivity databases for lead and drug discovery. In *Chemical Biology: From Small Molecules to Systems Biology and Drug Design*, SL Schreiber, T. K., G. Wess, Ed. Wiley-VCH: 2007; pp 760-786.

EMBL-EBI, ChEMBL StARlite, http://www.ebi.ac.uk/chembl/. In 2009.

Gaon, I.; Turek, T. C.; Weller, V. A.; Edelstein, R. L.; Singh, S. K.; Distefano, M. D., Photoactive analogs of farnesyl pyrophosphate containing benzoylbenzoate esters: synthesis and application to photoaffinity labeling of yeast protein farnesyltransferase. *J. Org. Chem.* **1996,** *61*, 7738-7745.

DeGraw, A. J.; Hast, M. A.; Xu, J.; Mullen, D.; Beese, L. S.; Barany, G.; Distefano, M. D., Caged protein prenyltransferase substrates: tools for understanding protein prenylation. *Chem. Biol. Drug. Des.* **2008,** *72*, 171-181.

Lingham, R. B.; Silverman, K. C.; Jayasuriya, H.; Kim, B. M.; Amo, S. E.; Wilson, F. R.; Rew, D. J.; Schaber, M. D.; Bergstrom, J. D.; Koblan, K. S.; Graham, S. L.; Kohl, N. E.; Gibbs, J. B.; Singh, S. B., Clavaric acid and steroidal analogues as Ras- and FPP-directed inhibitors of human farnesyl-protein transferase. *J. Med. Chem.* **1998,** *41*, 4492-4501.

Frye, S. V., Structure-activity relationship homology (SARAH); a conceptual framework for drug discovery in the genomic era. *Chem. Biol.* **1999,** *6*, R3-R7.

Jacoby, E.; Schuffenhauer, A.; Floersheim, P., Chemogenomics knowledge-based strategies in drug discovery. *Drug News Perspect.* **2003,** *16*, 93-102.

Maggiora, G. M.; Johnson, M. A., Introduction to similarity in chemistry. *Concepts Appl. Mol. Sim.* **1990**, 1-13.

Altschul, S. F.; Gish, W.; Miller, W.; Myers, E. W.; Lipman, D. J., Basic local alignment search tool. *J. Mol. Biol.* **1990,** *215*, 403-410.

Karlin, S.; Altschul, S. F., Methods for assessing the statistical significance of molecular sequence features by using general scoring schemes. *Proc. Natl. Acad. Sci. U. S. A.* **1990,** *87*, 2264-2268.

Pearson, W. R., Empirical statistical estimates for sequence similarity searches. *J. Mol. Biol.* **1998,** *276*, 71-84.

Roskoski, R., Jr.; Ritchie, P. A., Time-dependent inhibition of protein farnesyltransferase by a benzodiazepine peptide mimetic. *Biochemistry* **2001,** *40*, 9329-9335.